NPS62-87-003

# NAVAL POSTGRADUATE SCHOOL
Monterey, California

# THESIS

AN INVESTIGATION INTO THE POTENTIAL FOR DEVELOPING A SUCCESSFUL LOG-PERIODIC HALF SQUARE ANTENNA WITH DUAL FEED

by

John Richard Johnsen

December 1986

Thesis Advisor: R. W. Adler

Approved for public release; distribution is unlimited.

Prepared for:
Naval Ocean Systems Center(Code 822)
271 Catalina Blvd
San Diego, CA 92152

NAVAL POSTGRADUATE SCHOOL
Monterey, CA 93943

Rear Admiral R. Austin
Superintendent

D. A. Schrady
Provost

This thesis prepared in conjunction with research sponsored in part by Naval Ocean Systems Center, San Diego, California.

SECURITY CLASSIFICATION OF THIS PAGE

# REPORT DOCUMENTATION PAGE

| | |
|---|---|
| 1a REPORT SECURITY CLASSIFICATION<br>UNCLASSIFIED | 1b RESTRICTIVE MARKINGS |
| 2a SECURITY CLASSIFICATION AUTHORITY | 3 DISTRIBUTION/AVAILABILITY OF REPORT Approved for public release; distribution is unlimited |
| 2b DECLASSIFICATION / DOWNGRADING SCHEDULE | |
| 4 PERFORMING ORGANIZATION REPORT NUMBER(S)<br>NPS62-87-003 | 5 MONITORING ORGANIZATION REPORT NUMBER(S) |
| 6a NAME OF PERFORMING ORGANIZATION<br>Naval Postgraduate School<br>6b OFFICE SYMBOL (If applicable)<br>62 | 7a NAME OF MONITORING ORGANIZATION<br>Naval Postgraduate School |
| 6c ADDRESS (City, State, and ZIP Code)<br>Monterey, California 93943-5000 | 7b ADDRESS (City, State, and ZIP Code)<br>Monterey, California 93943-5000 |
| 8a NAME OF FUNDING / SPONSORING ORGANIZATION Naval Ocean Systems Center<br>8b OFFICE SYMBOL (If applicable)<br>822 | 9 PROCUREMENT INSTRUMENT IDENTIFICATION NUMBER |
| 8c ADDRESS (City, State, and ZIP Code)<br>271 Catalina Blvd<br>San Diego, CA 92152 | 10 SOURCE OF FUNDING NUMBERS<br>PROGRAM ELEMENT NO / PROJECT NO / TASK NO / WORK UNIT ACCESSION NO |

11 TITLE (Include Security Classification)
AN INVESTIGATION INTO THE POTENTIAL FOR DEVELOPING A SUCCESSFUL LOG-PERIODIC HALF SQUARE ANTENNA WITH DUAL FEED

12 PERSONAL AUTHOR(S)

| 13a TYPE OF REPORT | 13b TIME COVERED | 14 DATE OF REPORT (Year, Month, Day) | 15 PAGE COUNT |
|---|---|---|---|
| Master's Thesis | FROM ______ TO ______ | 1986 December | 147 |

16 SUPPLEMENTARY NOTATION

| 17 COSATI CODES | | | 18 SUBJECT TERMS (Continue on reverse if necessary and identify by block number) |
|---|---|---|---|
| FIELD | GROUP | SUB-GROUP | Log-Periodic Antenna; Half Square Antenna; Near Field Investigation |

19 ABSTRACT (Continue on reverse if necessary and identify by block number)

The investigation of a uniformly periodic half square array antenna with dual feed was conducted to provide more information about the potential of the structure as a log-periodic antenna for use by the military. Utilizing the Numerical Electromagnetics Code (NEC), an experimental investigation of the near field characteristics and the far field radiations patterns was conducted on a modeled version of the structure to identify the necessary performance characteristics of a successful log-periodic antenna. In the near field investigation, the Brillouin diagram was used extensively to analyze performance characteristics generated by the k to $\beta$ relationship where $\beta$ was determined from the relative amplitude and phase of the near magnetic field created by the structure under various conditions. The far field radiation patterns

| | |
|---|---|
| 20 DISTRIBUTION/AVAILABILITY OF ABSTRACT<br>☐ UNCLASSIFIED/UNLIMITED ☒ SAME AS RPT ☐ DTIC USERS | 21 ABSTRACT SECURITY CLASSIFICATION<br>UNCLASSIFIED |
| 22a NAME OF RESPONSIBLE INDIVIDUAL<br>Prof R. W. Adler | 22b TELEPHONE (Include Area Code)<br>(408)646-2352<br>22c OFFICE SYMBOL<br>62Ab |

DD FORM 1473, 84 MAR — 83 APR edition may be used until exhausted. All other editions are obsolete

SECURITY CLASSIFICATION OF THIS PAGE

were used to check the results of the Brillouin diagram and observe the presence of end and truncation effects.

The results of this study show that the potential of designing a successful log-periodic antenna with half square elements and a dual feed system exist, but further research is needed to establish optimum scaling and gain. The research did verify the dual polarization property, and the possibility of generating high and low angle propagation modes with the use of a dual feed system on the structure.

# An Investigation into the Potential for Developing a Successful Log-Periodic Half Square Antenna with Dual Feed

by

John Richard Johnsen
Captain, United States Army
B.S., United States Military Academy, 1979

Submitted in partial fulfillment
of the requirements for the degree of

MASTER OF SCIENCE IN ELECTRICAL ENGINEERING

from the

NAVAL POSTGRADUATE SCHOOL
December 1986

# ABSTRACT

The investigation of a uniformly periodic half square array antenna with dual feed was conducted to provide more information about the potential of the structure as a log-periodic antenna for use by the military. Utilizing the Numerical Electromagnetics Code (NEC), an experimental investigation of the near field characteristics and the far field radiations patterns was conducted on a modeled version of the structure to identify the necessary performance characteristics of a successful log-periodic antenna. In the near field investigation, the Brillouin diagram was used extensively to analyze performance characteristics generated by the k to $\beta$ relationship where $\beta$ was determined from the relative amplitude and phase of the near magnetic field created by the structure under various conditions. The far field radiation patterns were used to check the results of the Brillouin diagram and observe the presence of end and truncation effects.

The results of this study show that the potential of designing a successful log-periodic antenna with half square elements and a dual feed system exist, but further research is needed to establish optimum scaling and gain. The research did verify the dual polarization property, and the possibility of generating high and low angle propagation modes with the use of a dual feed system on the structure.

TABLE OF CONTENTS

# I. INTRODUCTION

## A. MILITARY HIGH FREQUENCY COMMUNICATION PROBLEM

Today's military forces have the capability to be highly mobile, strike quickly over long distances, and integrate complex intelligence resources and weapon systems to effectively deliver combat power at critical points. The coordination and control of these capabilities rely on dependable communications. To support the complex nature of the modern battlefield, the military employs numerous and varied communication systems.

High frequency (HF) communication systems provide the military short, medium, and long range communication for voice, digitally coded burst messages, radio teletype traffic, and radio telegraph (CW). The users of military HF communications vary from special operation teams operating in isolated areas to major military command headquarters controlling joint service operations. The demanding and varied requirements placed on military HF communications create a unique problem for the antenna engineer.

In designing antenna systems for military HF communications, the engineer has to consider the operating frequency range of 2 to 30 MHz, the variety of transmitting equipment utilized, and the proposed deployment of the equipment.

Understanding the various conditions imposed on an antenna, the engineer must establish the conditions which the antenna will be designed to operate in, and then design to optimize performance under those conditions. To obtain a useful antenna design, the engineer tries to achieve a balance between meeting operating conditions that allow the military to effectively deploy the structure while providing an acceptable performance. The engineer has historically faced a critical decision in achieving this balance by having to select an antenna size which supports a highly mobile force while compromising electrical performance if the physical size is small compared to the wavelength of operation, or selecting a size which enhances electrical performance at the sacrifice of limiting mobility and employment.

In response to design requirements, D. V. Campbell and associates at Fort Monmouth, New Jersey proposed a lightweight wire structure consisting of half square elements arranged in a log-periodic configuration with dual feeds (Figure 1). The antenna was designed to be mobile with on-site construction, support broadband communication requirements with a frequency range of 2 to 30 MHz and provide low and high angle propagation modes for short, medium, and long range communications. [Ref. 1] The focus of this paper is to provide more information about this proposed design and its potential for development as a military HF antenna system.

LOG–PERIODIC HALF SQUARE

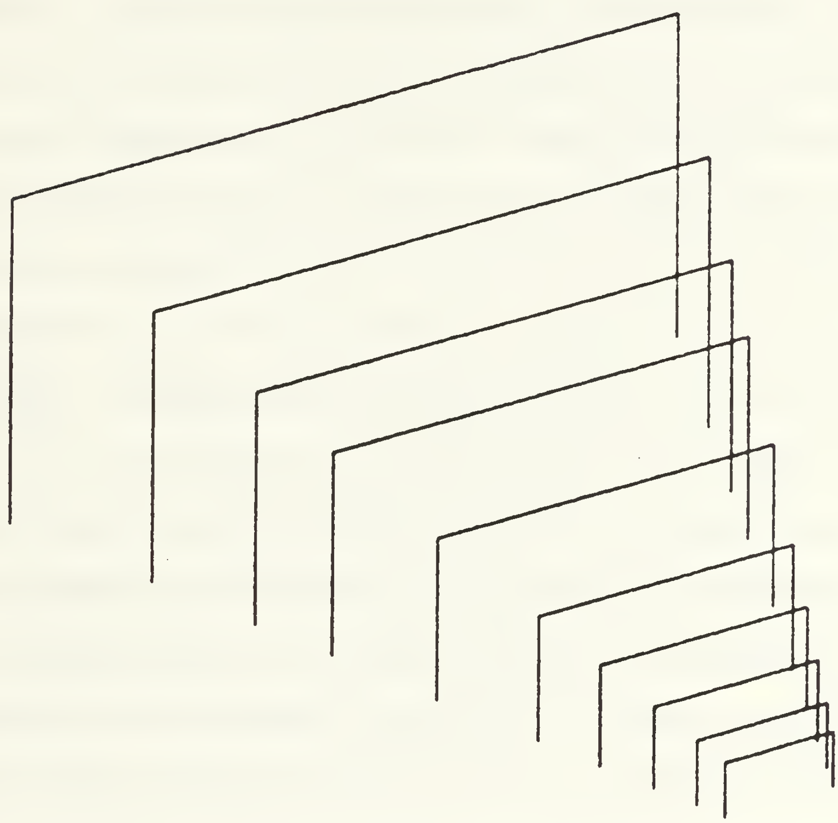

Figure 1. Log-periodic Half Square Antenna with Dual Feed

## B. HISTORICAL BACKGROUND

### 1. The Development of Log-Periodic Antennas

During the period from 1955 to 1958, research was conducted at the University of Illinois under the sponsorship of the United States Air Force to develop an antenna which was frequency independent. V. H. Rumsey noted that the characteristic length of the structure as compared to the operating wavelength ($\lambda_o$) introduced the frequency dependence observed in the antenna performance. Rumsey concluded that if a structure could be made self-scaling the characteristic length could be eliminated, and a structure that could be described by angles alone would provide such a characteristic. This conclusion is often referred to as the "angle concept." [Ref. 2] Structures which can be described by angles alone normally have an infinite length like the infinite biconical and if (bow tie) antennas. Since infinitely long structures can not be constructed, the finite length of the physical structure introduces a characteristic length property which eliminates the predicted frequency independent behavior.

Raymond DuHamel was the next to continue research on designing a broadband antenna with linear polarization. DuHamel interpreted the truncation problem observed by Rumsey in the work conducted on finite biconical and bifin antennas as the fact that the current on the structure had not demonstrated significant attenuation at the truncation

point. In his work, DuHamel observed that by introducing discontinuities into the structure in the form of teeth, he was able to increase radiation and the decay of current. Discovering that the teeth increased current decay in the structure, the investigation continued into the question of the effects that spacing and placement of the discontinuities on the structure had on the electrical performance. In his analysis of this problem, DuHamel recalled the work by Rumsey on the angle concept and on an equiangular spiral structure which had successfully demonstrated a broadand performance. From this information, the decision was made to cut teeth along circular arcs with a constant spacing ratio, $\tau$(Figure 2).

$$\tau = \frac{R_{n+1}}{R_n} \qquad \text{[Ref. 3]}$$

The finite length still created a characteristic length which eliminated the possibility of achieving complete frequency independence, but over a discrete frequency range, the structure exhibited a self scaling characteristic which allowed the antenna's performance for this frequency range to match the theoretical performance on an infinite structure over the same frequencies. DuHamel observed that the antenna demonstrated a performance in a periodic relationship to the operating frequency, and

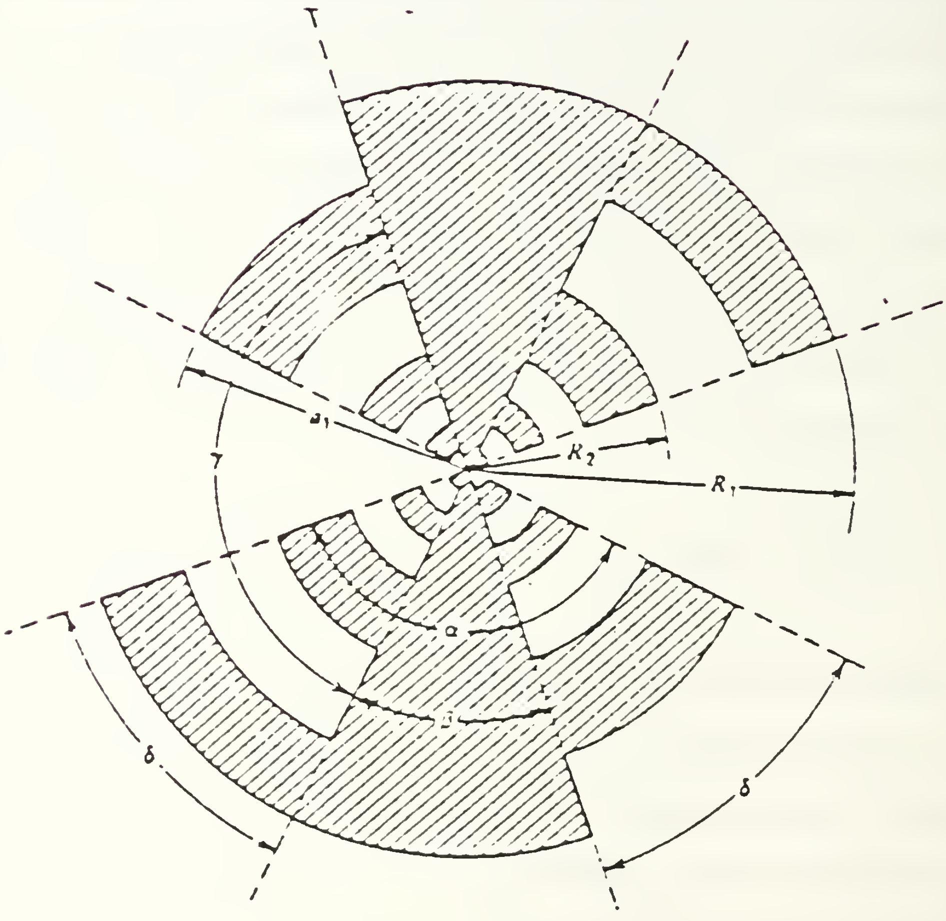


Figure 2. DuHamels' Log-periodic Structure

concluded that the antenna's performance was virtually identical for frequencies related logarithmically as

$$\log f_{n+1} = \log f_n + \log \left(\frac{1}{\tau}\right)$$

From the periodic performance of the antenna being related to the logarithm of the frequency, the structure was identified as a log-periodic antenna. [Ref. 4]

From Duhamel's work, many different structures were built and tested with varying degrees of frequency independence, but the next major contribution to the study of log-periodic antennas was made by a research assistant of DuHamel at the University of Illinois, D. E. Isabell. Isabell discovered by folding the structure into a wedge (Figure 3) the radiation pattern could be changed from a broad, bidirectional pattern into a unidirectional pattern with the primary direction of propagation being off the feed point of the structure. The new wedge shaped antenna demonstrated similar bandwidth properties but with lower impedance levels when compared to the equivalent unfolded structure. Continuing his research into log-periodic antennas, Isabell later discovered that the properties exhibited by the discontinuities on the structure were not dependent on the circular arc shape, as straight cut teeth provided the same performance characteristics (Figure 4). Isabell used the concepts of the wedge, the properties

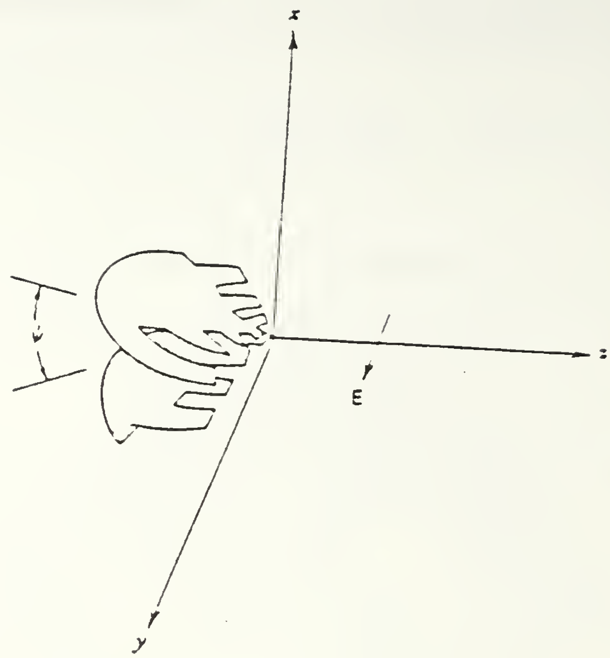


Figure. 3. Wedge Shape Antenna Proposed by Isabell

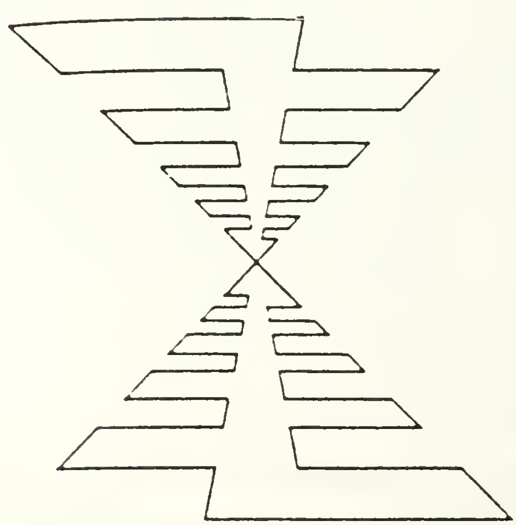

Figure 4. Periodic Structure with Straight Cut Discontinuities

observed in straight cut discontinuities and work by DuHamel which demonstrated that antennas formed by wire outlines of solid metallic structures provided similar performance characteristics to their sheet equivalent structure to develop a more conventional antenna using dipoles (Figure 5). Isabell established that the resonant elements must be staggered in a manner that will allow for a smooth transfer of the resonant region over the structure as a function of frequency. To accomplish this smooth transfer, the self scaling principle was employed to obtain overlapping response characteristics from the elements in the desired frequency range. The overlapping response was obtained by effective scaling of the dipole elements and scaling of the environment or spacing of the elements. Isabell proposed the use of an element scaling factor, $\tau$, defined by the relationship

$$\tau = \frac{L_n}{L_{n+1}} < 1$$

where $L_n$ is the length of the dipole, and a space factor, $\sigma$, defined as a ration of the spacing, $d_n$, between dipoles and the length of the dipole

$$\sigma = \frac{d_n}{2L_n}$$

The log-periodic dipole array antenna (LPDA) designed by Isabell has proven to be a successful broadband antenna. [Ref. 5]

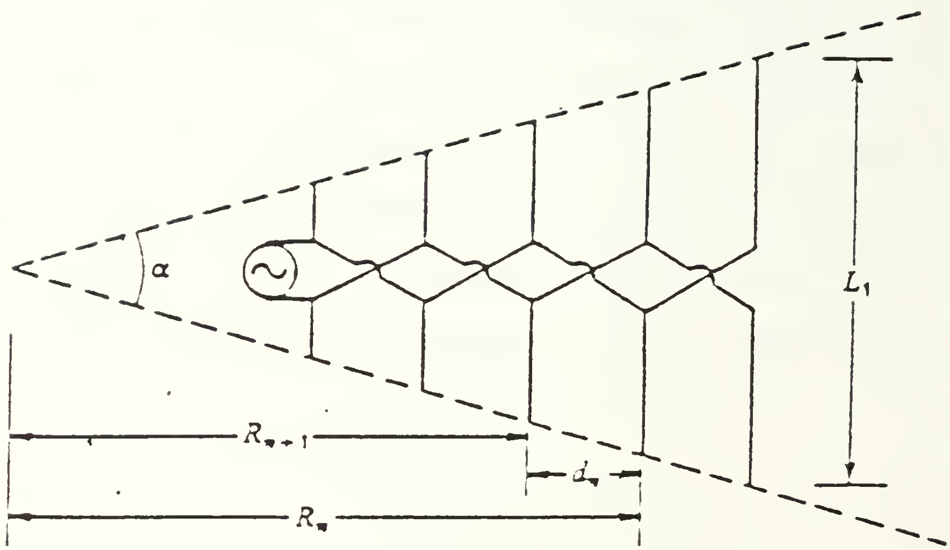


Figure 5. Log-periodic Dipole Antenna

The conventional structure of the LPDA allowed for the first time an opportunity to analyze a log-periodic structure with conventional analytic methods. R. L. Carrel made the first significant advances in the mathematical analysis of the performance characteristics of the LPDA. In 1961, Carrel, using early digital computer programming techniques, calculated the impedances on the structure, and then used the impedance values in a circuit type analysis of a loaded transmission line for the calculation of input impedance, voltage, and current on the transmission line. Using the calculated information about the transmission line and assumed current distribution along the elements, Carrel was able to calculate the radiation patterns for the structure. The comparison between the values of current calculated by Carrel and the values measured along the structure proved to be within experimental accuracy, and leading the engineering community to accept his analysis of the structure and a set of design curves he formulated relating scaling factors to design objectives (Figures 6 and 7). [Ref. 2]

### 2. The Development of the Half Square Log-Periodic Antenna

The half square antenna (Figure 8) served as the prototype for the elements implemented in this antenna. Ben Vester, an amateur radio operator, first noted that success of the half square antenna when he discovered that a bobtail

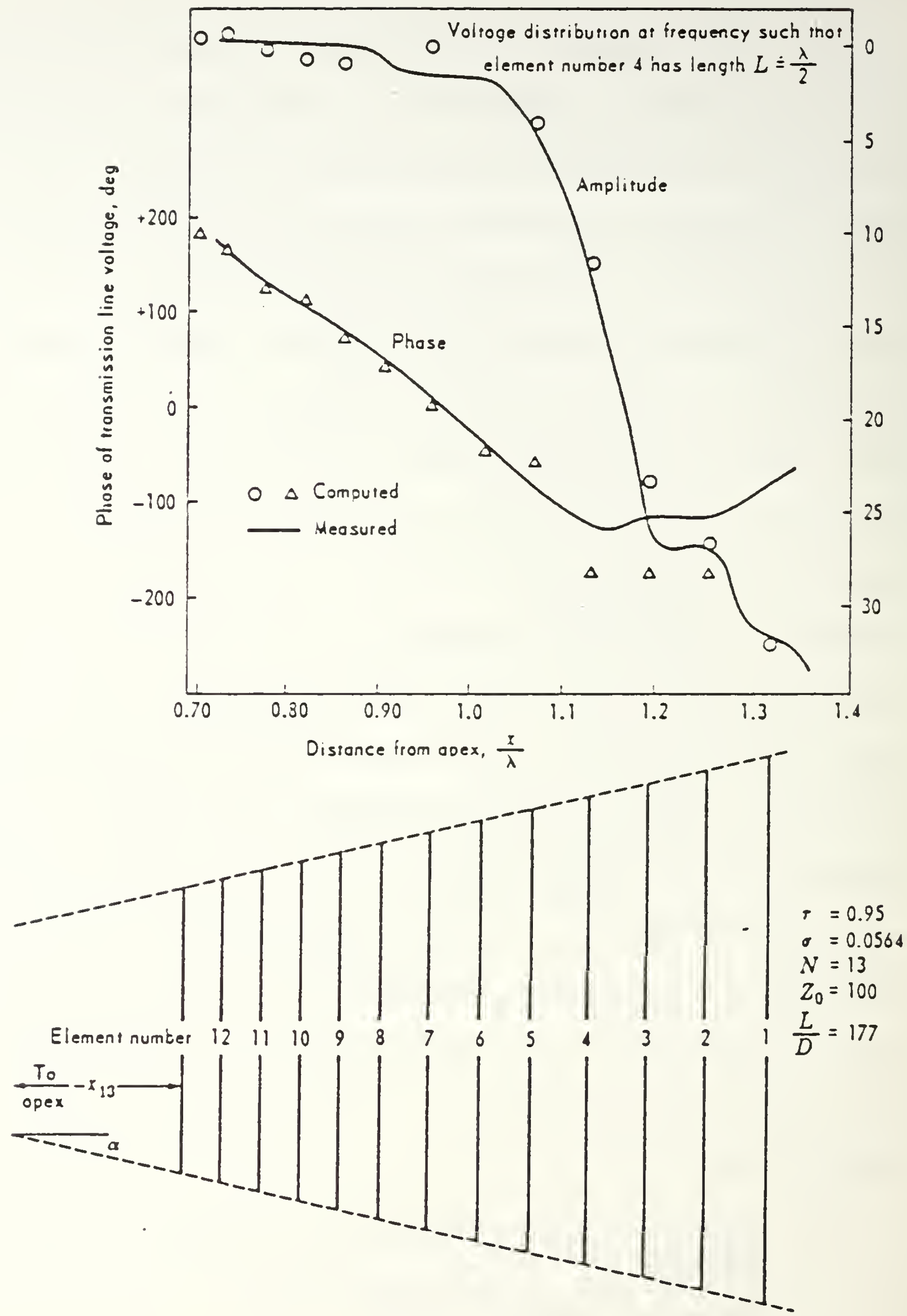


Figure 6. Experimental Values Compared to Carrel's Calculations

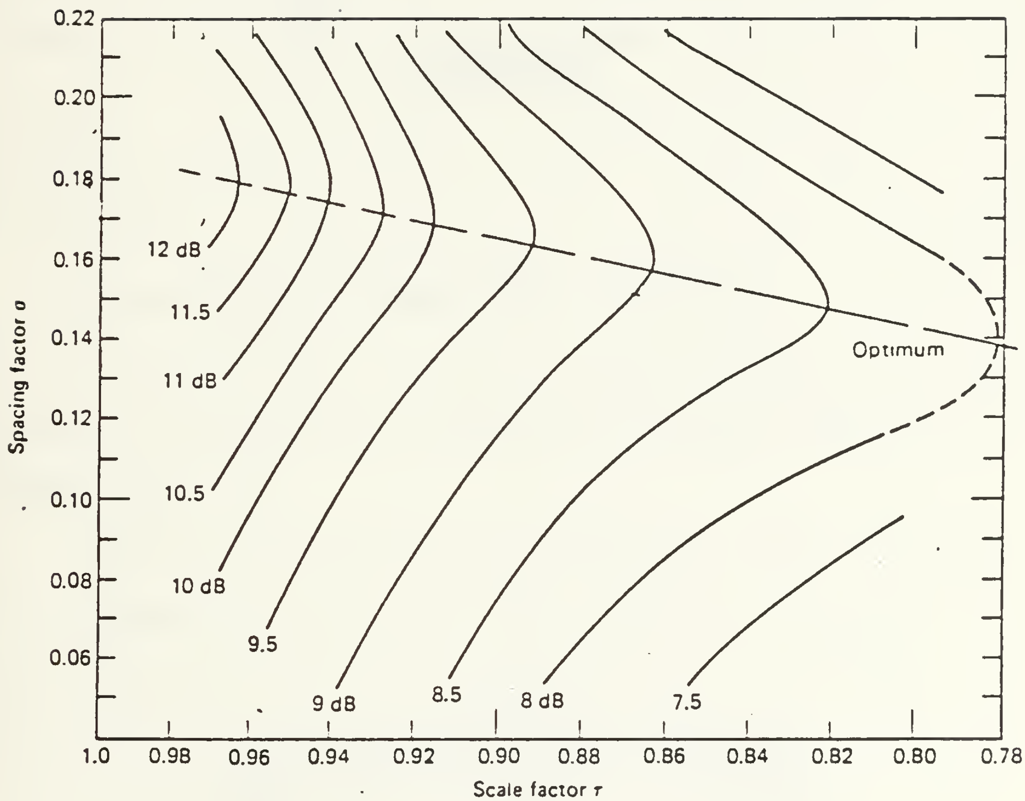


Figure 7. Carrel's Design Curves

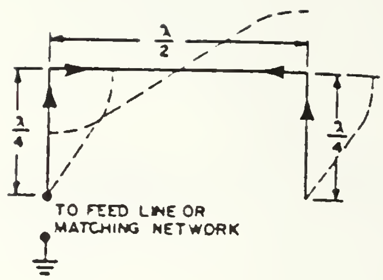


Figure 8. Half Square Antenna

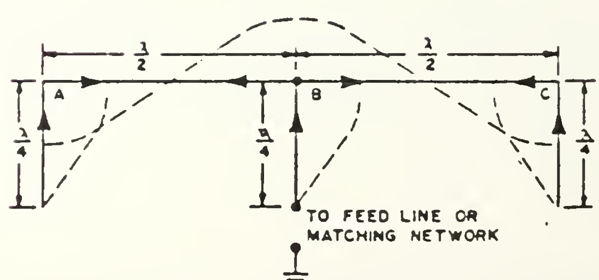


Figure 9. Bobtail Antenna

antenna (Figure 9) which had accidentally broken in half, demonstrated very little change in impedance and radiation pattern from the successful bobtail antenna. The current distributions on the half square antenna elements appear as if they were generated by a full wavelength antenna center fed with current loops located at quarter-wave points. The current distributions on the vertical wires are generated in phase resulting in broadside radiation patterns. From further investigation, Vester noted that a two element half square array antenna provided a wider bandwidth performance than the single element, and by moving the feed point to different positions along the transmission line, a directionality change was observed in the radiation pattern. Vester's half square antenna has proven to be a successful high frequency antenna for amateur radio operators. [Ref. 6]

Campbell and associates postulated that the half square antenna developed by Vester could be implemented into a log-periodic structure for use in military HF communications based on the performance characteristics observed. The proposed design implemented a dual feed system which provided the capability to alter the current distribution along the wires and support either low angle or high angle radiation. By observing that the current distributions on the half square structure demonstrated characteristics of current loops placed at the corners of the structure,

Campbell proposed that a dual feed system could be employed by feeding the corners that would provide current distributions similar to a single feed system if coupling was reduced by an insulator at the midpoint of the structure. The dual feed system allows for the vertical wires to be excited in either an in-phase or anti-phase mode. The in-phase mode provides a current distribution along the structure similar to the currents observed in a single feed structure; consequently, provides a radiation pattern of primarily vertical polarization. The anti-phase mode creates currents in the vertical wires which are out of phase with each other eliminating the vertically polarized radiation, but allowing the currents along the horizontal wires to provide a horizontally polarized radiation pattern.

Utilizing the dual feed concept proposed, a prototype of the log-periodic half square antenna was constructed at Fort Monmouth for testing a frequency range of 8 to 30 MHz. Campbell reported in his initial paper on the antenna that during the testing, the antenna exhibited impedance behavior common to a log-periodic structure, and computer modeling efforts demonstrated acceptable gain and pattern performance to warrant further investigation. [Ref. 1]

## C. GENERAL CHARACTERISTICS OF SUCCESSFUL LOG-PERIODIC ANTENNAS

From the work conducted by the individuals discussed in the previous section and others, some general characteristics

of successful log-periodic structures can be concluded from experimental results despite the complexity observed in attempting theoretical analysis of such structures. For a structure to be considered log-periodic in nature, the electrical properties must repeat periodically with the logarithm of the frequency. It has been shown in previous work that the periodic relationship appears to be a necessary, but not a sufficient characteristic condition to ensure broadband performance. In some log-periodic structures, large variations in electrical performance over a period or truncation effects destroy the periodic characteristics in certain frequency ranges and eliminate the broadband performance. To maintain the relative frequency independence of the structure, variations of the electrical properties over a period must be small and the structure must demonstrate a rapid decay in the current over an "active region" (or region of radiation) to eliminate end effects caused by finite truncation of the electrical length of the structure. Backward wave radiation is another characteristic observed in successful log-periodic designs. If a structure is being excited by a feed point providing a wave travelling on a transmission line from left to right, backward radiation occurs if the magnitude of the current is sharply attenuated as it travels across the left-most element of the active region and if the phase of the current in the element on the right

leads or increases in phase from the element on the left. This relationship results in a beam forming to the left and a null to the right creating a wave which propagates back in the direction of the feed, backward radiation. General amplitude and phase relationships along with the resulting rediation patterns are shown in Figure 10. Typical amplitude and phase relationships from backward radiation regions of loop and dipole arrays are shown in Figures 11 and 12.

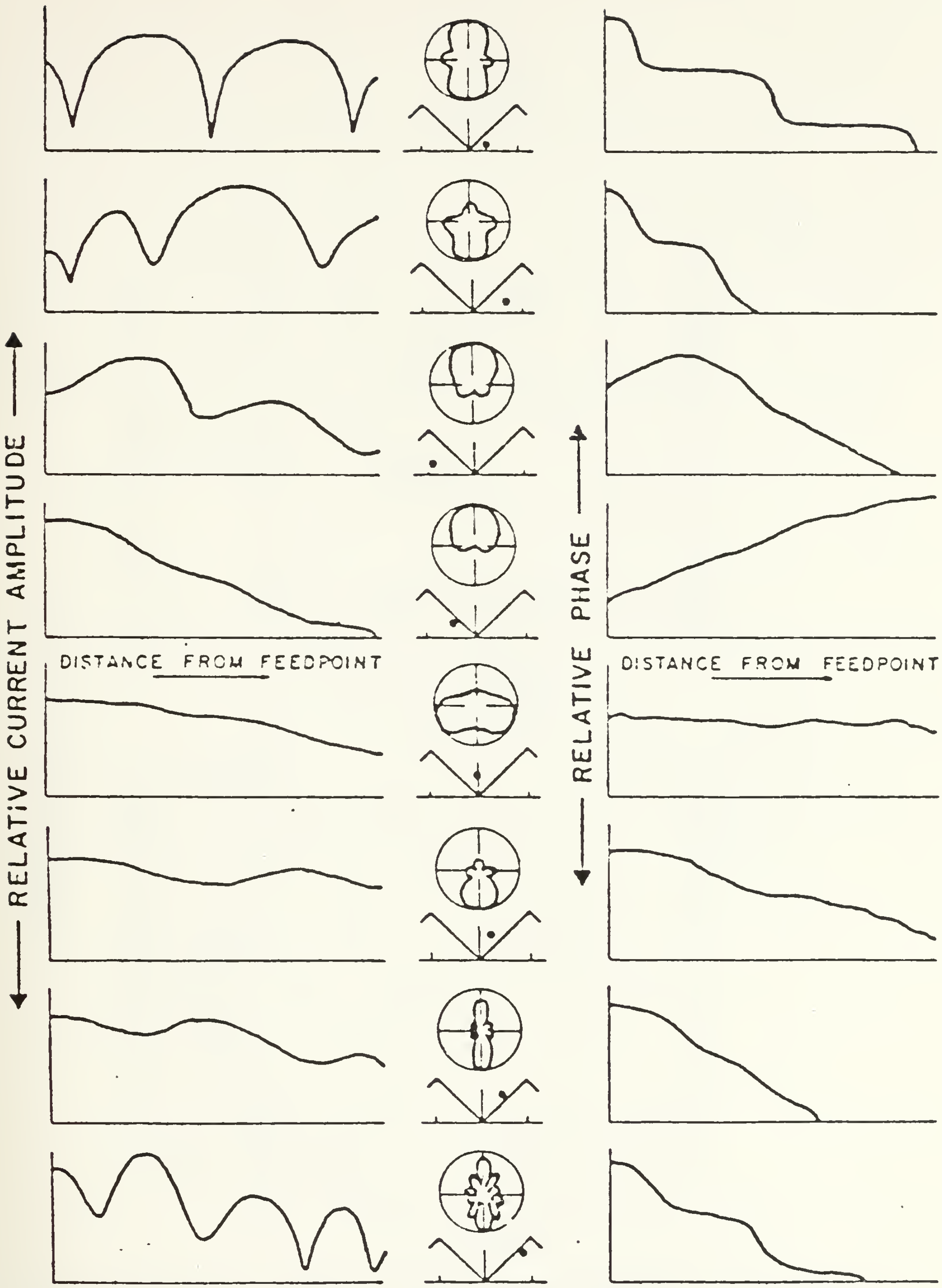


Figure 10. Amplitude and Phase Relationship for Various Areas of the Radiation Region

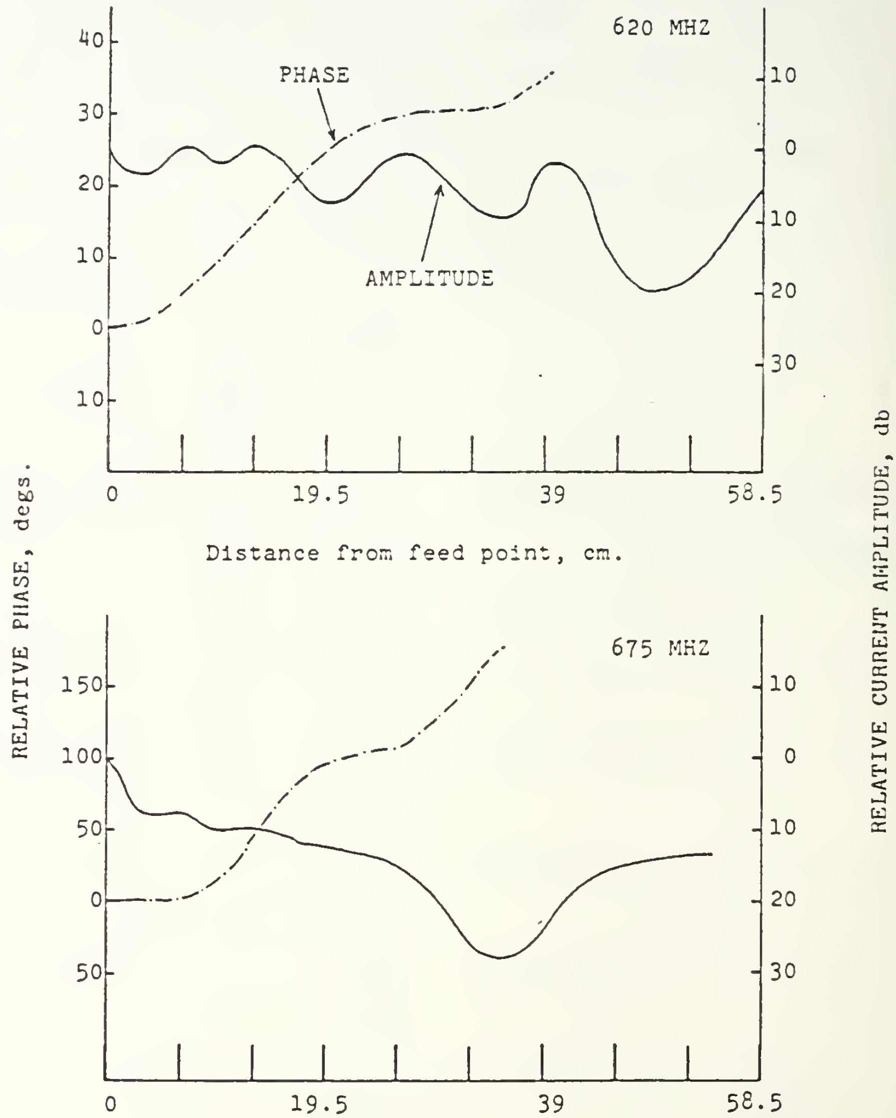


Figure 11. Current Amplitude and Phase in the Backward Wave Radiation Region for a Small Loop Array

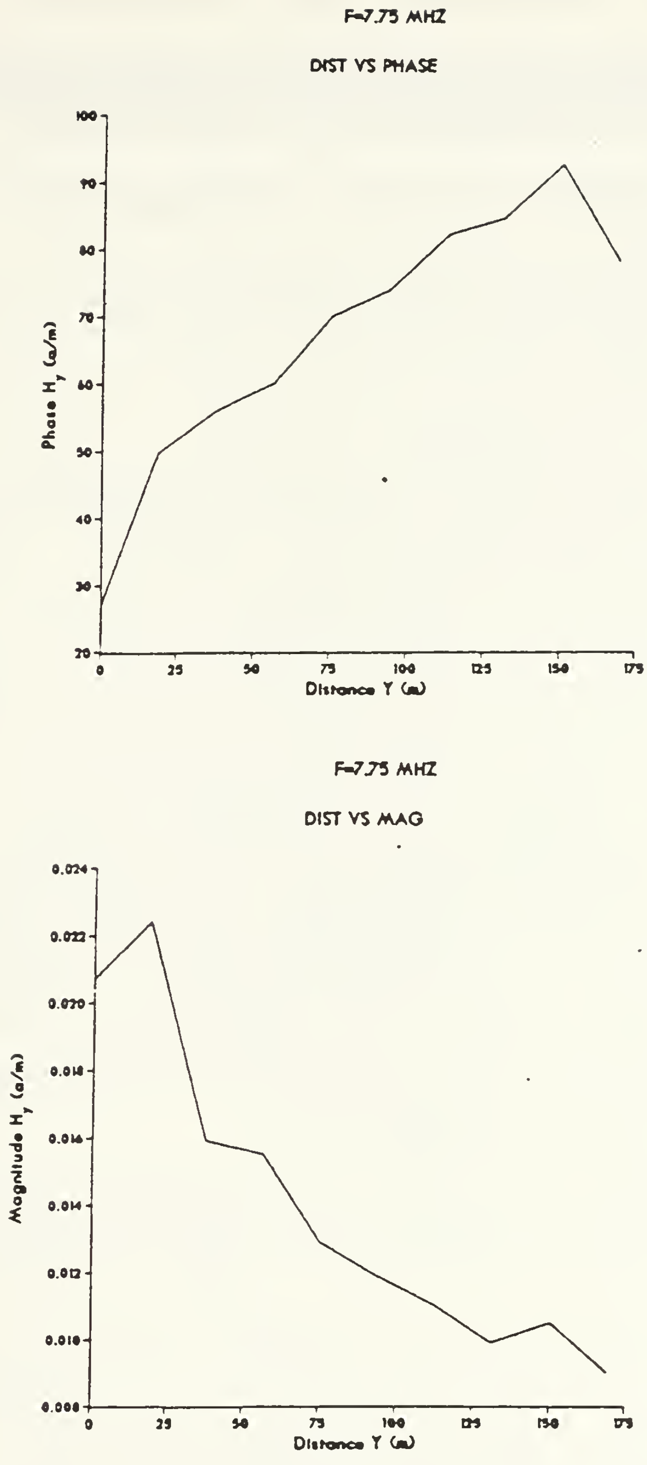


Figure 12. Current Amplitude and Phase in the Backward Wave Radiation Region of a Dipole Array

## II. THE SELECTED APPROACH FOR FURTHER INVESTIGATION OF THE LOG-PERIODIC HALF SQUARE ANTENNA

### A. THE TECHNIQUE OF UTILIZING A UNIFORMLY PERIODIC STRUCTURE

To provide more detailed information about the potential of the log-periodic dual feed half square antenna, the method proposed by Mayes, Deschamp, and Patton of investigating the near field properties of a uniformly periodic structure was selected as the starting point for research. Their proposed method suggested that a log-periodic structure could be interpreted to be a tapered or scaled version of a uniformly periodic array, and the near field properties of the uniform array could be analyzed over a frequency range to identify the necessary characteristics for a successful log-periodic structure. [Ref. 7] In independent research projects, Hudock and Tezmen utilized this approach to investigate the potential of monopole arrays and small loop arrays as log-periodic antennas. [Refs. 8, 9]

Utilizing this technique, a uniformly periodic half square array antenna (UHSA) with a dual feed could be analysied to determine if the characteristics of a log-periodic structure could be identified with a method similar to the one employed by Hudock and Tezmen. For the structure to be considered as having potential for development as a log-periodic antenna, the analysis should provide

information to demonstrate that the structure can support backward radiation, does not lend itself to large variations in electrical properties over the frequency range of interest, and creates sufficient current decay to eliminate end effects. The identification of the characteristic properties indicates that with proper scaling a log-periodic antenna can be developed.

## B. THE APPLICATION OF THE BRILLOUIN DIAGRAM TO THE NEAR FIELD INVESTIGATION

Backward wave radiation has been identified as a key characteristic to successful log-periodic antennas. The backward-travelling wave is created by the effective coupling of the forward-travelling wave on the transmission line and the space harmonics of the elements. To achieve this desireable condition, the feeder wave medium must produce a fast-wave along the structure to facilitate radiation. The determination of whether a wave is considered fast or slow is based on the relationship between the phase propagation constant of the wave on the structure, $\beta$, and the free space phase constant or wave number, k,

$$k = 2\pi/\lambda \ .$$

The comparison of the two phase constants determines the relative phase velocity of the feeder wave. A slow wave is defined to exsist when $\beta>k$ or equivalently when the

phase velocity of the feeder wave is travelling on the structure faster than the phase velocity of a wave radiating in free space, and conversely, a fast-wave is generated when $k>\beta$ condition exists.

The accepted method of analyzing the k to $\beta$ relationship is the Brillouin or k-$\beta$ diagram (Figure 13). Mittra and Jones discussed the significance of the k-$\beta$ diagrams in the analysis of log-periodic antenna designs in a paper published in 1956. [Ref. 10] In their analysis of the k-$\beta$ diagram, three distinct regions were defined based on performance characteristics observed on structures when a particular k-$\beta$ relationship existed. The regions defined are normally referred to as the propagation region, the complex region, and the radiation region. The propagation or P region is identified to exist in regions of the diagram where very little or no attenuation is observed on the feeder wave, and is normally found in the slow-wave areas. The complex or C region exists in the slow wave portion of the diagram where appreciable attenuation of the feeder wave is observed. The presence of the high level of attenuation in a slow wave area indicates the structure does not lend itself to the necessary coupling of energy to space which would facilitate radiation, but instead acts as a stopband filter region. The C region will not be present in the k-$\beta$ relationship for many structures, but will probably be present in structures that demonstrate

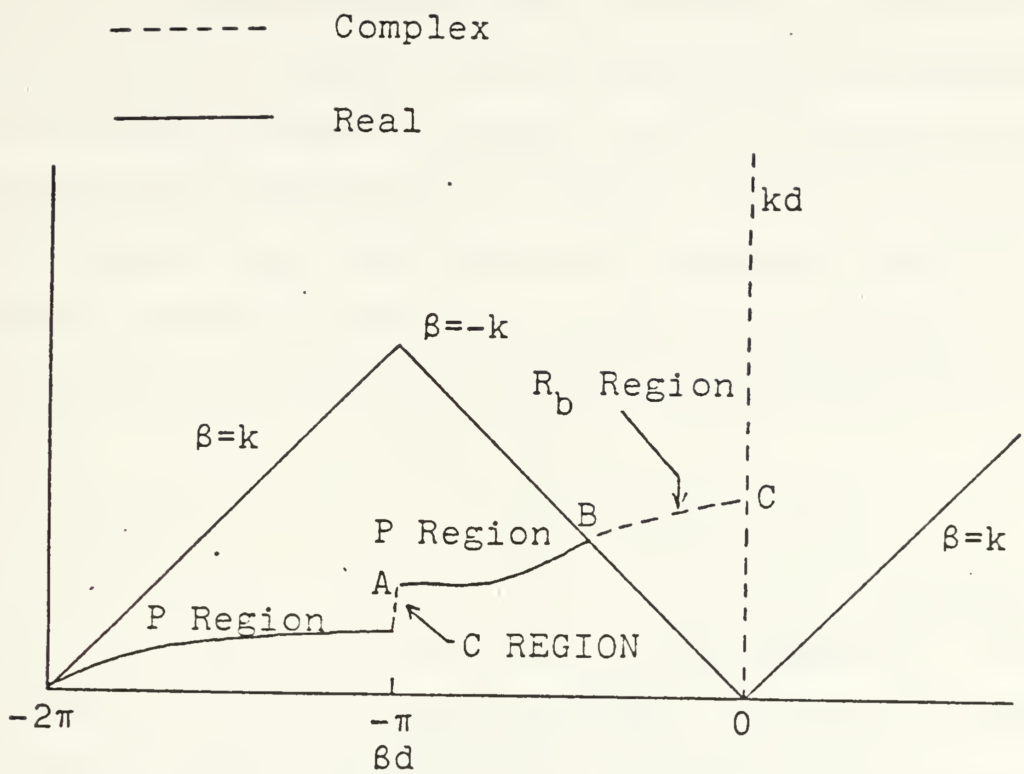


Figure 13. Brillouin Diagram

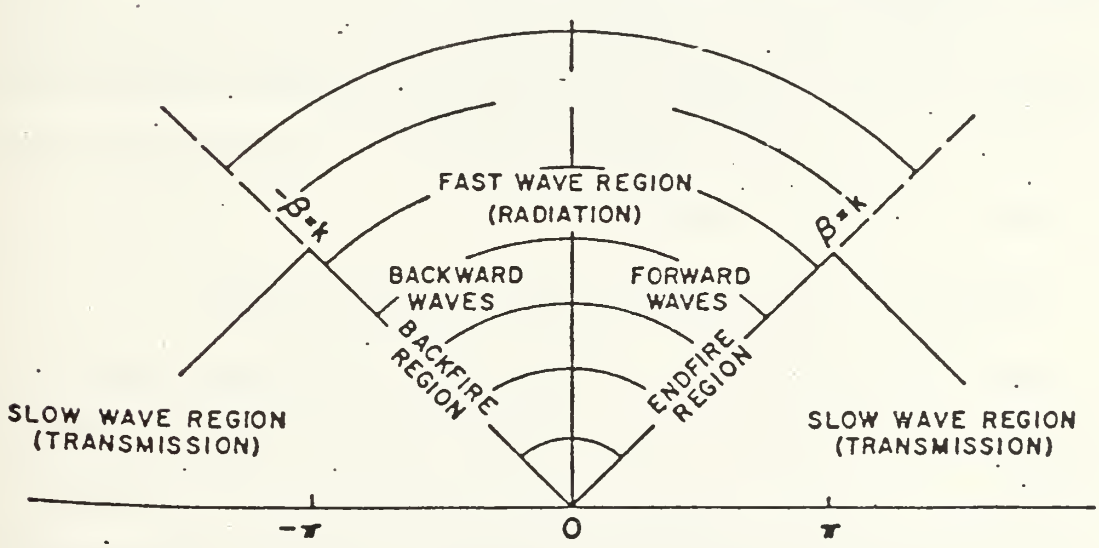


Figure 14. Radiation Region of a Brillouin Diagram

large variations in electrical performance. The radiation or R region is located in the fast-wave portion of the diagram and is characterized by a complex $\beta$ with a significant attenuation. The R region is normally sub-divided into a forward radiation region, $R_f$, located near the boundary, $k = \beta$, and a backward radiation region, $R_b$, located near the boundary $k = -\beta$ (Figure 14). The direction of propagation for the waves radiated under these conditions is given by

$$\theta = \cos^{-1} \frac{\beta}{k} \qquad \text{[Ref. 7]}$$

where $\theta$ is measured from the axis of the structure. In Hudock's study of a uniform monopole array, he closely examined the relationship between the subdivisions of the R region and the far field propagation patterns (Figure 15). The transition from backward radiation to forward radiation appears to occur gradually across the fast wave region with the most directional radiation patterns occuring close to the fast to slow boundary.

## C. TECHNIQUE FOR OBTAINING THE k-β RELATIONSHIP

The k-$\beta$ relationship for periodic structures can be obtained from either a theoretical approach which involves developing a characteristic function for $\beta$, or an experimental approach which investigates the near field properties of a periodic structure. The theoretical approach involving

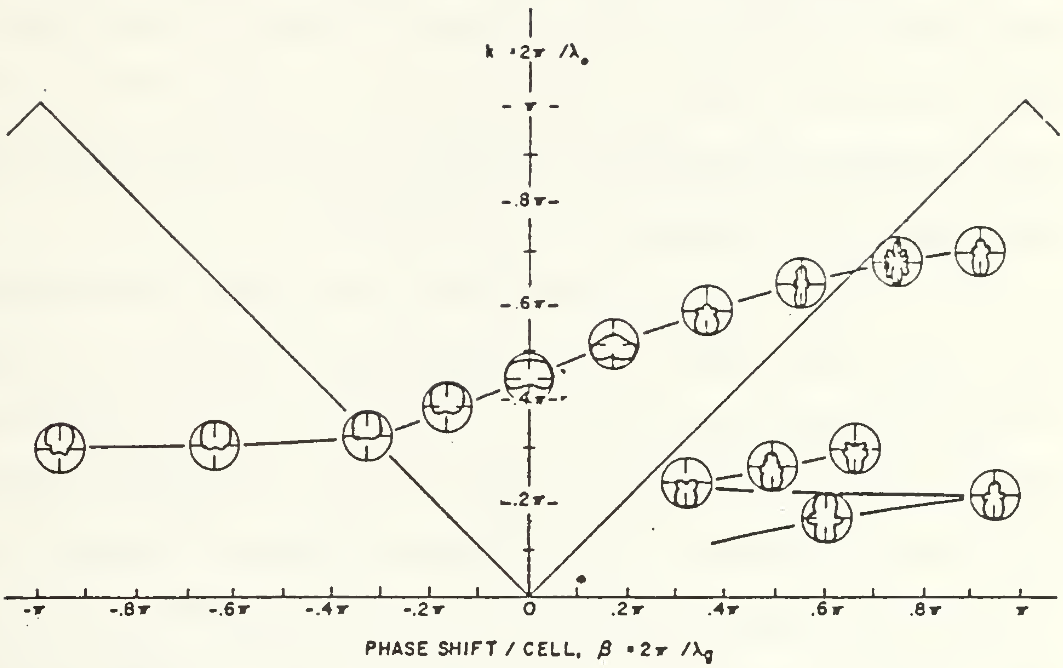


Figure 15. Hudock's Diagram Relating k-β Relationship to Far Field Radiation Patterns

a characteristic function in terms of $\beta$ is a very complex method which is developed in detail by Mittra. [Ref. 11] Due to the complexity of the analytical approach proposed by Mittra, the experimental approach was selected for the investigation of the k-$\beta$ properties of the uniform half square array antenna with a dual feed system. The experimental approach of investigating the near field characteristics has been previously employed on several structures, and has proven to be a fiarly simple and satisfactory method of obtaining the characteristics of a structure from which the phase relationship can be obtained.

The purpose of the experiment is to take measurements which will determine the propagation constant, $\beta$, present on the structure for different frequencies. To determine $\beta$, the amplitude and phase of the current along the transmission line must be measured from the near field of the structure to determine the properties of the feeder wave. In early experiments, a current loop was placed in the near magnetic field as a method of measuring field strength along the structure. Since the magnetic near field is proportional to the current along the conducting elements, the relative current phase and amplitude can be determined from the measurements.

In frequency regions located away from the resonant wavelengths, standing wave patterns will normally be observed for the current distribution along the transmission line of

the structure. The standing wave pattern lends itself to analysis of the structure as a simple transmission line; therefore, measuring the distance between nulls or minima points, d, determines the guide wavelength, $\lambda g$.

$$\lambda g = 2d$$

Knowing $\lambda g$, $\beta$ can be calculated from the measurement,

$$\beta = 2\pi / \lambda g = \pi / d$$

As the frequency approaches the resonant wavelength, the feed wave and current distribution demonstrate an attenuation in amplitude as it travels down the structure. The attenuation virtually eliminates the reflected wave and resulting standing wave pattern. The incident feeder wave appears as a travelling wave along the structure with a resultant phase to distance relationship. $\beta$ in this frequency is now dependent on the change in phase, $\Delta\phi$, with respect to distance, and is defined as the slope of the phase change with distance,

$$\beta \triangleq \frac{\Delta\phi}{\Delta d}$$

In earlier experiments performed by Hudock and Tezmen, measuring the phase change in the current with distance was based on the concept of comparison of a measured point to a reference point.

For this experiment, the measurements will be made in a similar manner to earlier experiments, but instead of constructing a prototype structure and employing a laboratory environment to measure the near field, the structure will be modeled on a computer using the Numerical Electromagnetics Code (NEC). Experimental data will be obtained from numerous simulation runs with controlled parameter variations to observe the calculated response of the structure. Utilizing the capabilities of NEC, a near magnetic field investigation can be conducted on the UHSA which will provide data that allows for the determination of $\beta$ in the manner employed in earlier experiments. The NEC code allows for an ideal analysis of the structure to be undertaken without imposing size limitations on the structure to facilitate laboratory use or introducing human error into the measurement of phase change.

## D. DESCRIPTION OF THE NUMERICAL ELECTROMAGNETICS CODE (NEC)

NEC can be simply described as a computer code designed to provide analysis of the electromagnetic response to metal structures. The code was developed as an upgraded version of the Antenna Modeling Program (AMP) at Lawrence Livermore Laboratory to obtain numerical solutions for integral equations which describe the current distribution on a

structure. [Ref. 12] By employing a method known as the method of moments, the code reduces integral equations of the form

$$\int I(Z')K(Z,Z')dZ' = -E^{i}(Z) \qquad \text{[Ref. 3]}$$

to a system of simultaneous linear algebraic equations developed in terms of the unknown current component, $I(Z')$. The method of moments approach to solving for current distributions eliminates the need to restrict the current distributions along the structure to simplifying assumptions allowing a larger number of antenna structures to be analyzed. The NEC code provides accurate solutions to the current distributions of a particular structure, and then utilizes the current values to evaluate structure impedances, radiation patterns, and near electric and magnetic fields. The NEC code installed on the Naval Postgraduate School mainframe employs single and double precision versions of the code to enhance accuracy of the calculations.

# III. EXPERIMENTAL CONSIDERATIONS AND PROCEDURE

## A. ESTABLISHING AN EXPERIMENTAL STARTING POINT

The purpose of the experimental portion of the research was to provide additional information about the characteristic performance of the log-periodic half square antenna with dual feed. In order to provide this information, research was conducted into two areas of interest. The first and primary area of experimental research was an investigation into the near magnetic field of a uniformly periodic half square array antenna (UHSA) with a dual feed system to establish the k-$\beta$ relationship for the structure. The second portion of the experiment was the evaluation of the far field radiation patterns of the single element antenna, and the uniform array of half square elements.

### 1. Determining the Size of the Uniform Array of Half Square Elements

Since the method selected to analyze performance was based on the experimental evaluation of a uniform array, the size of the array structure had to be established both in terms of element lengths and element spacing. The utilization of NEC removes laboratory restrictions on construction size of the antenna; therefore, considering the fact that the antenna is being designed for military high frequency communications, the frequency range of operation will be 2

to 30 MHz. A mid range frequency of 8 MHz was selected for the resonant wavelength of construction as it represents a midpoint frequency two octaves above the low frequency and approximately two octaves below the high frequency of operation. The uniform spacing between elements was selected arbitrarily to be a half wavelength at the resonant frequency. The selection of spacing was considered arbitrary as the spacing of elements can be considered to be a function of the input frequency; consequently, changing the frequency at the input is the same as varying the element spacing at a constant frequency. The radius of the wire was established for the model as .000814 meters based on the prototype construction which utilized number 14 gauge wire. The use of a 10 element array was an arbitrary selection, but made with the consideration that the array should be at least one wavelength long for the lowest frequency of interest. The experimental structure is shown in Figure 16. For modeling purposes, the insulator placed at the midpoint of the horizontal wire on the prototype was replaced by an open circuit on the model to act as an ideal insulator.

2. <u>Determination of a Transmission Line for the Model</u>

In the initial design and construction of a prototype antenna for testing, a 300 ohm open wire transmission line was utilized. From the results of the initial test, an impedance value of 300 ohms was accepted as a valid starting value for the impedance of the transmission line in

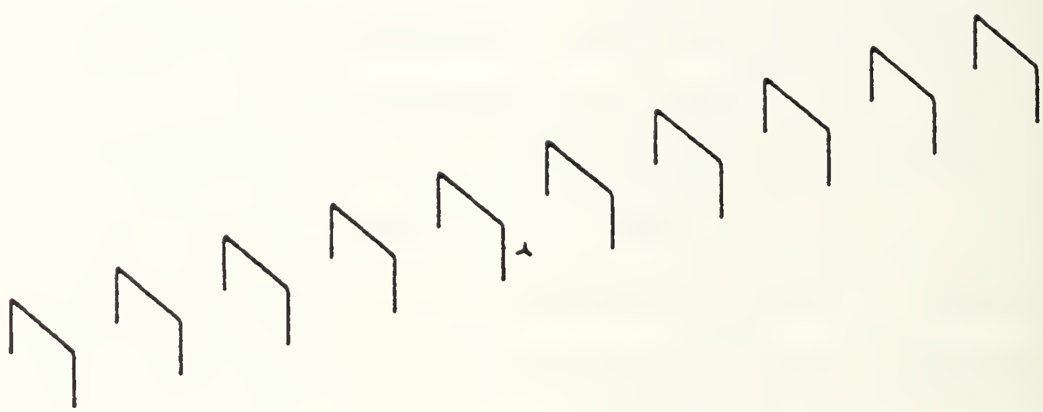

Figure 16. Uniformly Periodic Half Square Array Antenna Model

the NEC model. NEC allows transmission lines to be modeled either as implicit transmission line equations for balanced structures or explicitly as wires on the structure. The use of implicit transmission line equations allows the code to treat the transmission lines as two port networks using the defining parameters of characteristic impedence and length to calculate their response characteristics. Implicit transmission lines create a more general model of the structure, and reduce the number of wire segments in the model consequently, the size of the matrix necessary to evaluate currents is reduced for equivalent structures. In explicit transmission line models, the transmission line is represented as open wires on the structure with an impedance value determined by the spacing and the redius of the wire input into the model geometry. The explicit transmission line provides for more accurate modeling and the ability to model unbalanced structures; however, the addition of extra wires increases the size of the matrix required to calculate the current values. The larger matrix created by the addition of wires results in a longer run time for the code, and if the matrix is expanded beyond the size limitation of the code, steps must be taken to reduce the total number of current segments on the structure. The number of current segments may be reduced by reducing the size of the structure or eliminating the number of current segments by increasing the size of segments on each wire.

These alternatives may not produce desireable or accurate modeling results for the structure.

Since the half square may not be a well balanced structure, an evaluation of the two methods was conducted to insure that modeling accuracy is not compromised for computer costs and modeling simplifications, or that complex models do not waste computer assets unnecessarily when an accurate model can be achieved with the use of implicit transmission lines. The evaluation process consisted of a two part analysis. The first step of the analysis was to construct a 300 ohm two wire transmission line model using NEC. The second part of the analysis was to evaluate the antenna utilizing an implicit transmission line and an identical antenna utilizing an explicit transmission line.

The two wire transmission line equation for the characteristic impedance, $Z_o$, under an assumed low loss condition is

$$Z_o \simeq 120 \ln \left(\frac{D}{a}\right). \qquad \text{[Ref. 13]}$$

The wire separation distance, D, can be determined knowing the radius, a, of the wire used in the construction. For this model, the wire radius was established as .000814 meter, number 14 gauge wire, and D determined to be approximately .01 meters. A model of a two wire transmission line was constructed using the calculated values with NEC, and was

evaluated to determine $Z_o$. To find $Z_o$, one wavelength (1λ) and 3/8λ lengths of transmission line were evaluated under open and short circuit conditions with double precision NEC to provide impedance values for the structure. Using the NEC calculated values for the open circuit impedance $Z_{OC}$, and the short circuit impedance $Z_{SC}$, $Z_o$ was calculated by

$$Z_o = \sqrt{Z_{OC} Z_{SC}} \; .$$

The separation of .01 meters produced a NEC modeled transmission line with a characteristic impedance of approximately 356 ohms. To verify this technique of obtaining $Z_o$, a second technique of loading a 1λ length of transmission line with a load impedance, $Z_L$, equal to $Z_o$ was utilized. In the second technique, the currents calculated along the structure by NEC were analyzed for maximum and minimum magnitude points to establish a standing wave ration (SWR)

$$SWR = \frac{V_{MAX}}{V_{MIN}} = \frac{I_{MAX}}{I_{MIN}} \; . \qquad \text{[Ref. 13]}$$

Knowing that a matched load does not produce a reflection coefficient and results in a SWR of 1, the accuracy of the $Z_o$ could be verified for the structure. In this first run, the SWR was calculated to be 1.07 which demonstrated that the two techniques closely agreed and could be utilized to determine $Z_o$ for a modeled transmission line.

The model analysis showed that a separation of .01 meters was too large to provide a 300 ohm impedance. Utilizing an iterative procedure of varying the spacing value, D, and experimentally evaluating the new structure for characteristic impedance, a value of D equal to .0076 meters was determined to provide the closest approximation to a $Z_o$ of 300 ohms in a NEC modeled explicit transmission line.

In the second part of the analysis, a 2 element uniform dipole array antenna and a 2 element uniform half square array antenna were selected for testing performance variations between implicit and explicit transmission line models. The dipole array was selected to be a control for the experimental evaluation since the conventional dipole structure is balanced and commonly modeled with the implicit transmission line. By evaluating the dipole antenna with the two transmission line models (Figures 17 and 18), a comparison standard was achieved for current distributions and far field radiation patterns (Figures 19 and 20) for the different models which could be applied to the half square antenna. The performance comparison of the dipole antenna showed a maximum current value deviation of 6.5%, nearly identical radiation patterns, and a difference in maximum gain of .24 dB. The half square antenna (Figures 21 and 22) demonstrated a current magnitude deviation from 4 to 12%, very similar radiation patterns (Figures 23 and 24), and a

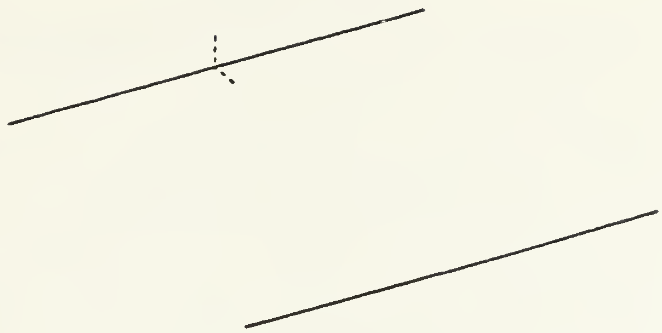

Figure 17. Dipole Antenna Implicit Transmission Line Model

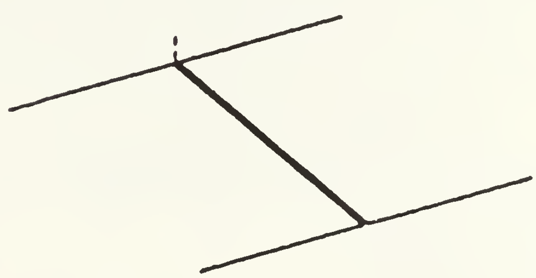

Figure 18. Dipole Antenna Explicit Transmission Line Model

IMPLICIT TRANSMISSION LINE

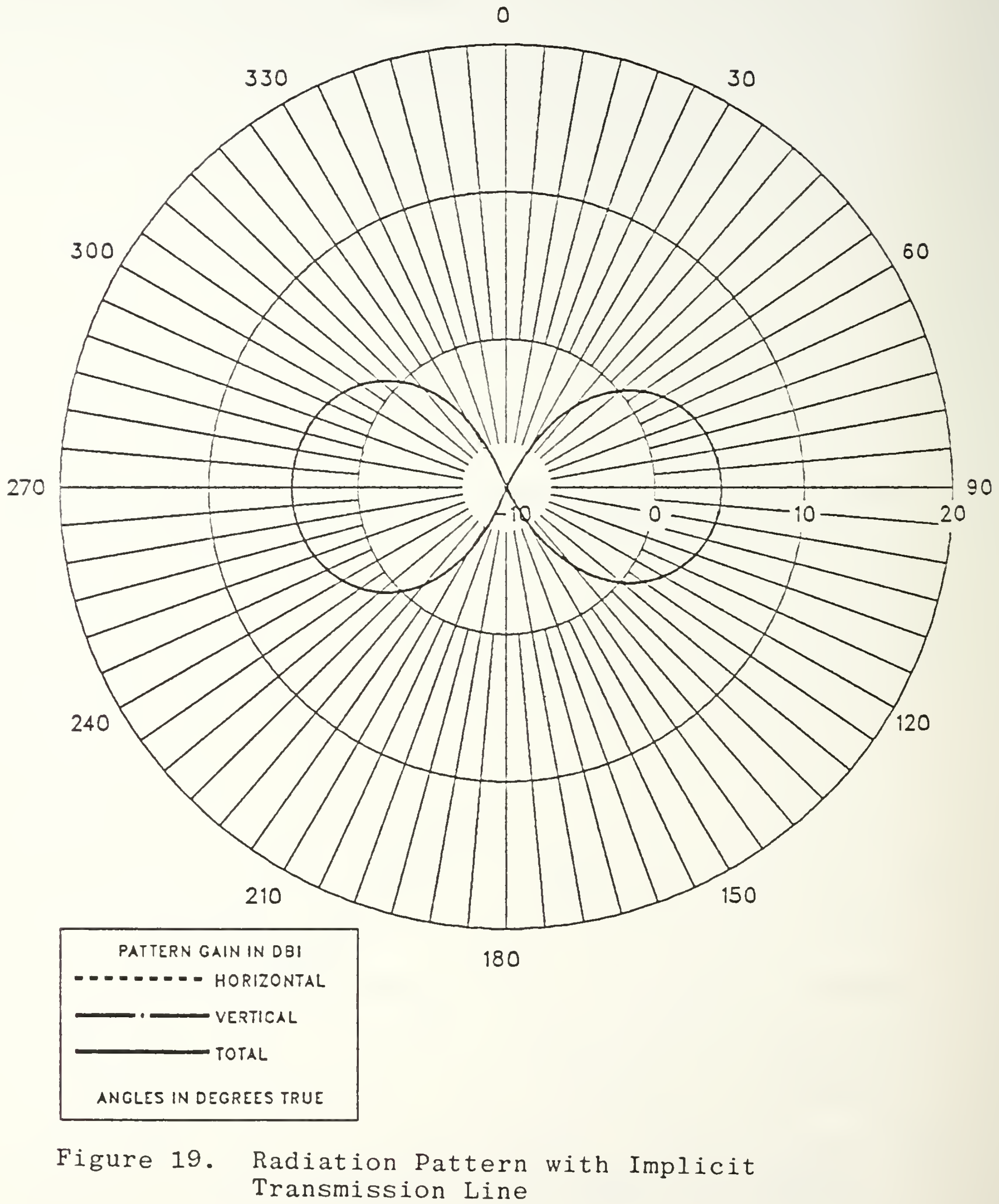


Figure 19. Radiation Pattern with Implicit Transmission Line

## OPEN 2 WIRE TRANSMISSION LINE

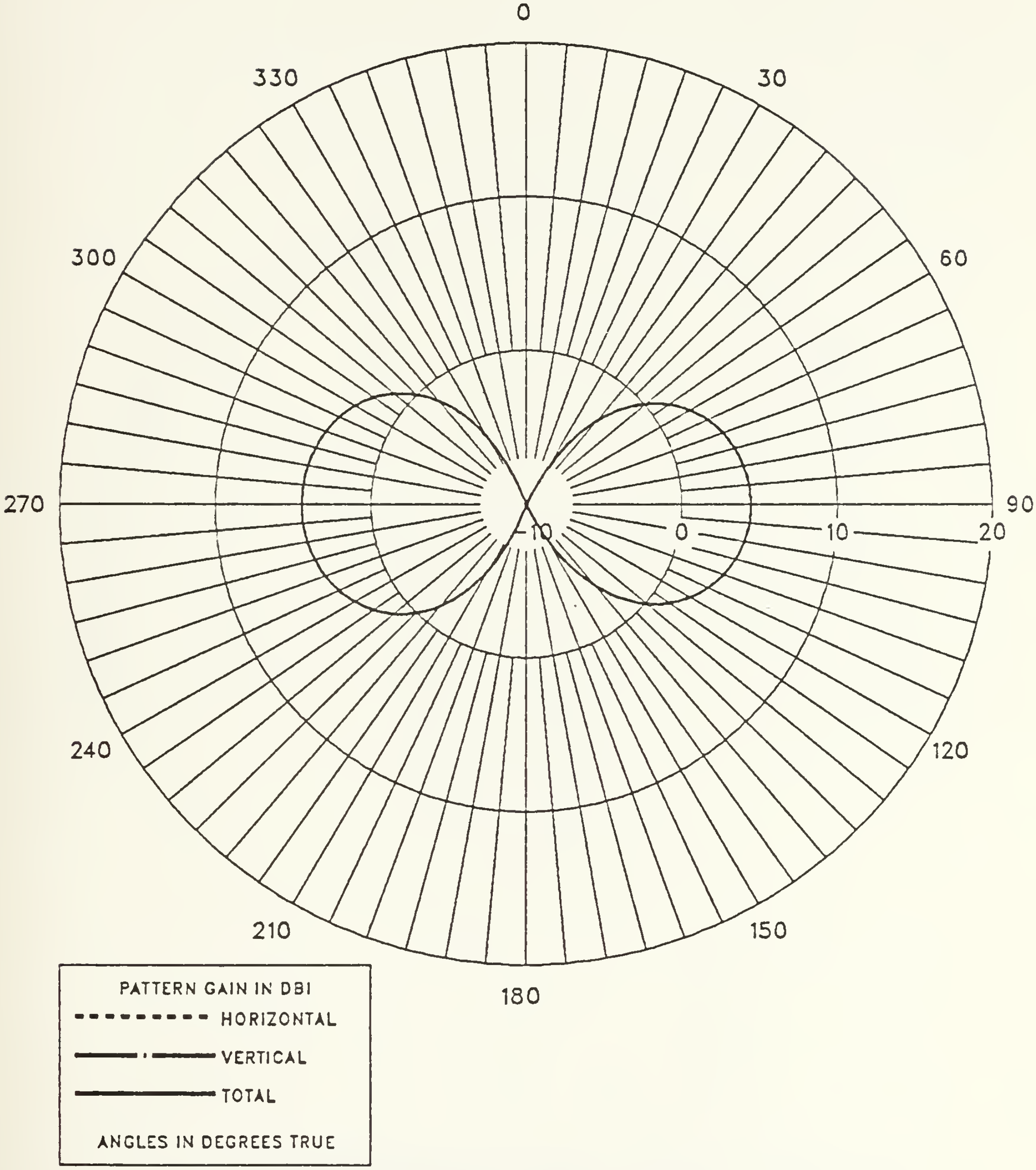


Figure 20. Radiation Pattern with Explicit Transmission Line

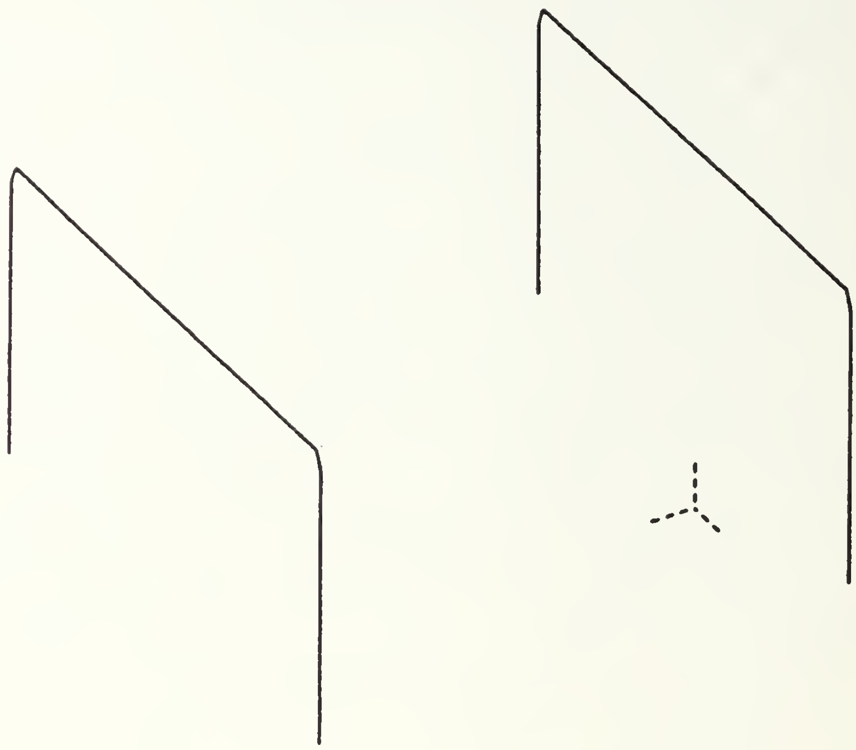

Figure 21. Half Square Antenna with Implicit Transmission Line

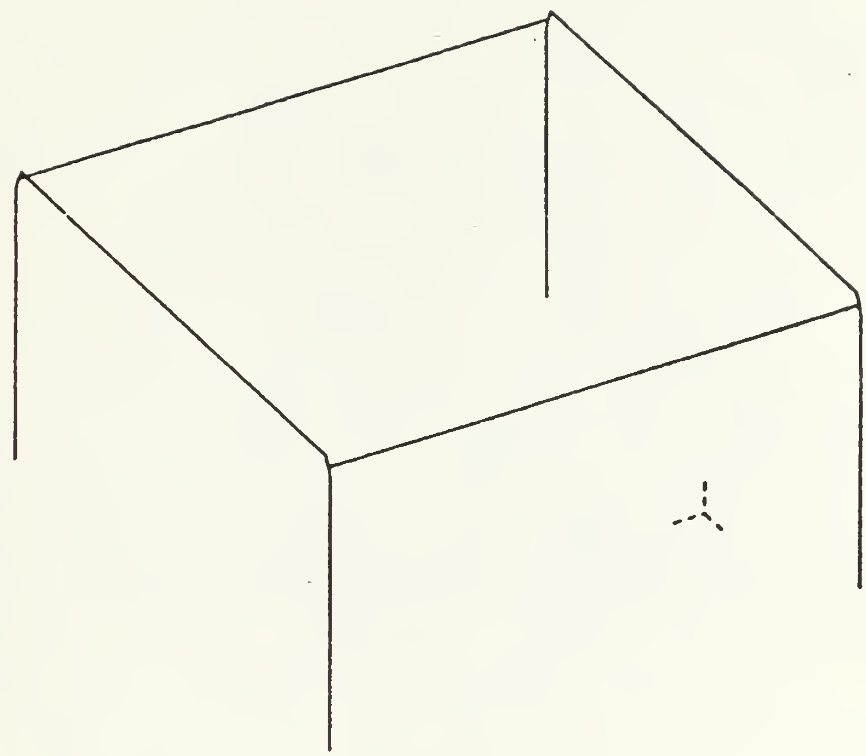

Figure 22. Half Square Antenna with Explicit Transmission Line

IMPLICIT TRANSMISSION LINE

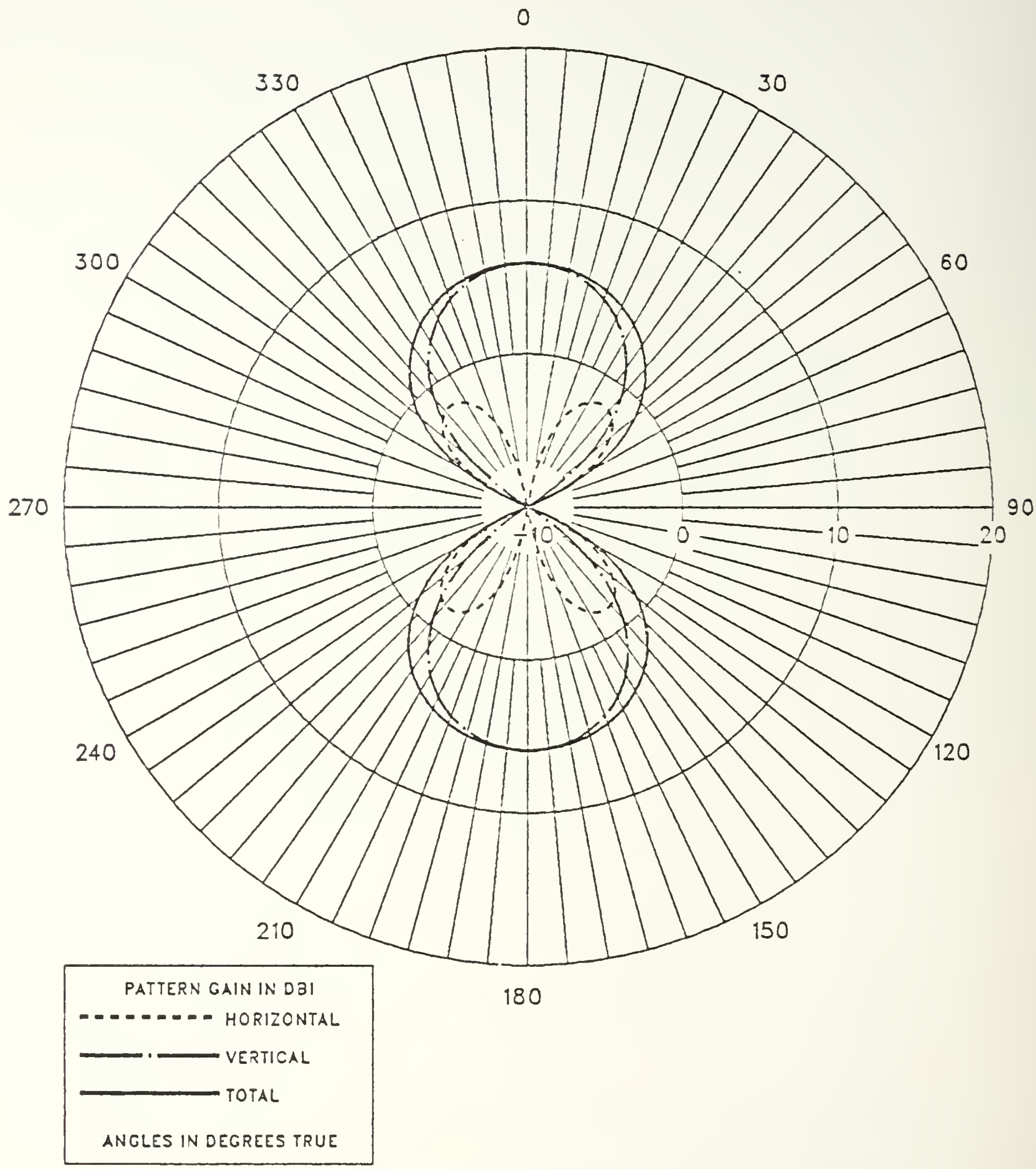


Figure 23. Radiation Pattern Half Square with Implicit Transmission Line

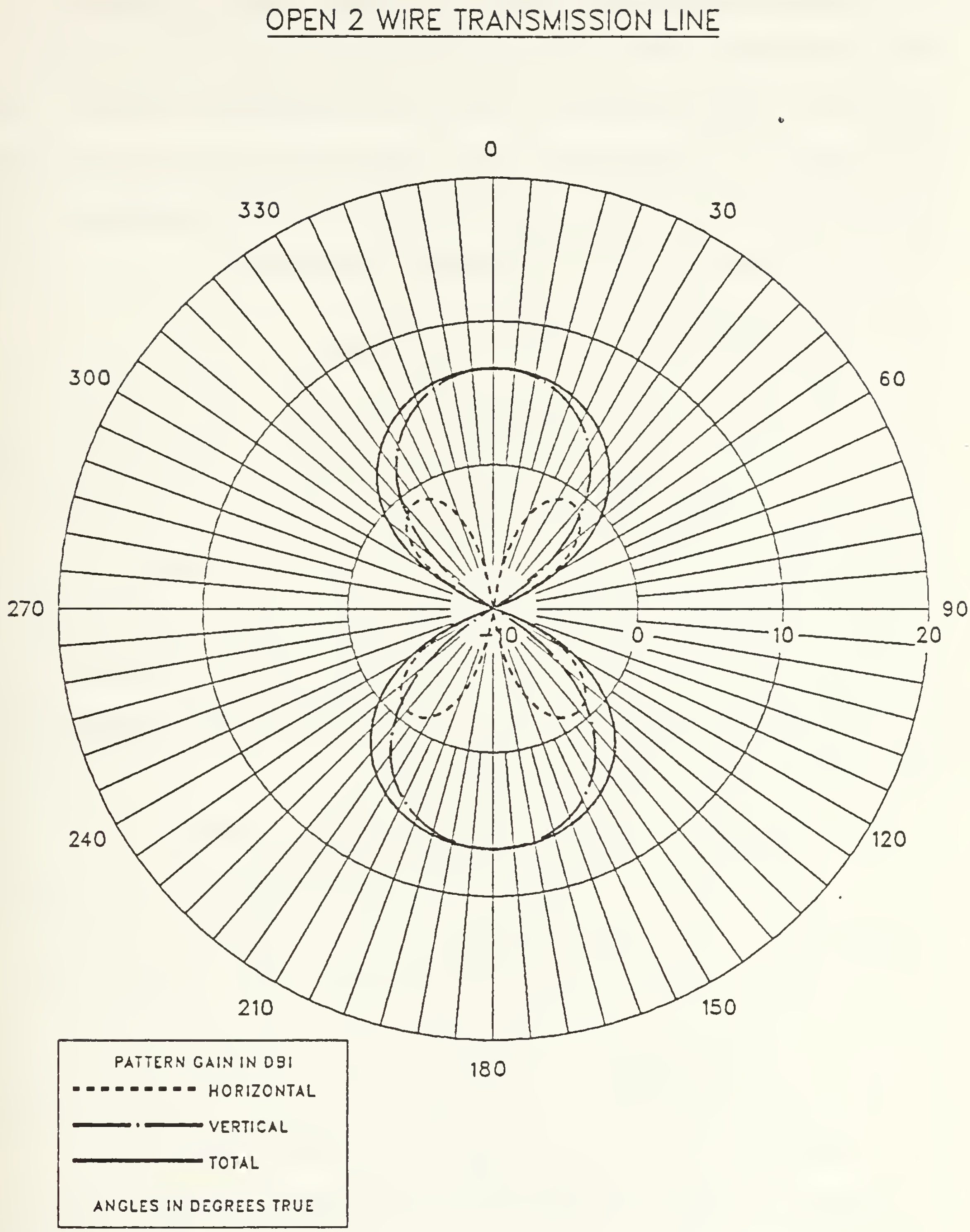


Figure 24. Radiation Pattern Half Square with Explicit Transmission Line

difference in maximum gain of .36 dB. From the analysis, the conclusion was drawn that the dual feed system allows the half square antenna to act as a balanced structure, and the implicit transmission line model will provide performance characteristics which will allow for valid experimental data to be obtained on the half square structure.

## B. OBTAINING DATA FOR THE k-$\beta$ DIAGRAM

The uniform half square array antenna with a dual feed system can be interpreted to be two quarter square antennas connected together by an insulated connector on the horizontal wires. To gain insight into the performance characteristics of the desired antenna, the decision was made to start the analysis in parts by first looking at the near field characteristics of the quarter square structure, and then the half square structure.

### 1. Uniformly Periodic Quarter Square Array

The quarter square antenna was modeled with identical dimensions to the half square, but the reflection (or the half of the structure which is produced by mirroring the structure across the X-Z plane) of the structure was eliminated (Figure 25). By eliminating the reflection and the second feed line, the physical properties of the structure's vertical and horizontal wires could be observed without the effects of coupling between sides of the antenna and the excitation of the second feed. Utilizing

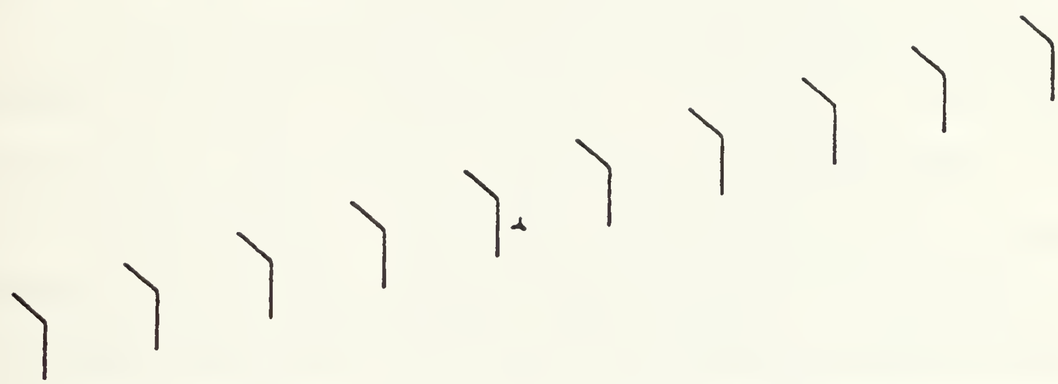

Figure 25. Uniformly Periodic Quarter Square Array Antenna

the capability of NEC to calculate the near magnetic field, near magnetic field data for the quarter square antenna was colle-ted for analysis by controlled parameter variation. Following the experimental procedures of Hudock and Tezmen, the input frequency was stepped through the range of interest for a given set of experimental conditions while collecting near field measurements for each frequency applied to the input of the antenna. The NEC code utilized to obtain this information was instructed to make near magnetic field calculations along the transmission line at points where the horizontal and vertical wires were connected to the line. The first set of conditions looked at the structure with a crossed transmission line in free space. In the second set, the effect of ground was investigated by applying the limiting condition of perfect ground under the structure. The final variation observed with the quarter square array was the effect of a straight transmission line in free space.

2. Uniformly Periodic Half Square Array

After testing the performance of the quarter square array, the uniformly periodic half square array was evaluated utilizing the same NEC procedure to accummulate near magnetic field data. For the half square array with dual feed, sets of near magnetic field data were collected for the following conditions:

1. Crossed transmission lines with in-phase feed voltages in free space.
2. Crossed transmission lines with in-phase feed voltages over perfect ground.
3. Crossed transmission lines with anti-phase feed voltages in free space.
4. Crossed transmission lines with anti-phase feed voltages over perfect ground.

## C. FAR FIELD RADIATION PATTERNS

The second portion of the experimental research was an evaluation of the far field patterns. This portion of the experiment first looked at the radiation patterns of the half square antenna with dual feed as one element of the array, and the effects of in-phase and anti-phase feed voltage sources had on the element pattern over the frequency range. Next, the far field radiation patterns were calculated for the uniform half square array over the frequencies identified as being in the radiation region of the k-$\beta$ diagrams for in-phase and anti-phase voltage sources. The far field patterns were calculated by the NEC code utilizing the structure models created for the near field investigation.

# IV. EXPERIMENTAL RESULTS

## A. NEAR MAGNETIC FIELD INVESTIGATION

A plotting program was used to assist in the analysis of the near field data collected. By plotting the magnitude and phase relationship of the near magnetic field, characteristic regions could be identified for more in depth investigation and the necessary technique for calculating the propagation constant, $\beta$, could be determined. $\beta$ was calculated for the various frequencies from the numerical values provided by NEC using the relationships defined by Mittra and utilized by Hudock and Tezmen. Along with the calculation of $\beta$, the attenuation of the field over the structure was calculated by a normalized ratio of the magnitude values. The calculated data for $\beta$ and attenuation was then plotted in a Brillouin diagram to allow for an analysis of the structures properties and potential for development as a log-periodic antenna to be evaluated.

### 1. Uniformly Periodic Quarter Square Array

In analyzing the data for the three sets of conditions applied to a quarter square array (Appendixes A, B, and C), similar responses were observed for the switched transmission line in free space and perfect ground while the unswitched transmission line demonstrated

a radically different response. The similarity of the responses over the extreme ground parameters can be observed in the magnitude and phase of the calculated near field and in the k-$\beta$ diagram (Figures 26 and 27). The switched transmission line structure demonstrated properties conducive to backward radiation in the frequency region of 6.1 to 7.9 MHz, and the k-$\beta$ diagram pictorially shows that the propagation region is immediately followed by a backward radiation region. The unswitched transmission line displayed very different responses over the frequency range as summarized by the k-$\beta$ diagram for the unswitched transmission line structure (Figures 28 and 29). The k-$\beta$ diagram shows a propagation region followed by a complex region. The presence of the complex region demonstrates that the unswitched transmission line created a condition which did not facilitate the coupling of energy into space; consequently, the complex region identifies the structure as an ineffective radiator.

From the experimental data, three conclusions can be drawn. First, the switched transmission line is an ineffective radiator; therefore, the structure with the unswitched feed system will not have the potential to become a successful log-periodic antenna. Secondly, ground parameters appear to have very little effect on the near field response of a quarter square structure with a switched transmission line. Finally, the near field characteristics

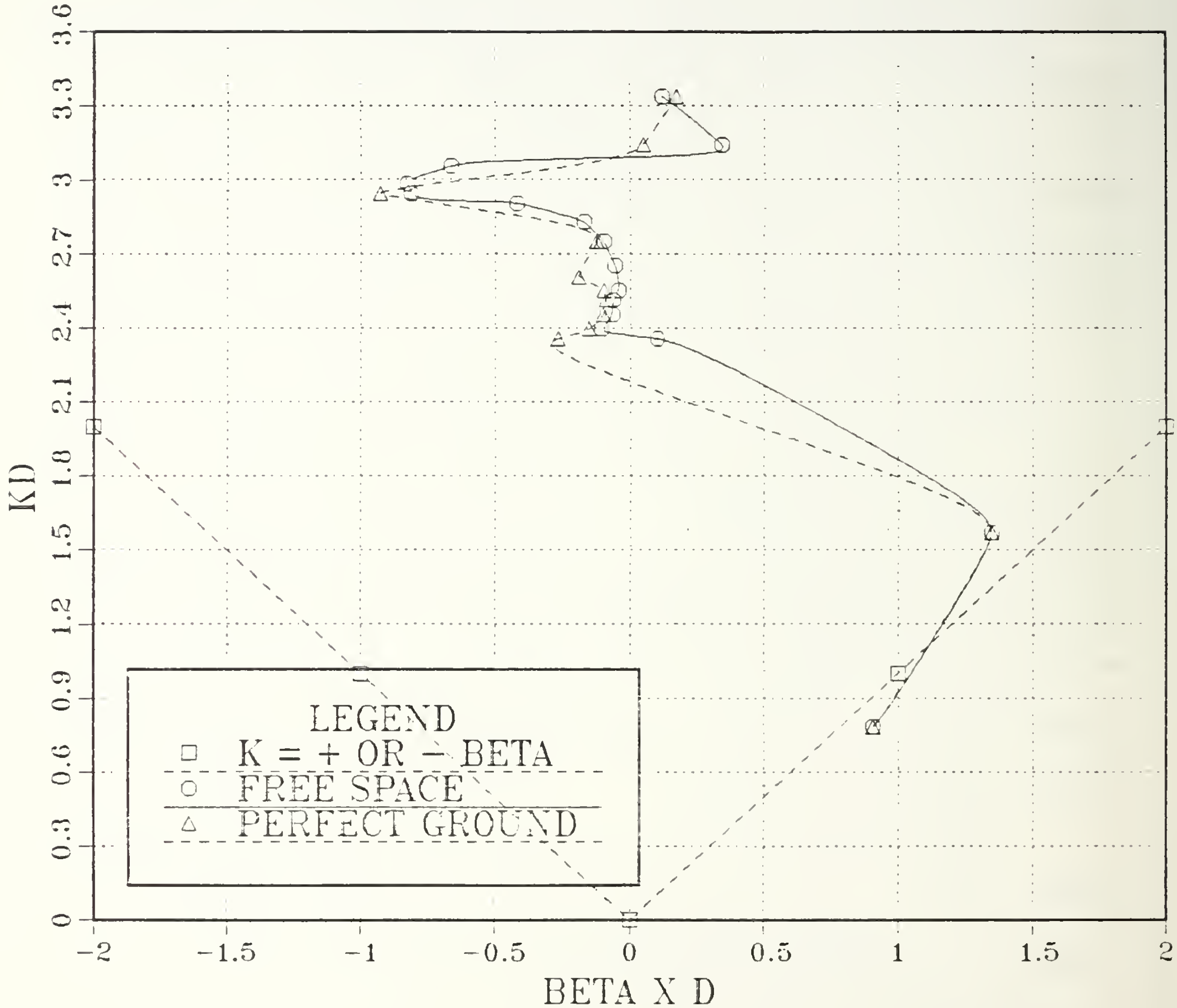


Figure 26. k-$\beta$ Relationship for a Quarter Square Array with a Switched Transmission Line

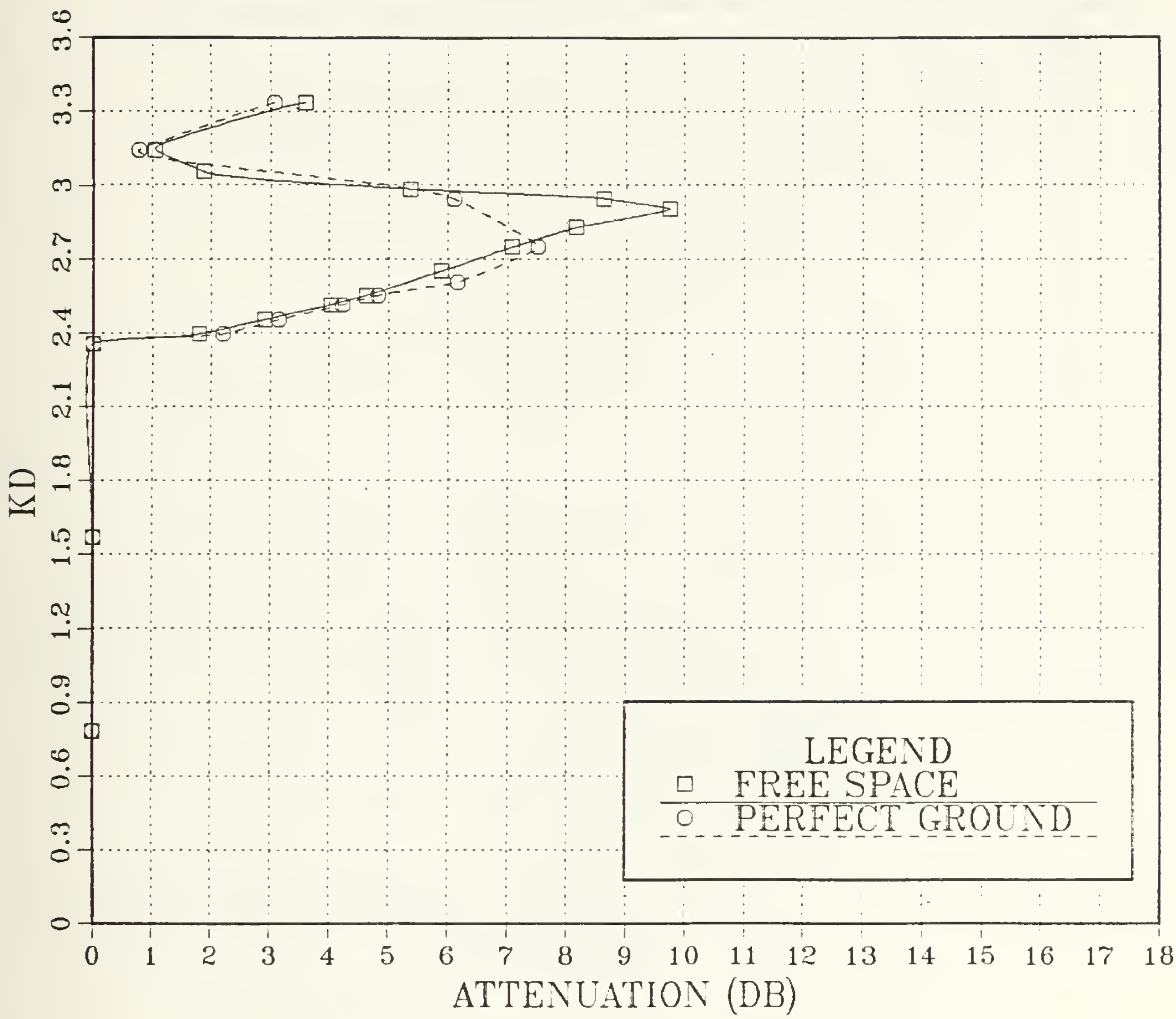


Figure 27. The Observed Attenuation on the Quarter Square Array with a Switched Transmission Line

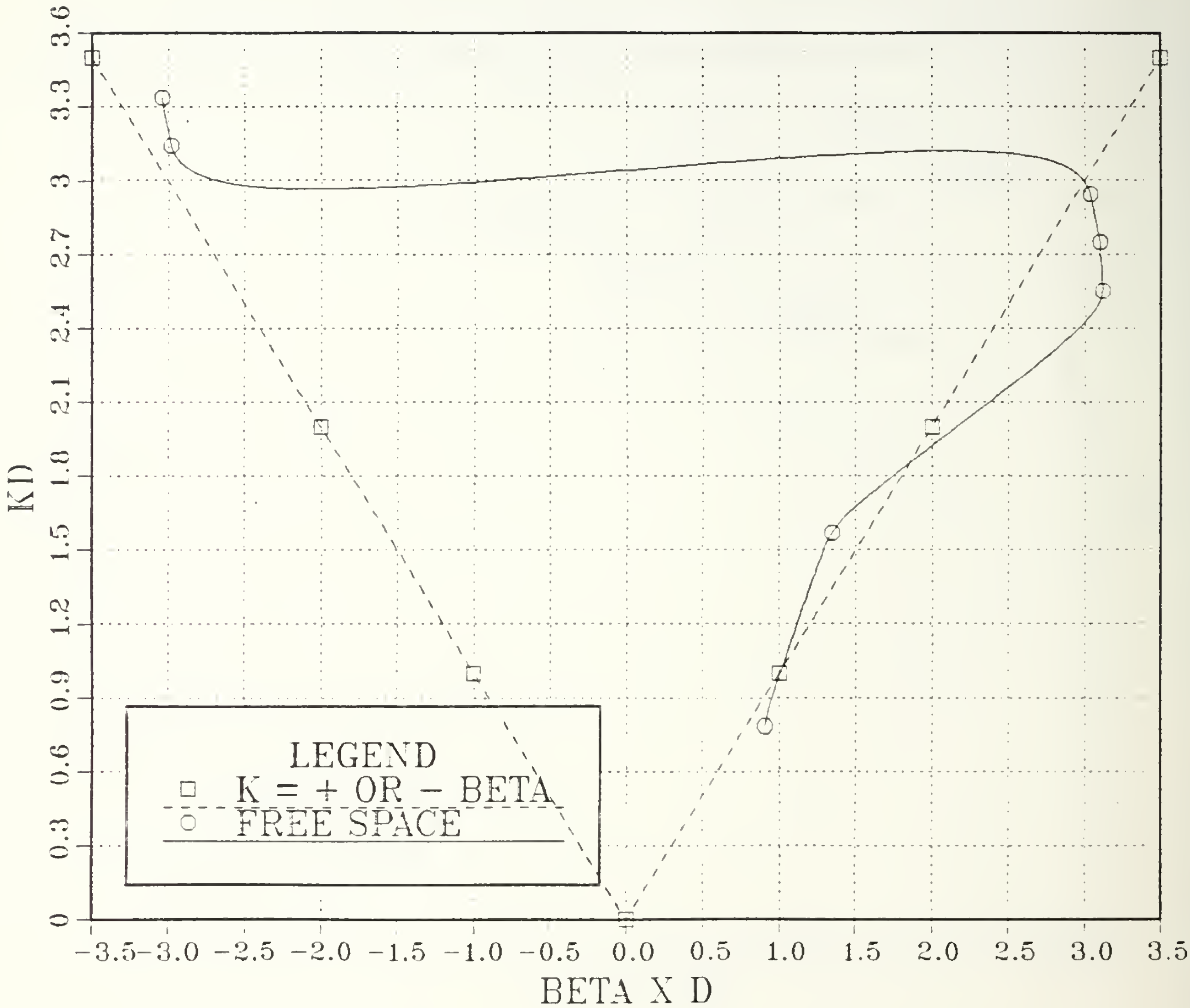


Figure 28. k-β Relationship for a Quarter Square Array with a Unswitched or Straight Transmission Line

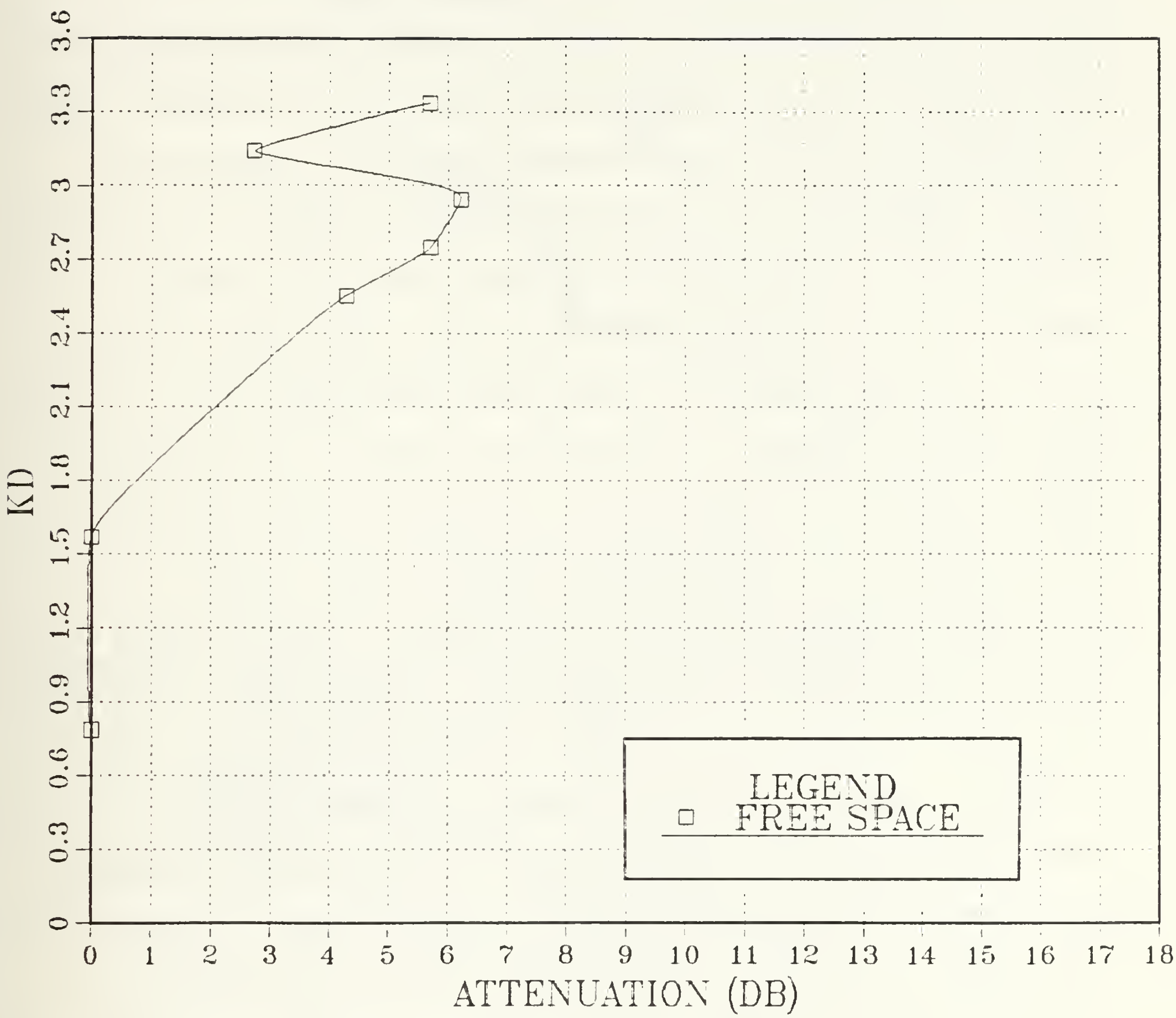


Figure 29. The Observed Attenuation on a Quarter Square with a Unswitched or Straight Transmission Line

demonstrated by the switched transmission line structure show potential for the structure as a log-periodic antenna and warrant further investigation.

2. <u>Uniformly Periodic Half Square Array</u>

The near magnetic field investigation continued with the analysis of the uniform half square array antenna. The analysis of the half square array data again showed very similar results for the limiting ground parameters evaluated for both the in-phase and anti-phase excitation modes; therefore, to alleviate repetition, the experimental results for the in-phase and anti-phase modes are shown only for the free space condition in Appendixes D and E. The in-phase mode of excitation produced the expected results that the half square array would produce similar near field performance characteristics to the quarter square array. The k-$\beta$ diagram for the in-phase half square array (Figures 30 and 31) identifies a backward radiation region in the frequency range of 6.25 to 7.9 MHz, the same frequency region as the quarter square array. The anti-phase excitation condition produced a very unexpected result in that the region of backward radiation occurred in a frequency range of 3.5 to 4.0 MHz. The k-$\beta$ diagram for the anti-phase mode (Figures 32 and 33) graphically depicts a propagation region followed by this small region of backward radiation.

The near field investigation of the uniformly periodic half square array showed that the structure will

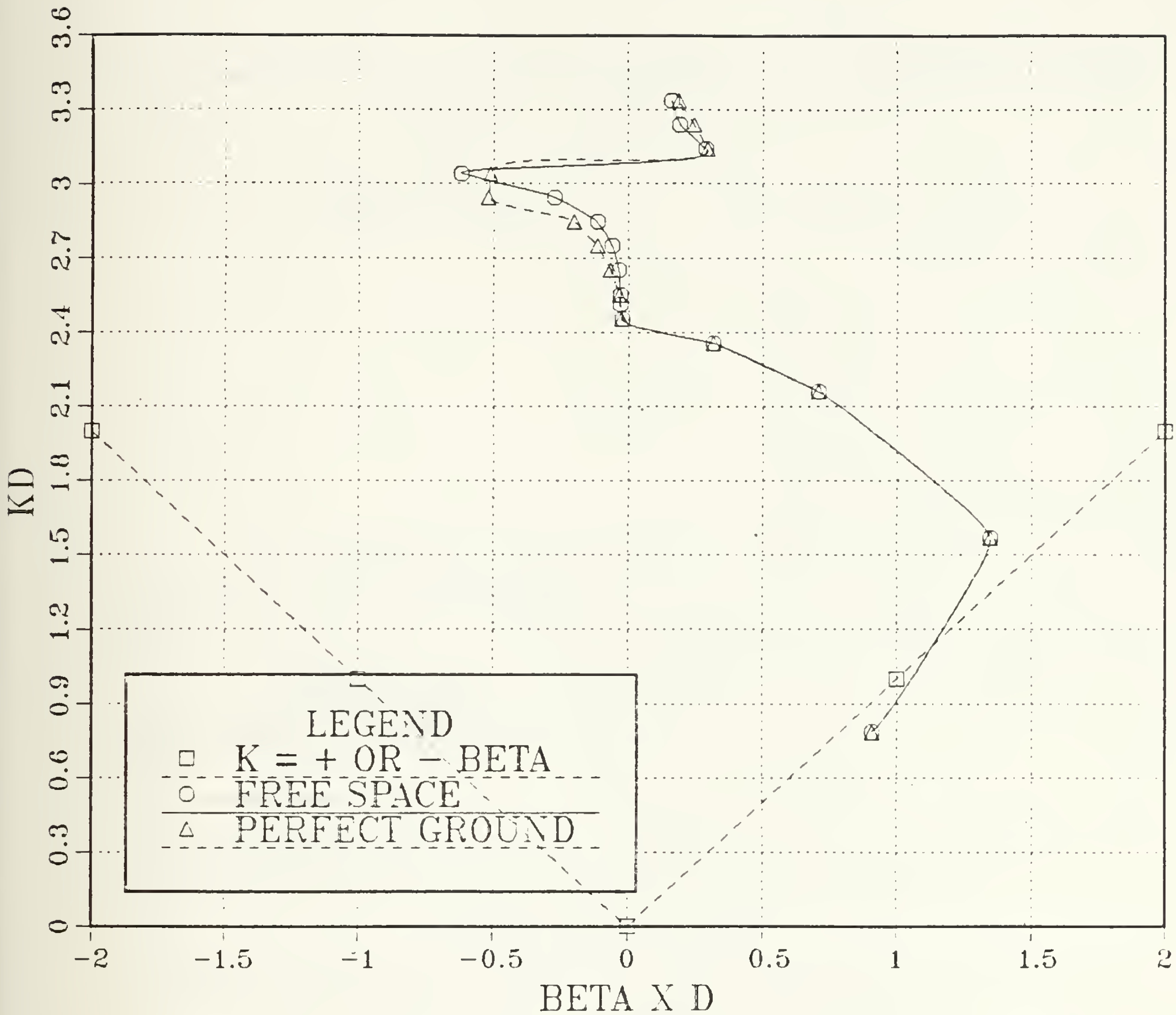


Figure 30. k-$\beta$ Relationship of a Half Square Array with In-Phase Feed Sources

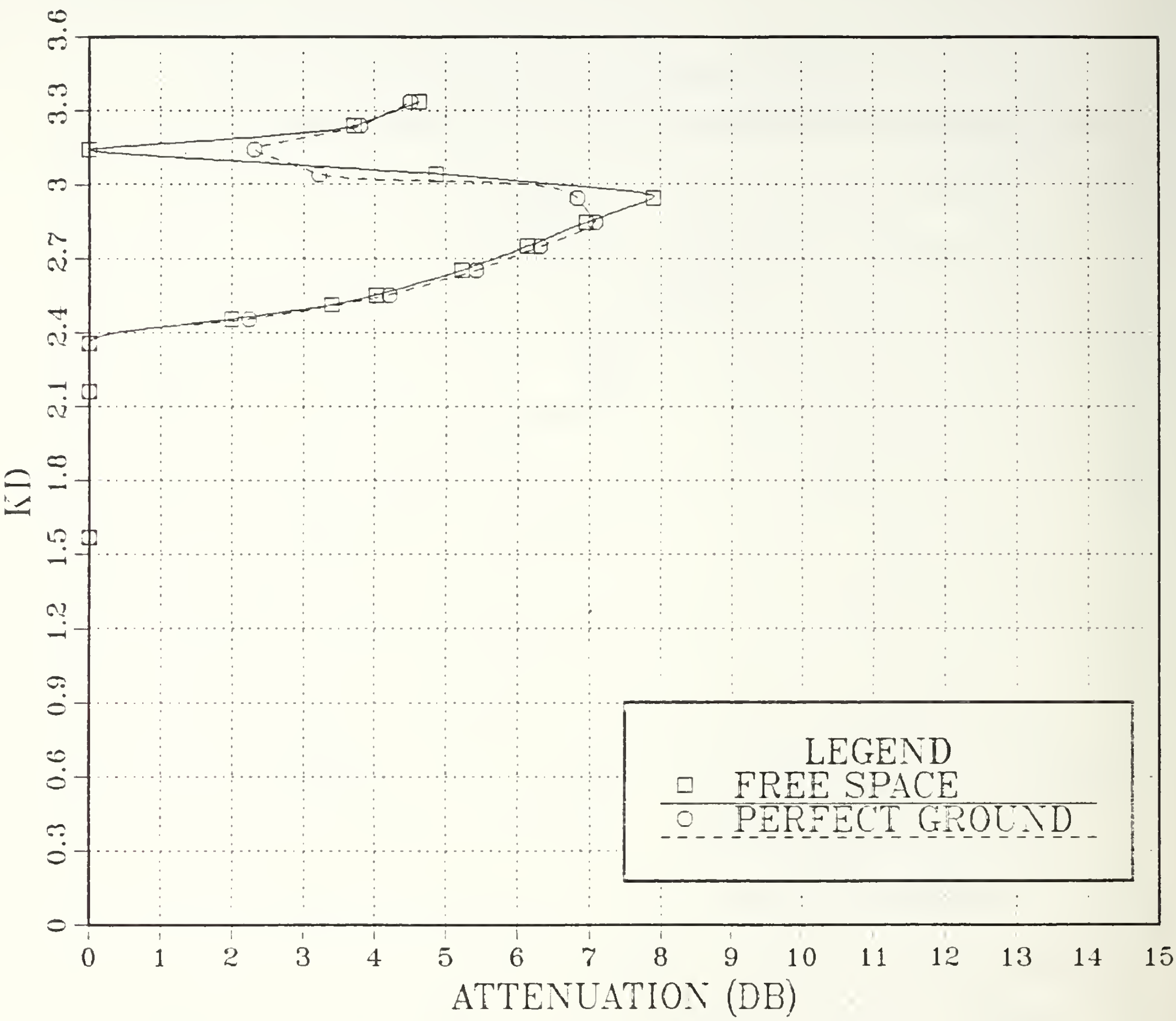


Figure 31. The Observed Attenuation of the Half Square Array with In-Phase Feed Sources

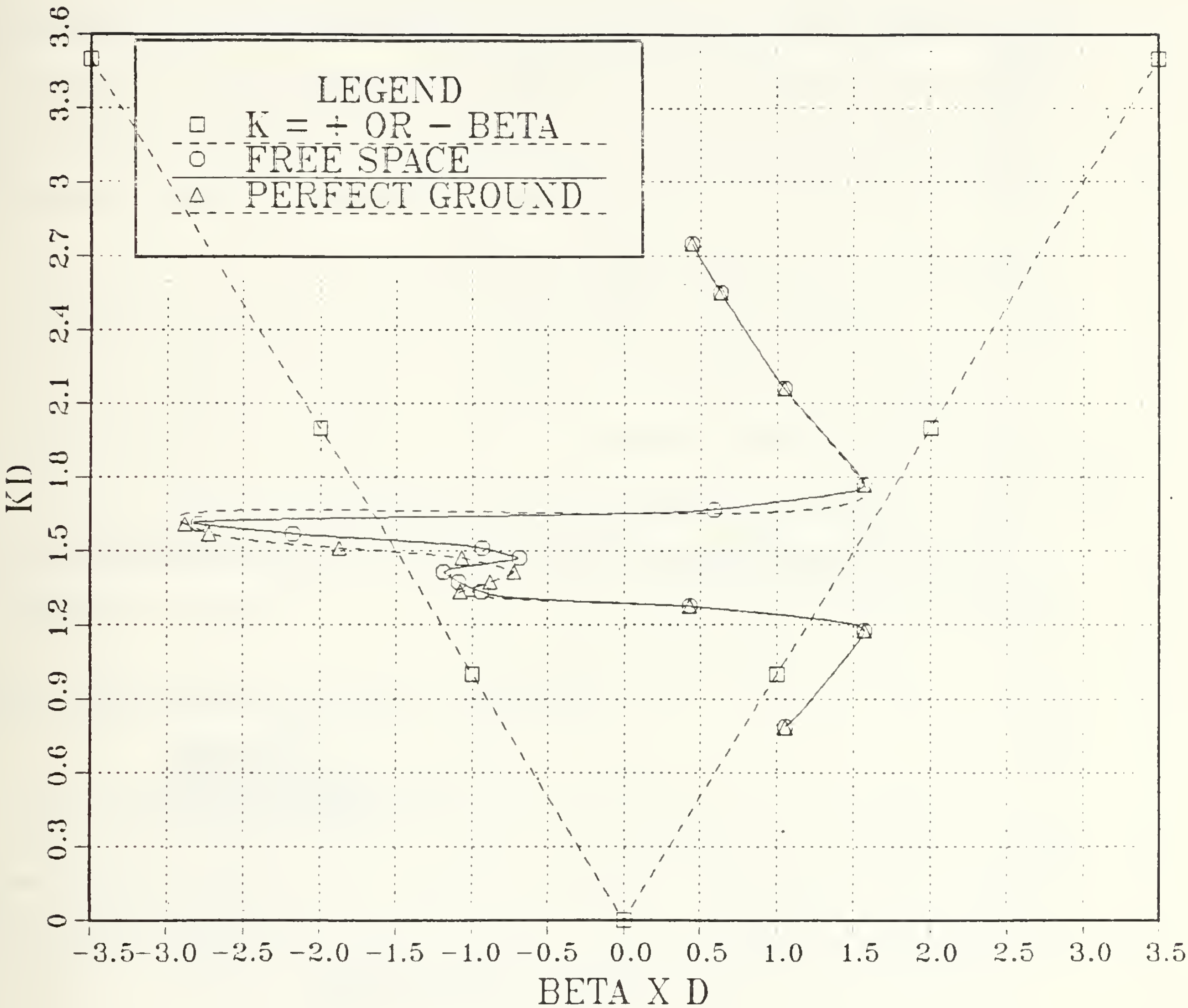


Figure 32. k-$\beta$ Relationship for the Half Square Array with Anti-Phase Feed Sources

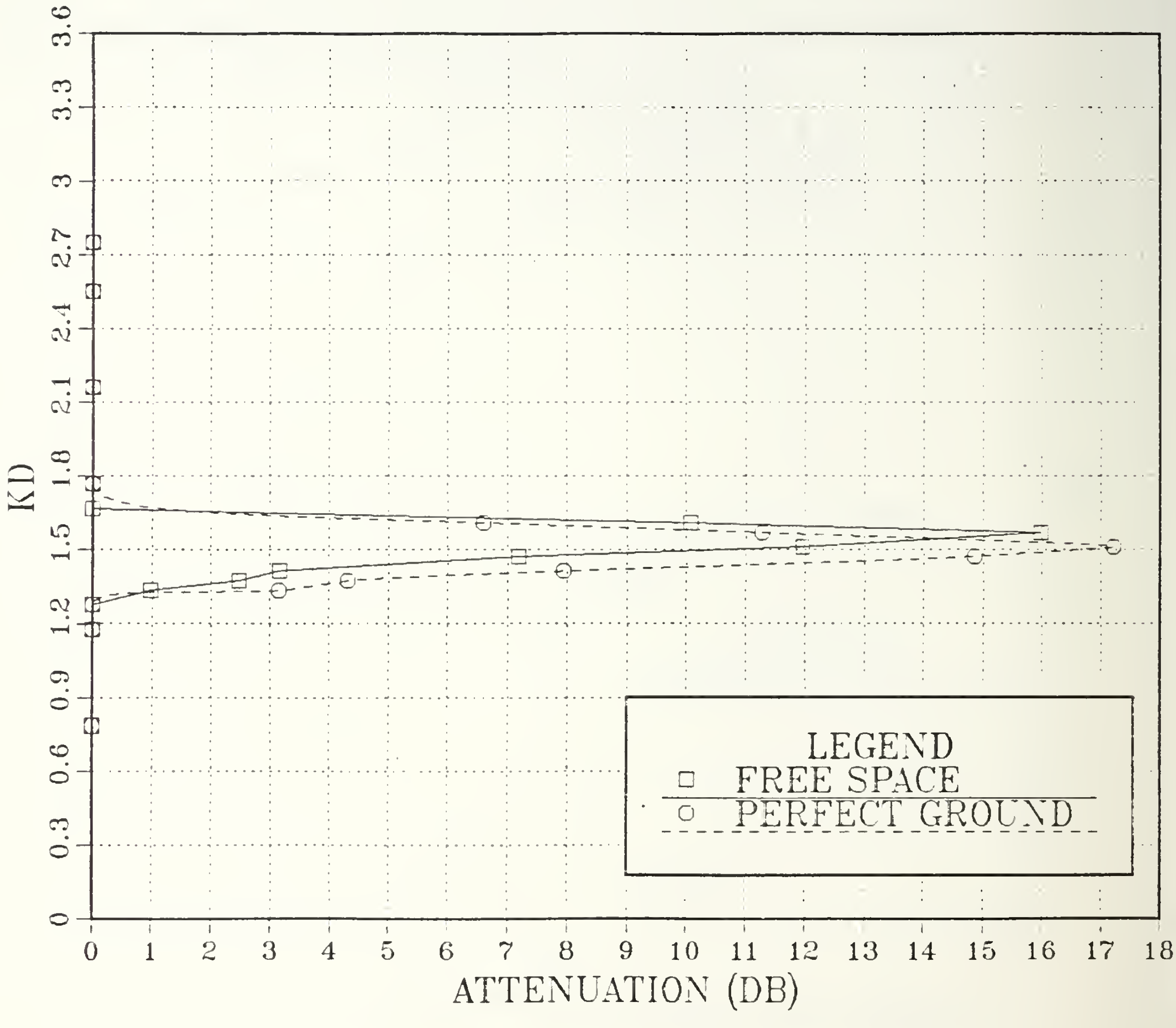


Figure 33. The Observed Attenuation on the Half Square Array with Anti-Phase Feed Sources

support backward radiation for both the in-phase and anti-phase excitation modes, but noted that the backward radiation regions occur in different frequency ranges or element spacing intervals. The identification of two different regions of backward radiation supports the projection that the dual feed system will support both low and high angle propagation modes. Recalling that the direction of propagation angle, $\theta$, is a function of $\cos^{-1}$ of the ratio of $\rho/k$, it was observed that the in-phase mode will support backward radiation with a high angle of propagation, and the anti-phase mode will create a low angle of propagation. The ability of the structure to support backward radiation in the frequency range of interest for both modes allows for the possibility of a successful log-periodic antenna design to exist.

## B. FAR FIELD RADIATION PATTERNS

### 1. Half Square Antenna

The far field radiation patterns were calculated and plotted for the half square antenna to determine performance characteristics of the elements. The radiation patterns for the half square antenna with both in-phase and anti-phase excitation are shown in Appendix F for the frequency range determined to be of interest by the k-$\beta$ diagrams. The patterns were calculated for the free space condition in order that both verticle and horizontal polarization

patterns could be observed without ground effects. The in-phase mode generated patterns with primarily vertical polarization, and the maximum gain condition occured when the input frequency matched the design resonant frequency. The anti-phase mode generated interesting radiation pattern results. For the 2 to 4 MHz region, the radiation patterns showed endfire gain with primarily horizontal polarization, but as the frequency increased the pattern changed to show horizontally polarized endfire radiation with 0 dB gain, and vertically polarized broadside radiation with 0 dB gain. From the far field radiation pattern information and the k-$\beta$ diagrams, there appears to be a correlation developing between the frequency regions of maximum gain and the regions identified as supporting backward radiation for each excitation mode.

2. Uniformly Periodic Half Square Array

The half square array far field radiation patterns were calculated for the in-phase and anti-phase excitation modes using the frequencies determined by the k-$\beta$ diagram to support backward radiation (Appendix G). By observing the resulting radiation patterns, the k-$\beta$ relationship calculated from the near field could be verified.

The in-phase excitation mode patterns demonstrated a predominant vertically polarized gain, and the patterns behaved in the manner predicted by Hudock. The frequency points close to the $R_b$-$R_f$ boundary (7.2 MHz) demonstrated

a bidirectional pattern with only slightly higher gain in the backward direction. As the frequency points moved away from the boundary (7.6, 7.8 and 7.9 MHz), the pattern showed a more unidirectional gain characteristic, but still demonstrated some forward radiation. This forward radiation was predicted by Hudock, and probably results from the truncation effects of the structure and the predicted high angle propagation.

The anti-phase excitation mode produced horizontally polarized radiation patterns. For the anti-phase mode, the $R_b$ region identified in the k-$\beta$ diagram was very small and close to the slow-fast wave boundry. Hudock predicted in his work with monopoles that the area very close to the boundry would produce the most unidirectional radiation characteristic, and the radiation patterns calculated for the half square array with anti-phase excitation demonstrated this unidirectional characteristic. The radiation patterns calculated for 3.6 and 3.8 MHz both showed unidirectional patterns in the backward radiation direction.

Reviewing the radiation patterns, it can be concluded that the k-$\beta$ diagram properly identified the backward radiation region for the structure as predicted. It also should be noted that the dual polarization property was observed for the dual feed system as predicted in the design by Campbell with vertical polarization dominant in the

in-phase excitation mode and a dominant horizontal polarization pattern with the anti-phase mode.

## V. CONCLUSIONS AND RECOMMENDATIONS

The purpose of this research was to provide information about the potential development of the log-periodic half square antenna with dual feed as a military HF antenna. This information was provided through an analysis of a uniformly periodic half square array with dual feed. The experimental objective of this research was accomplished with a near field investigation to determine regions from a k-$\beta$ diagram with the potential for providing the characteristic backward radiation of log-periodic antennas, and with a far field radiation pattern analysis to verify the presence of backward radiation in the frequency region identified by the k-$\beta$ diagram and to observe end and truncation effects of the structure.

From the experimental data, k-$\beta$ diagrams were constructed for both the in-phase and anti-phase excitation modes. The k-$\beta$ diagrams identified backward radiation regions for both modes of excitation. The in-phase mode identified characteristics of backward radiation in the frequency region of 6.2 to 7.9 MHz. Despite being in the $R_b$ region of the diagram, the identified k to $\beta$ relationship was very close to the $R_b$-$R_f$ boundry, and this relationship caused the far field radiation patterns to exhibit backward radiation but with noticeable forward radiation. The anti-phase mode identified

regiorward radiation in the region of 3.5 to on thegram. In the case of the anti-phase e ideregion was very close to the fast-slow ndry iagram, and the far field radiation demora primarily unidirectional radiation ackwarion.

result experiment lead to the conclusion that ntial ning a successful log-periodic half ntennal feed does exist with proper scaling ing tc HF communications in the frequency 2 to Before the possibility of the being for support of military HF ationsdiscussed, further research is nto thg and spacing of the log-periodic and tting radiation patterns for the must lted for beamwidth and gain.

APPENDIX A-NEAR FIELD EXPERIMENTAL RESULTS FOR THE QUARTER SQUARE ARRAY WITH A SWITCHED TRANSMISSION LINE IN FREE SPACE

F=2MHZ

DIST VS MAG

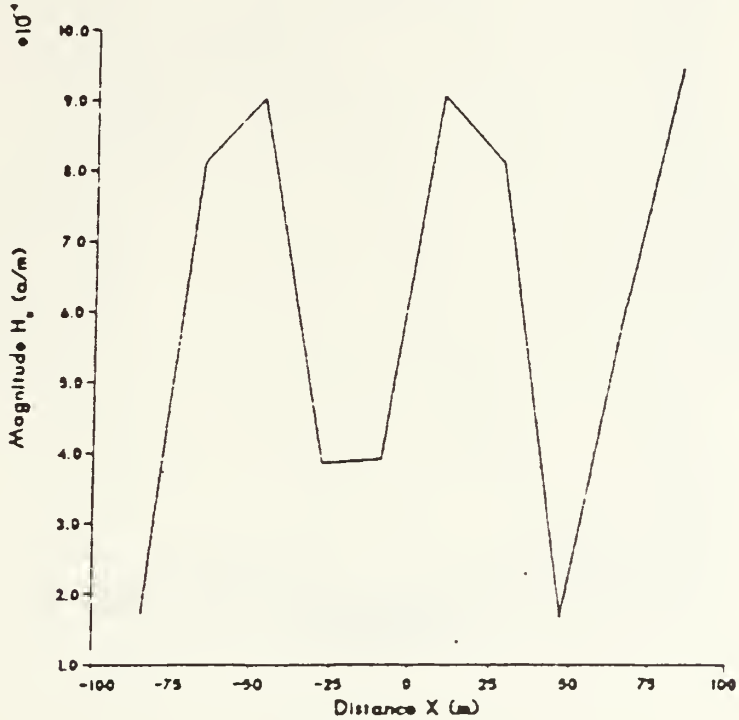


F=4MHZ

DIST VS MAG

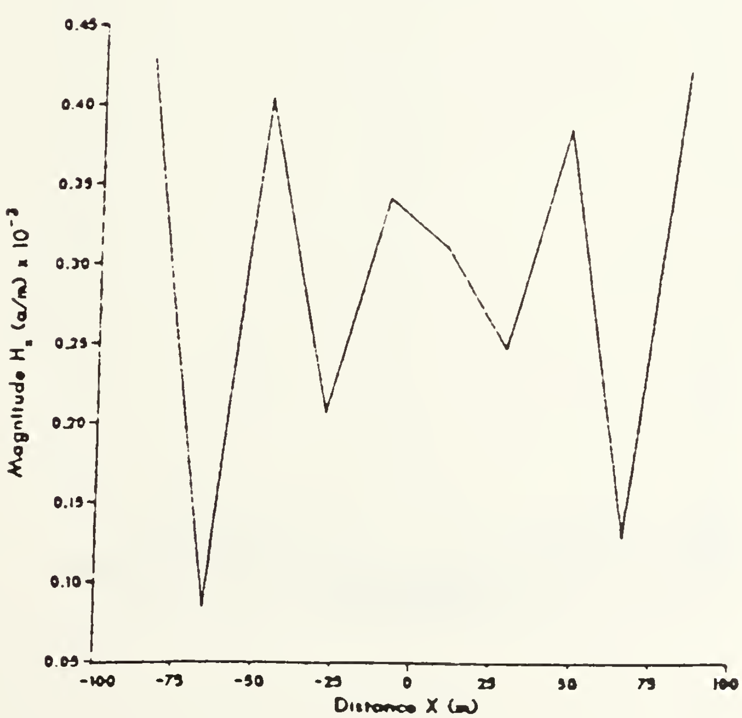

F=6MHZ

DIST VS MAG

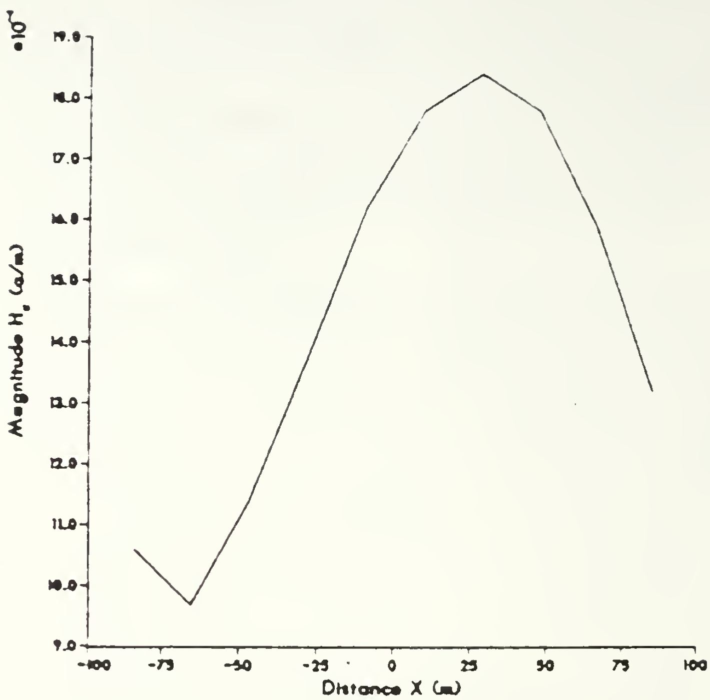


DIST VS PHASE

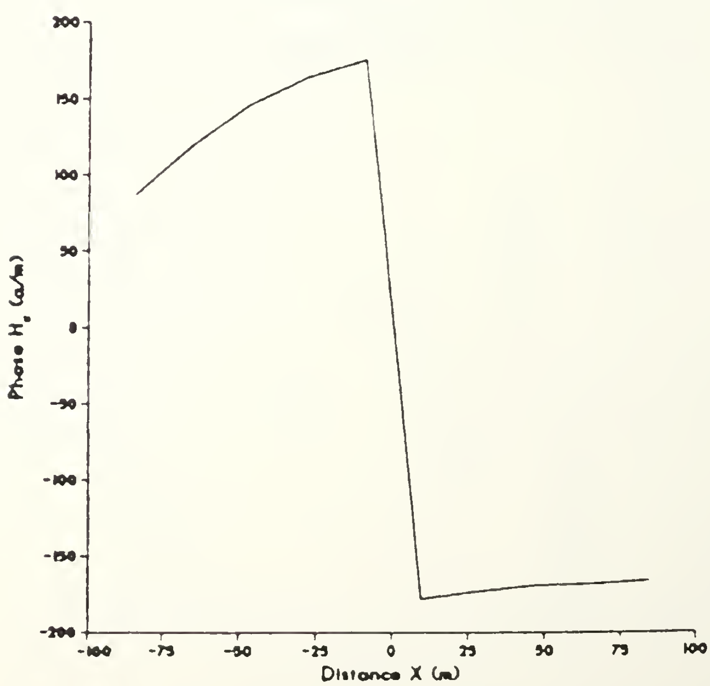

F=6.05 MHZ

DIST VS MAG

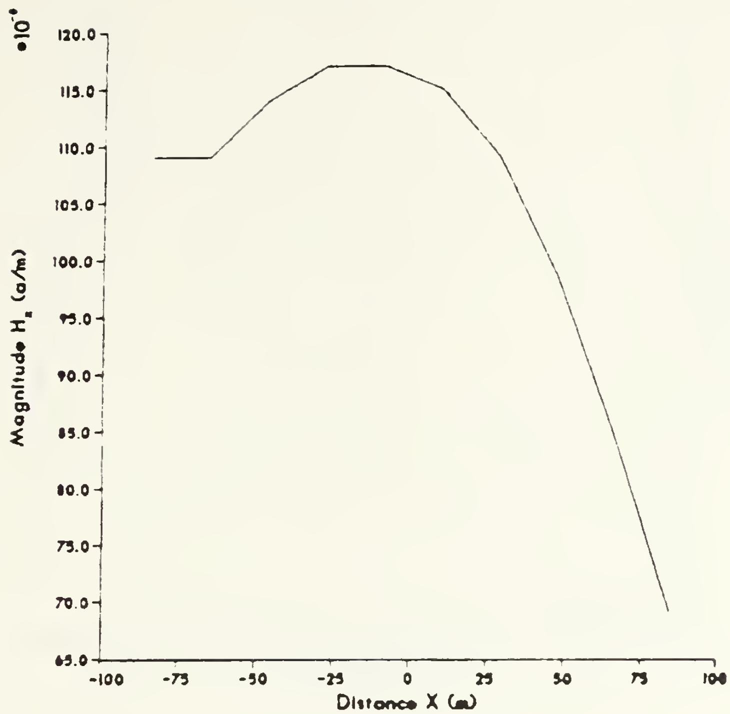


DIST VS PHASE

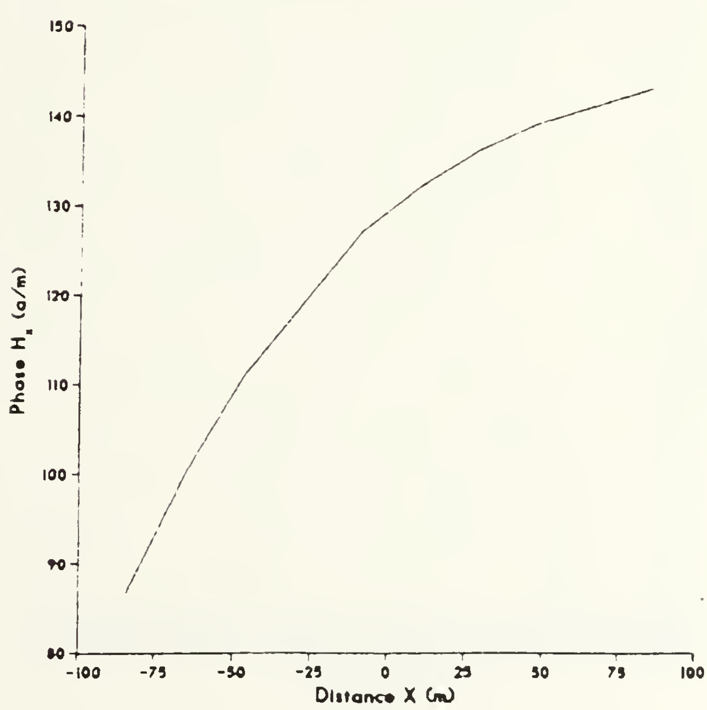

F=6.1MHZ

DIST VS MAG

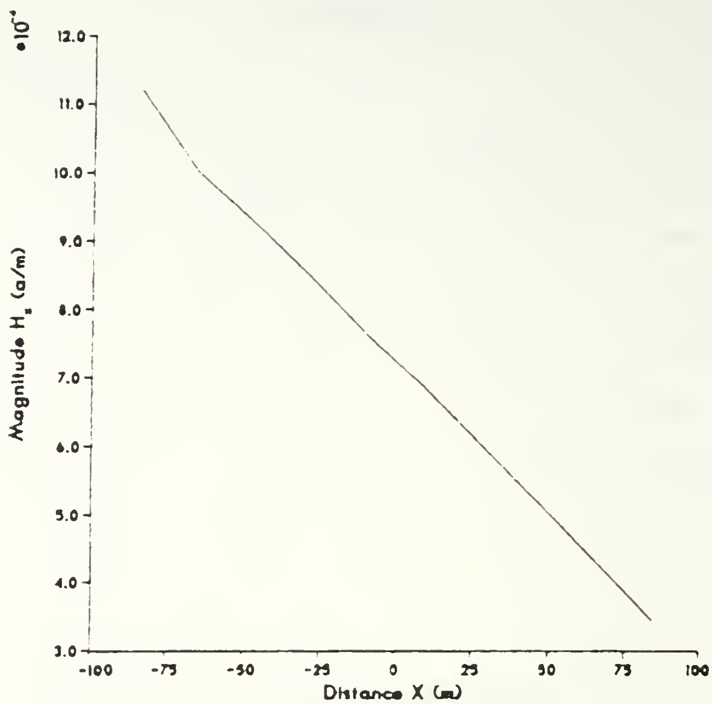


DIST VS PHASE

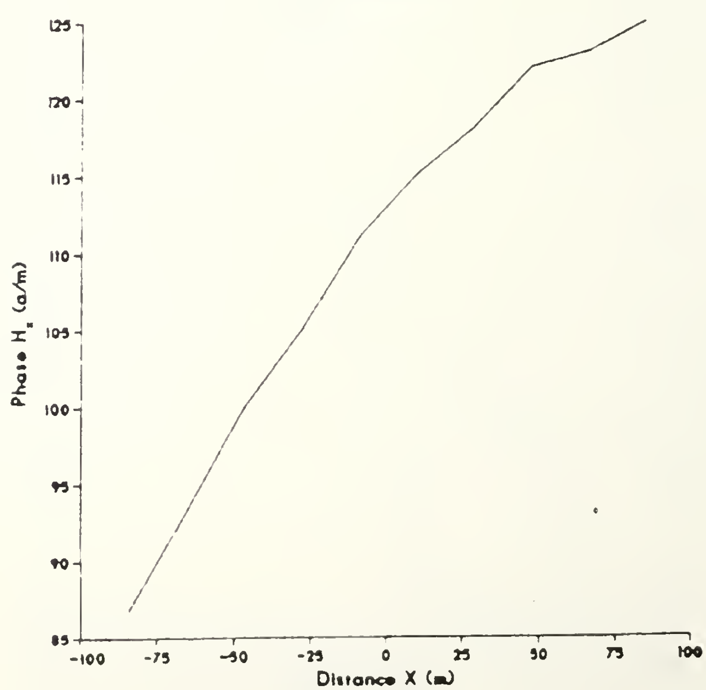

F=6.25MHZ

DIST VS MAG

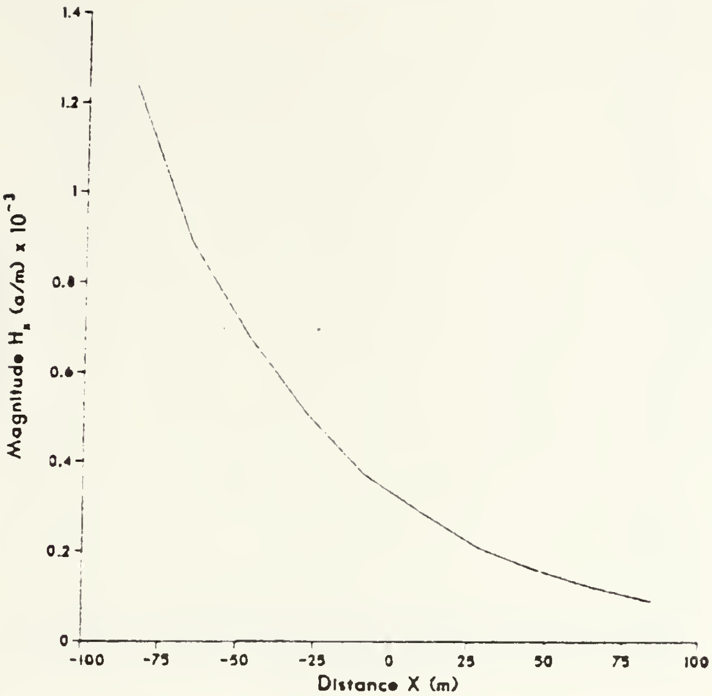


DIST VS PHASE

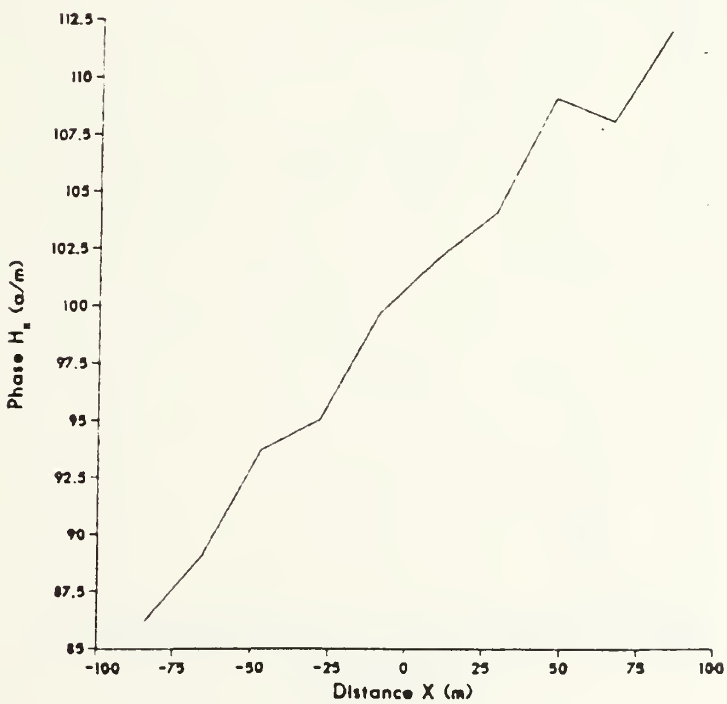

F=6.5 MHZ

DIST VS MAG

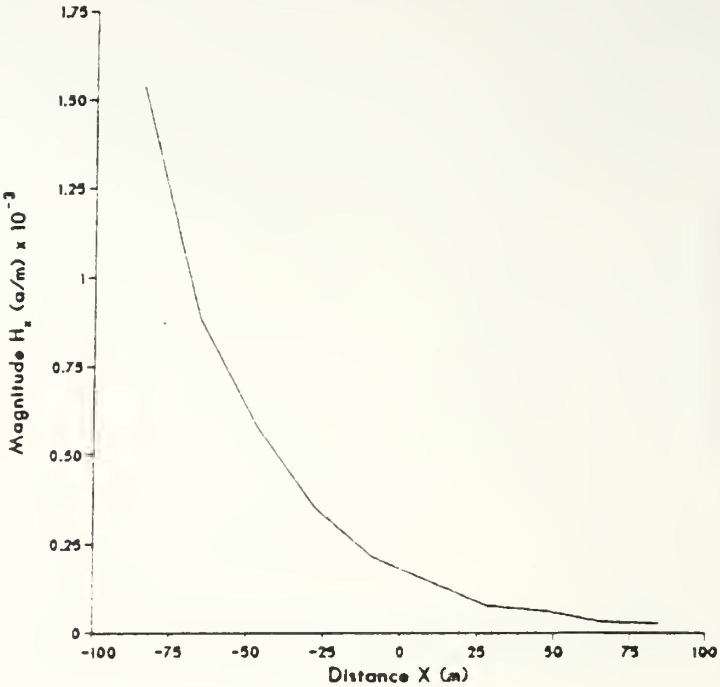


DIST VS PHASE

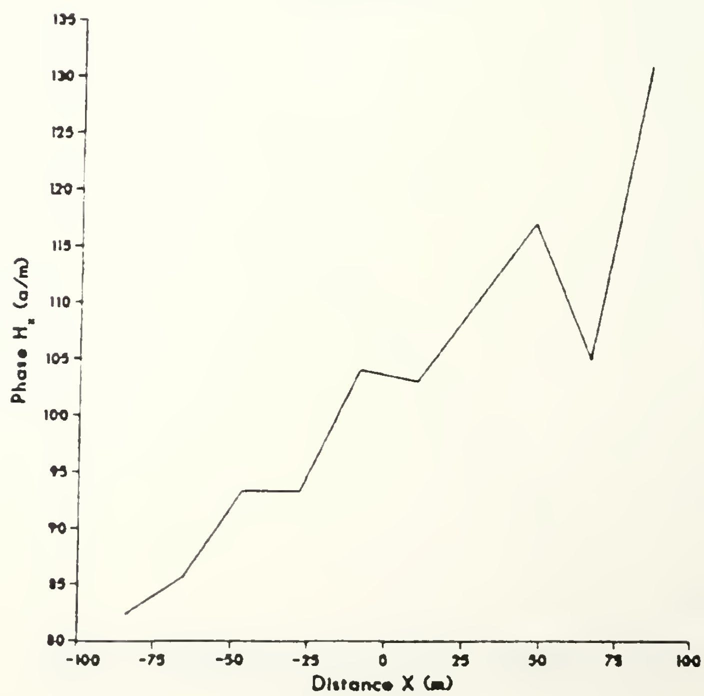

F=7MHZ

DIST VS MAG

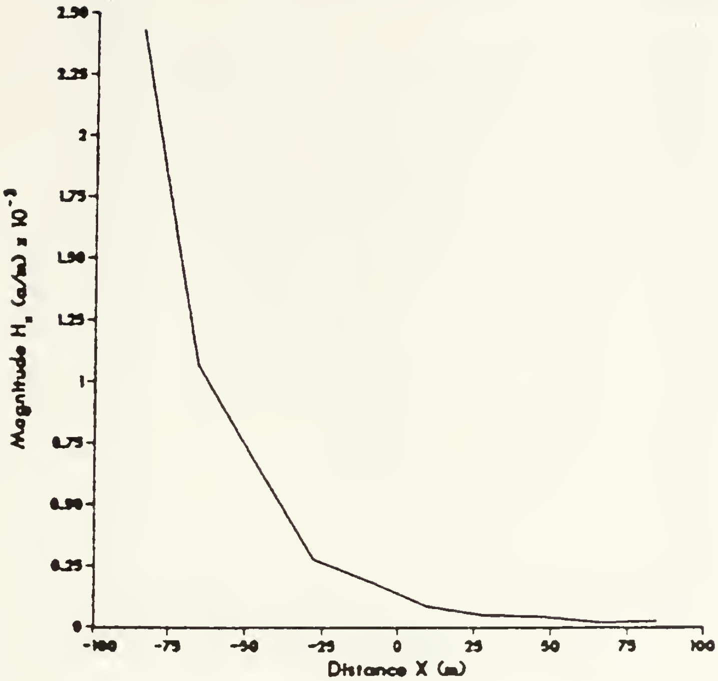


DIST VS PHASE

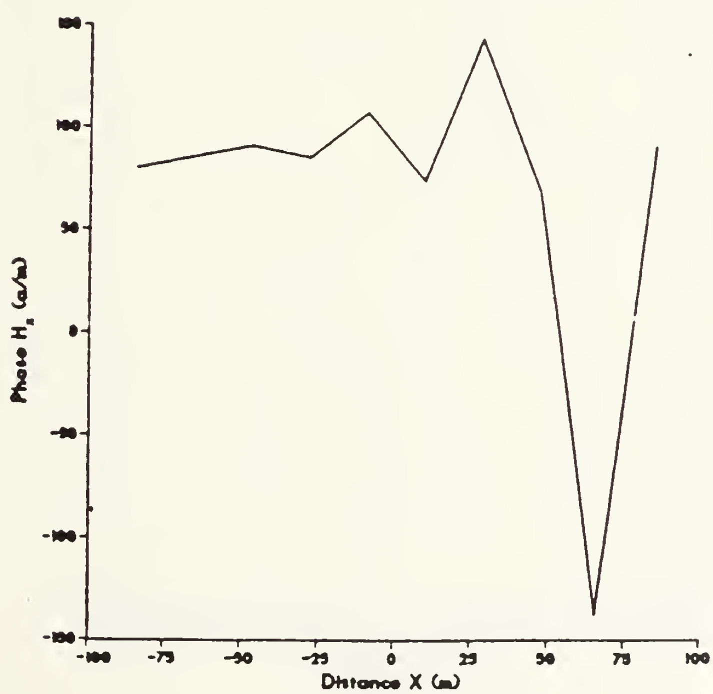

F=7.4MHZ

DIST VS MAG

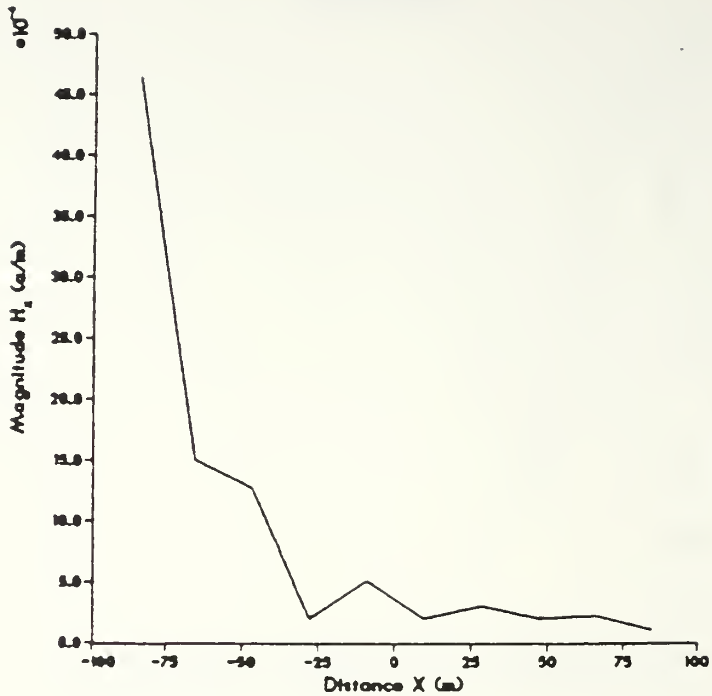


DIST VS PHASE

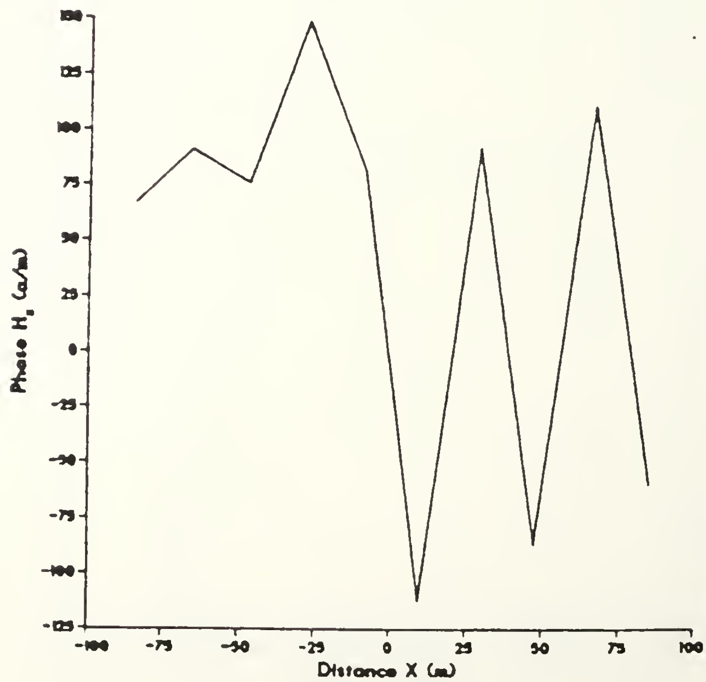

F=7.9MHZ

DIST VS MAG

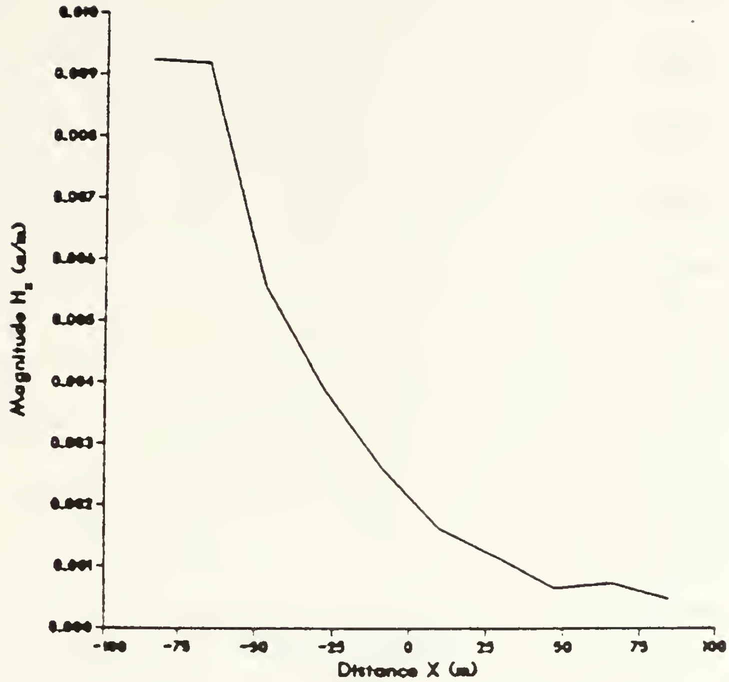


DIST VS PHASE

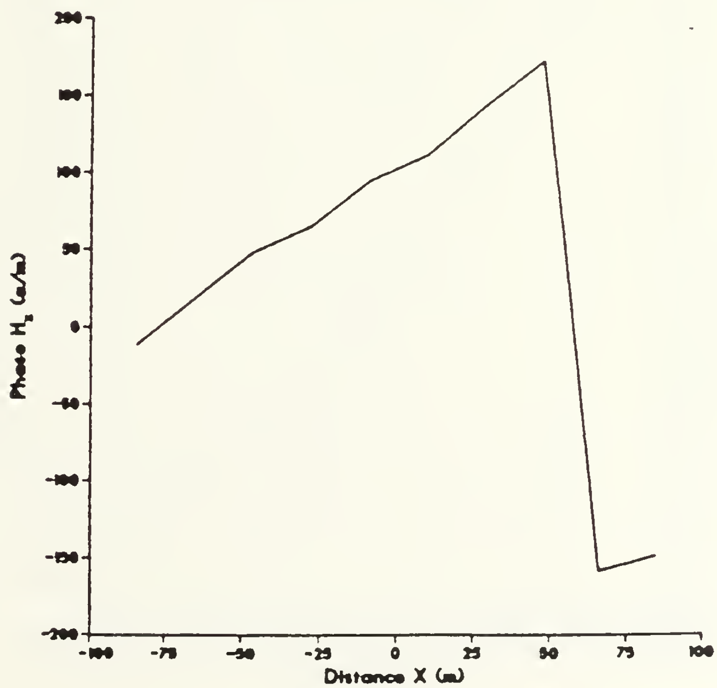

F=8MHZ

DIST VS MAG

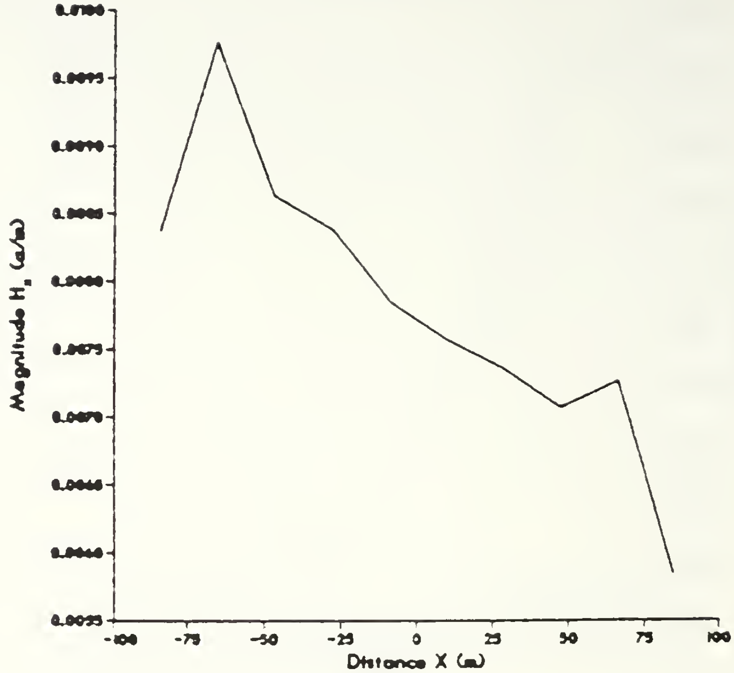


DIST VS PHASE

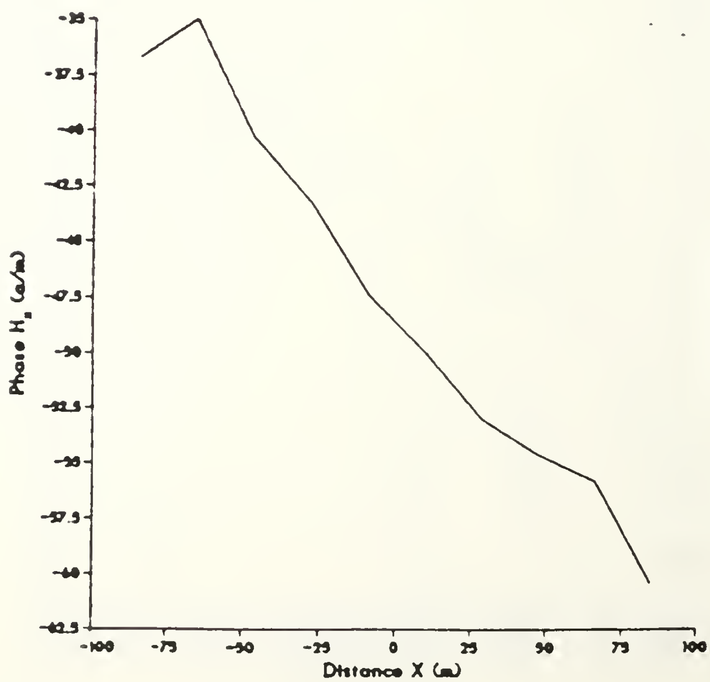

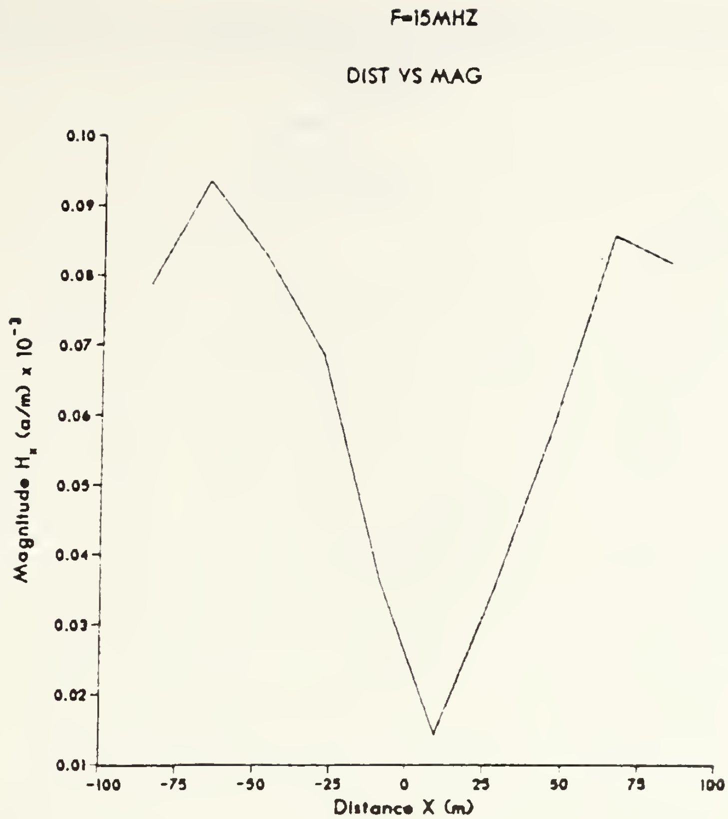

F=15MHZ
DIST VS MAG
Magnitude $H_x$ (a/m) x $10^{-3}$
0.10
0.09
0.08
0.07
0.06
0.05
0.04
0.03
0.02
0.01
-100
-75
-50
-25
0
25
50
75
100
Distance X (m)


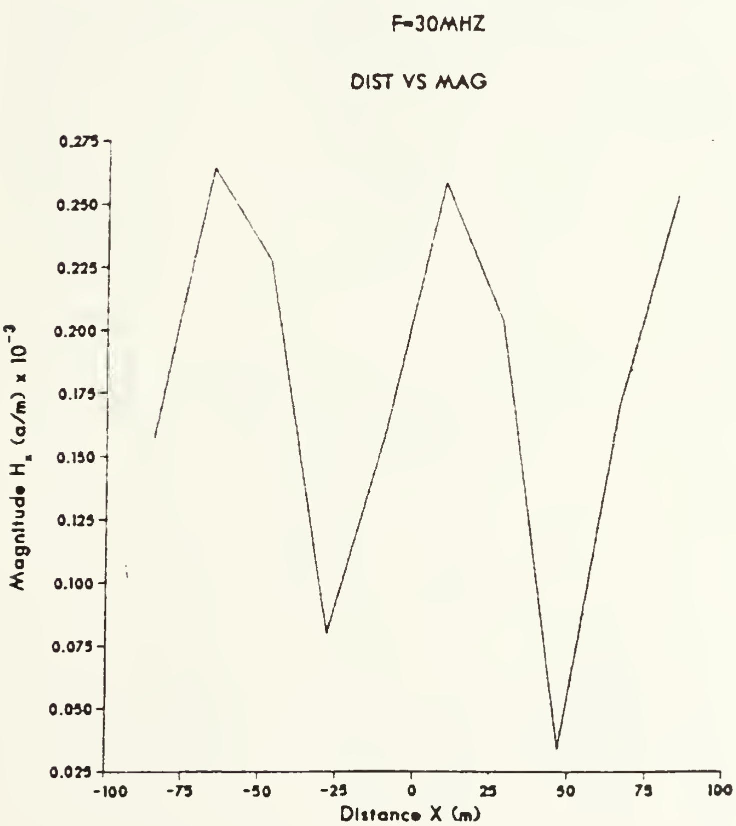

F=30MHZ
DIST VS MAG
Magnitude $H_x$ (a/m) x $10^{-3}$
0.275
0.250
0.225
0.200
0.175
0.150
0.125
0.100
0.075
0.050
0.025
-100
-75
-50
-25
0
25
50
75
100
Distance X (m)

# APPENDIX B-NEAR FIELD EXPERIMENT RESULTS FOR THE QUARTER SQUARE ARRAY WITH A SWITCHED TRANSMISSION LINE OVER PERFECT GROUND

F=2MHZ

DIST VS MAG

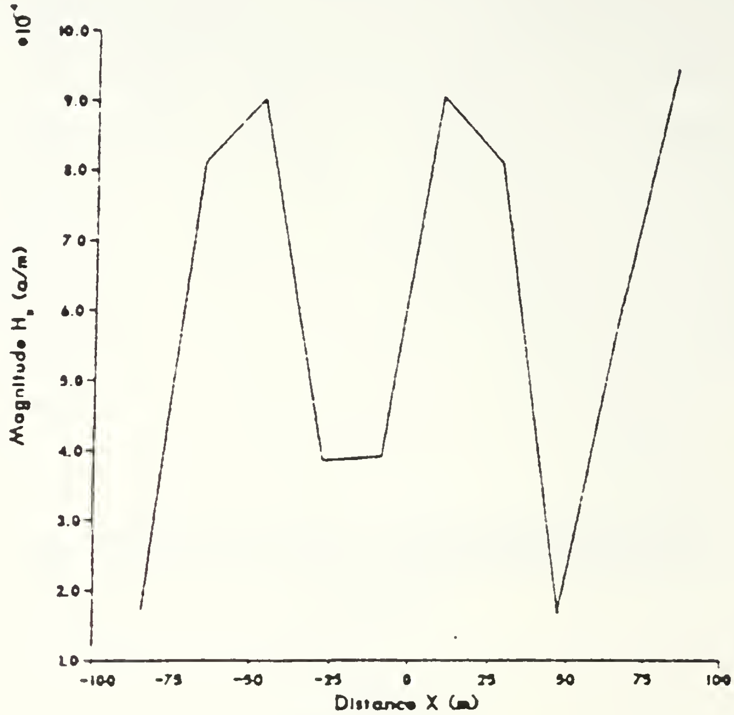


F=4MHZ

DIST VS MAG

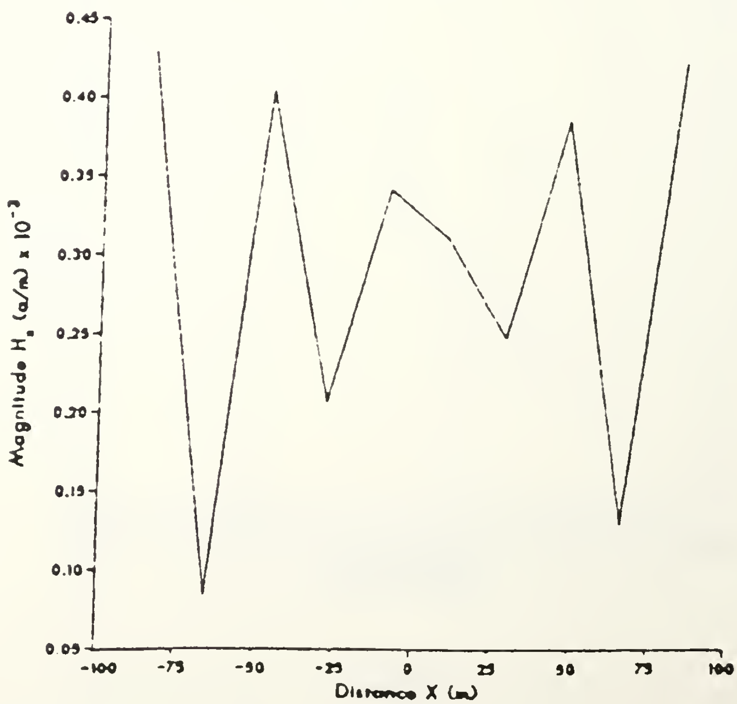

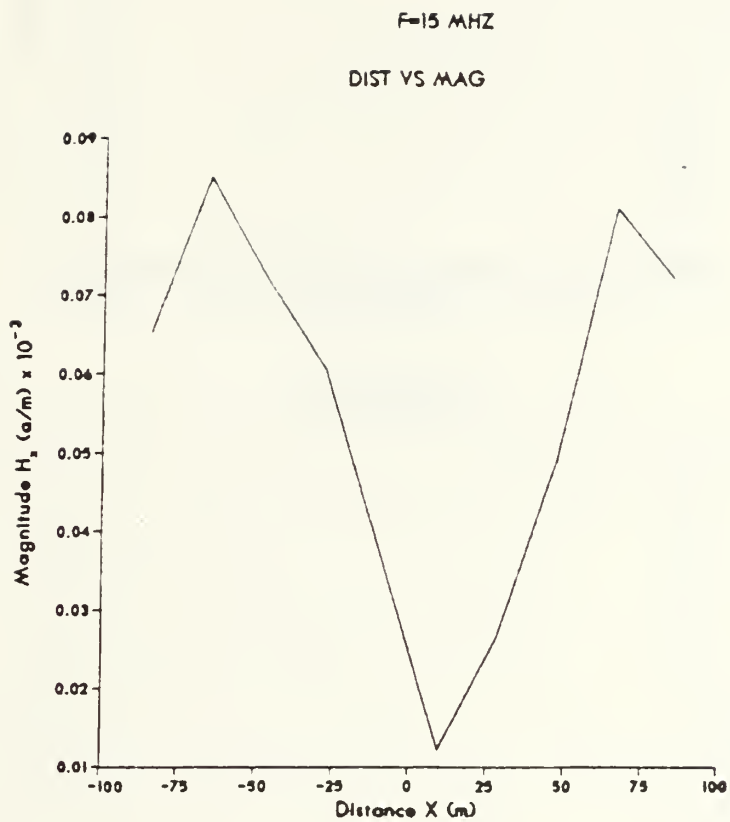
F=15 MHZ
DIST VS MAG
Magnitude $H_x$ (a/m) x $10^{-3}$
0.09
0.08
0.07
0.06
0.05
0.04
0.03
0.02
0.01
-100
-75
-50
-25
0
25
50
75
100
Distance X (m)

F=8.5 MHZ

DIST VS MAG

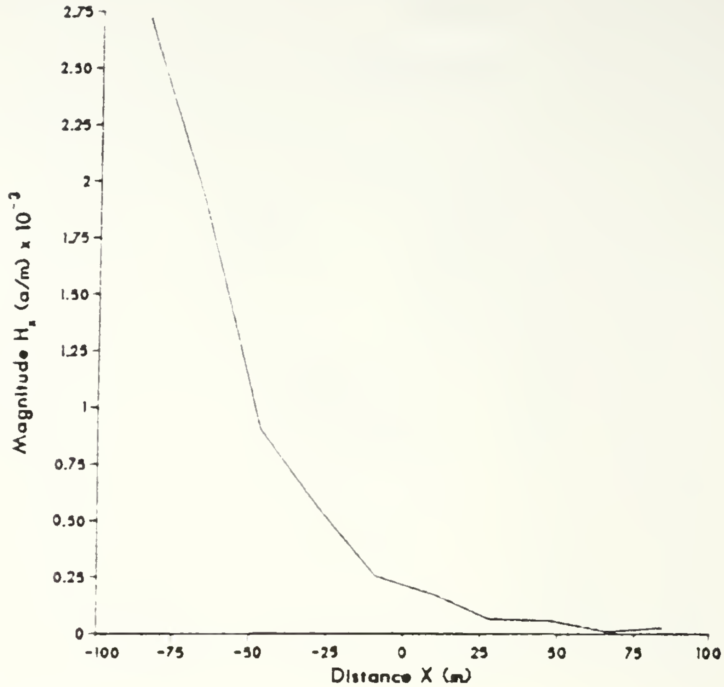


DIST VS PHASE

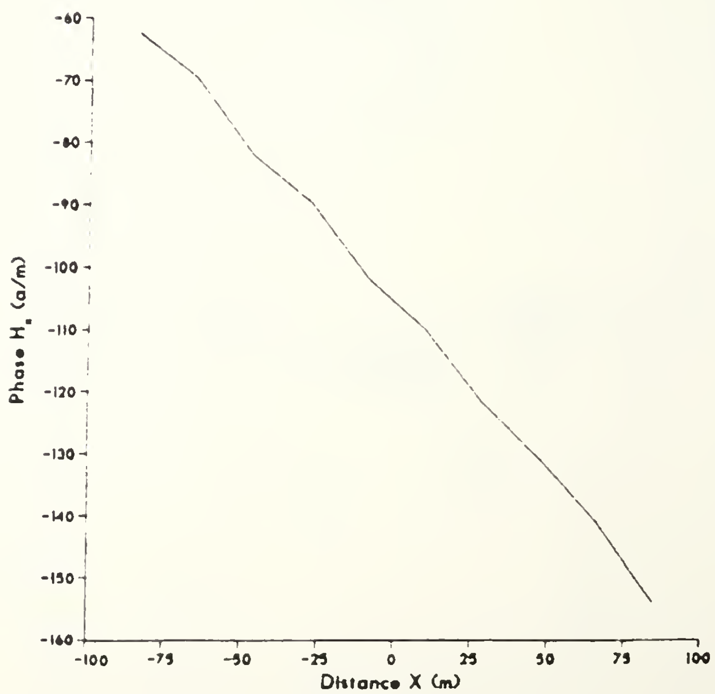

F=8 MHZ

DIST VS MAG

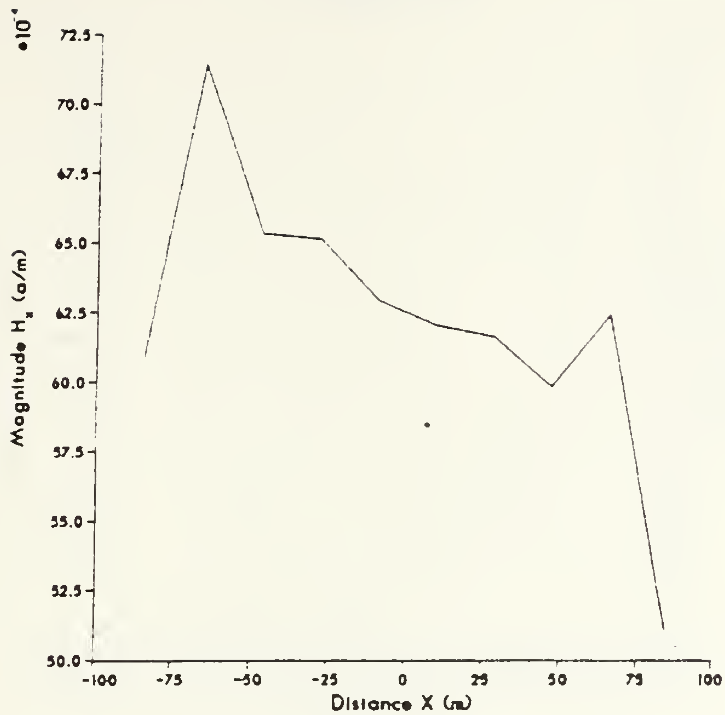


DIST VS PHASE

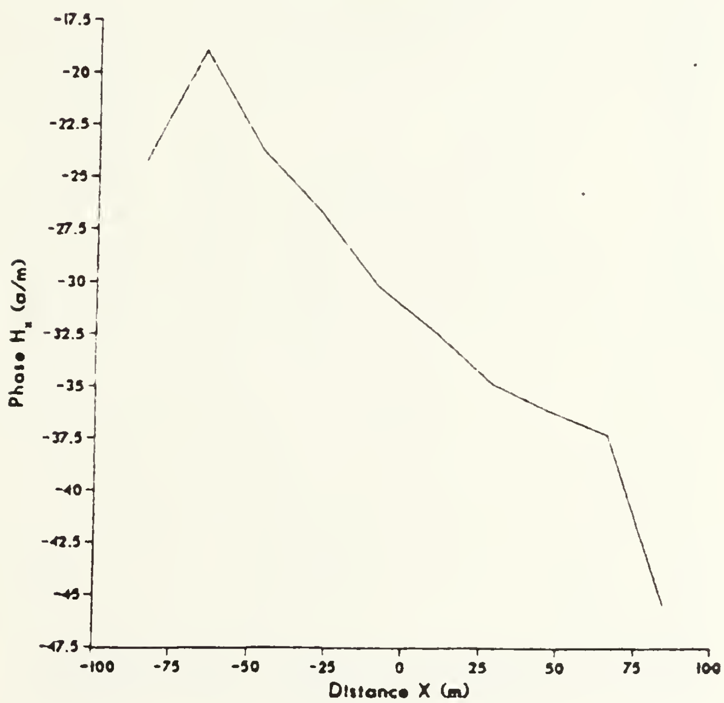

F=7.5 MHZ

DIST VS MAG

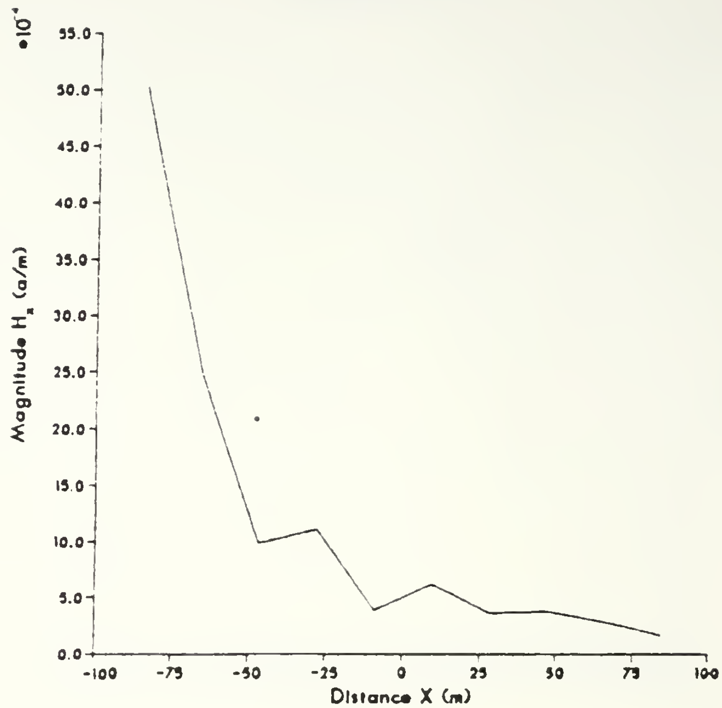


DIST VS PHASE

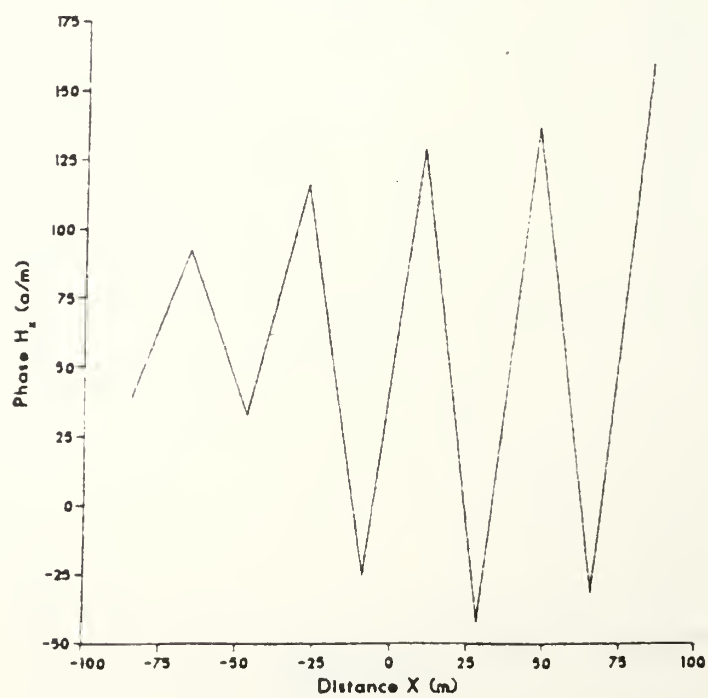

F=7 MHZ

DIST VS MAG

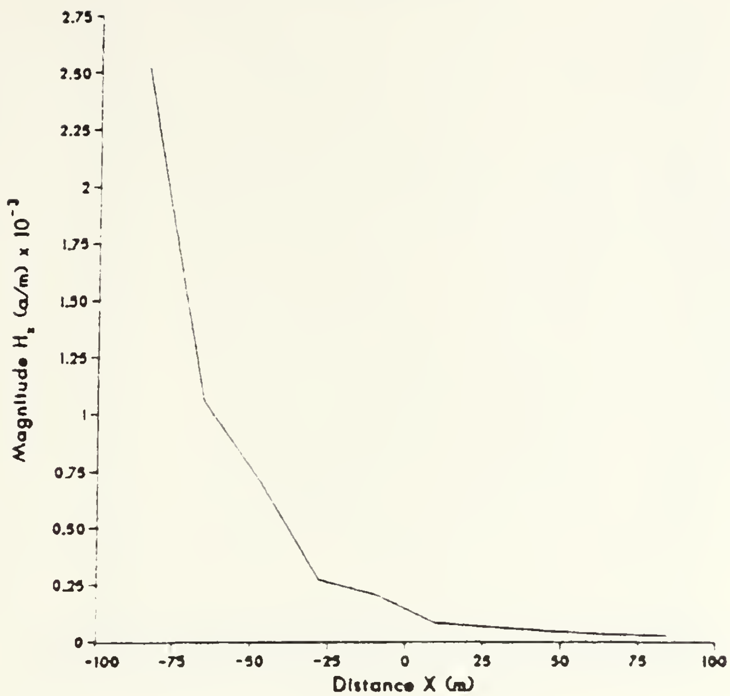


DIST VS PHASE

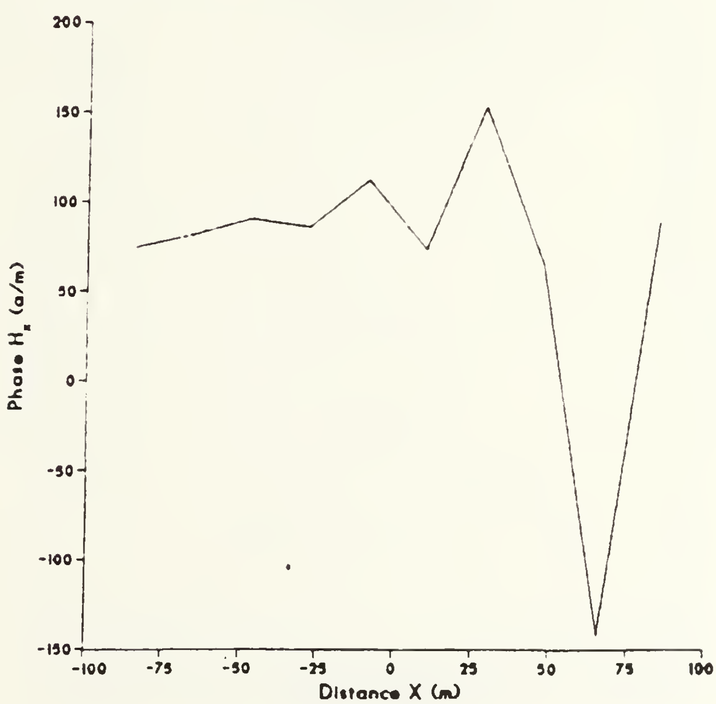

F=6.75 MHZ

DIST VS MAG

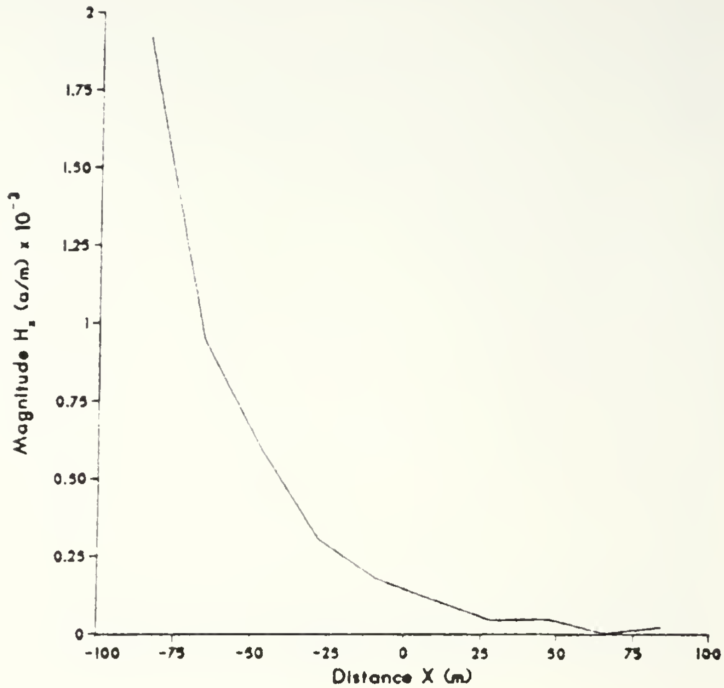


DIST VS PHASE

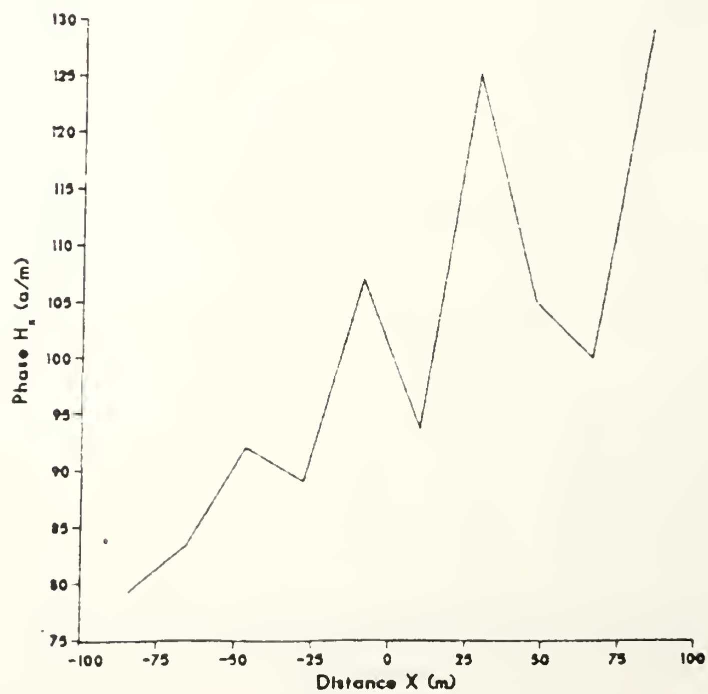

F=6.5 MHZ

DIST VS MAG

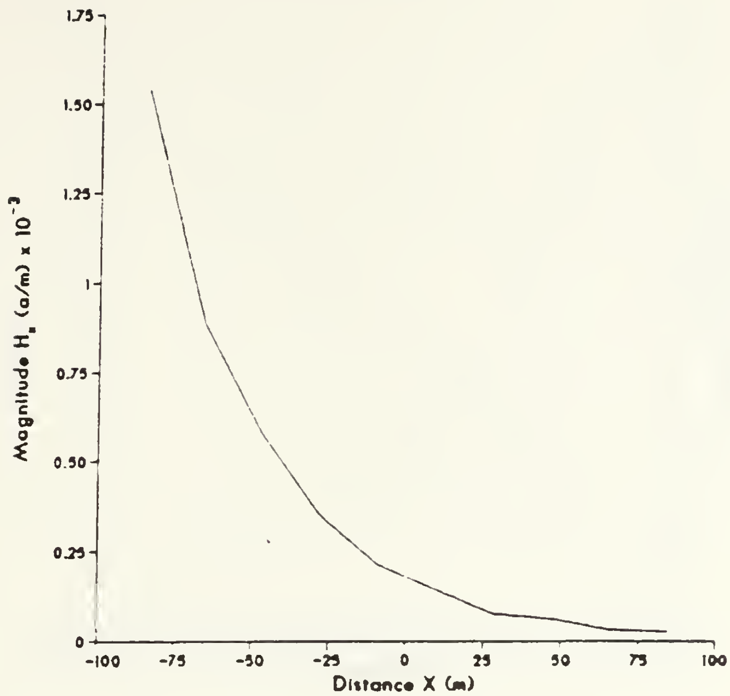


DIST VS PHASE

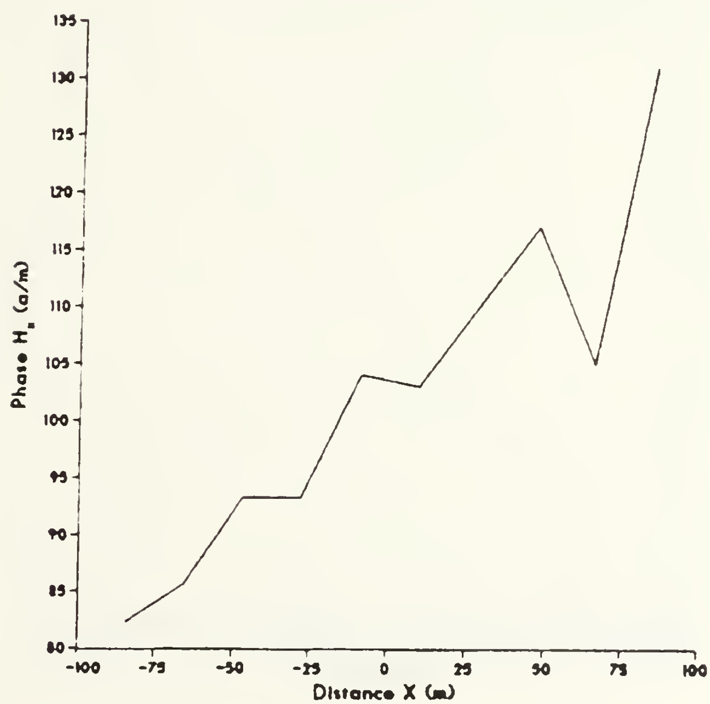

F=6.25 MHZ

DIST VS MAG

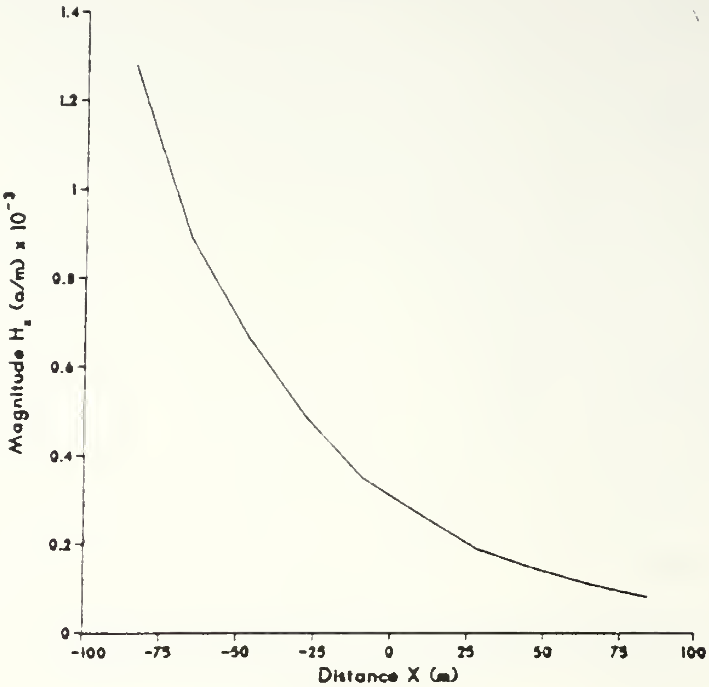


DIST VS PHASE

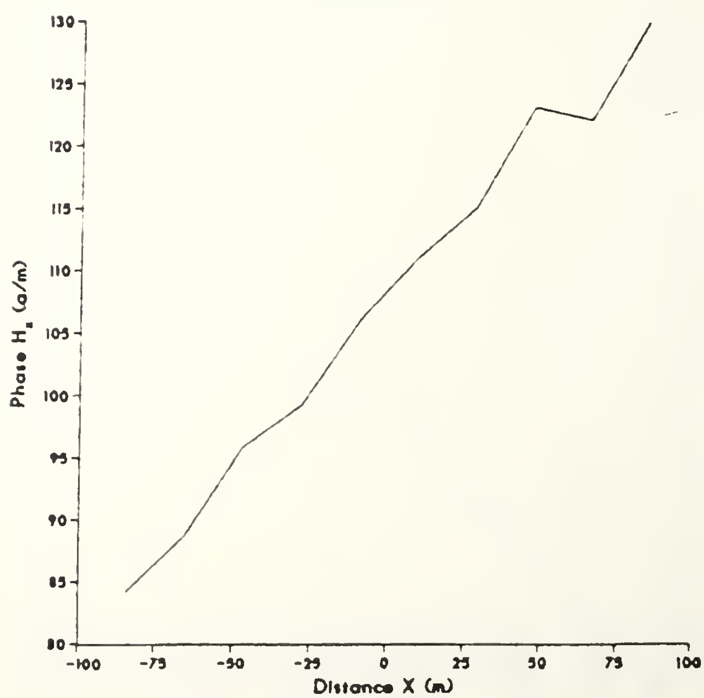

F=6.05 MHZ

DIST VS MAG

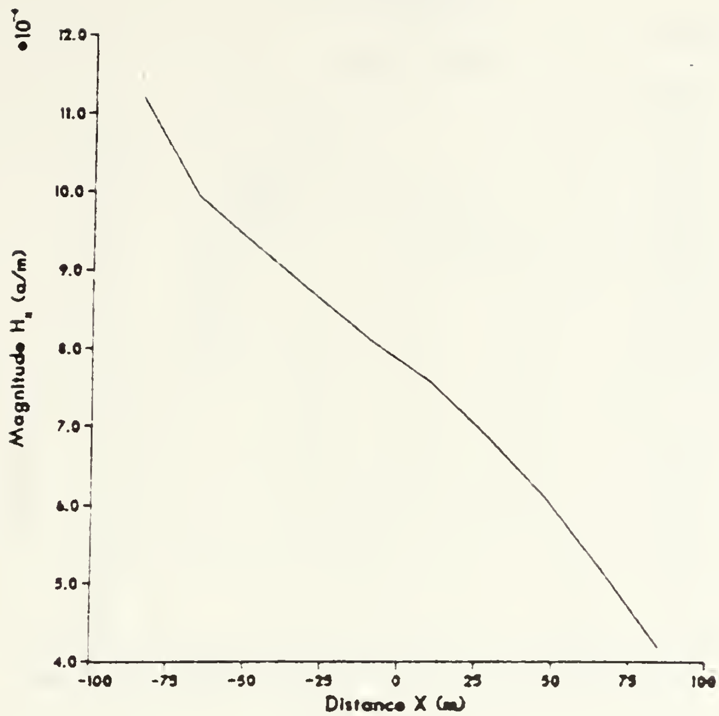


DIST VS PHASE

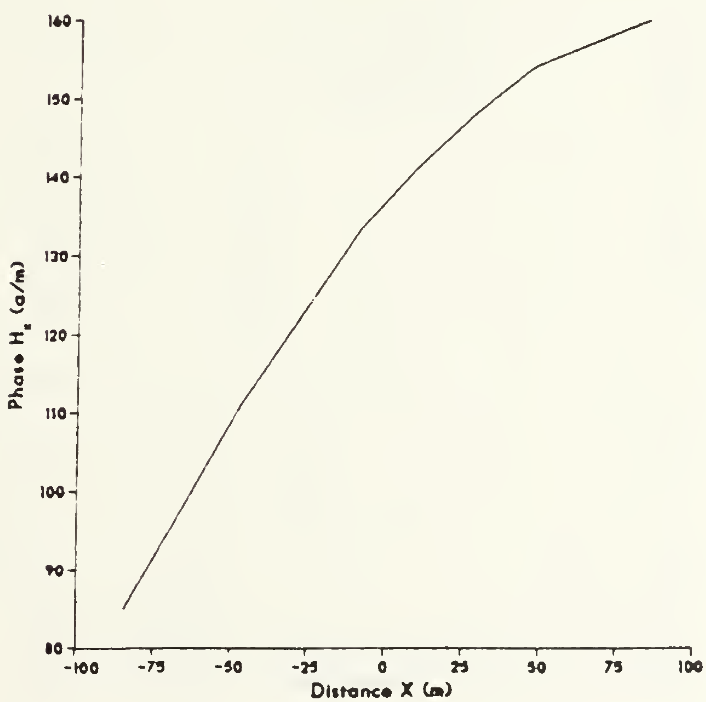

F=6 MHZ

DIST VS MAG

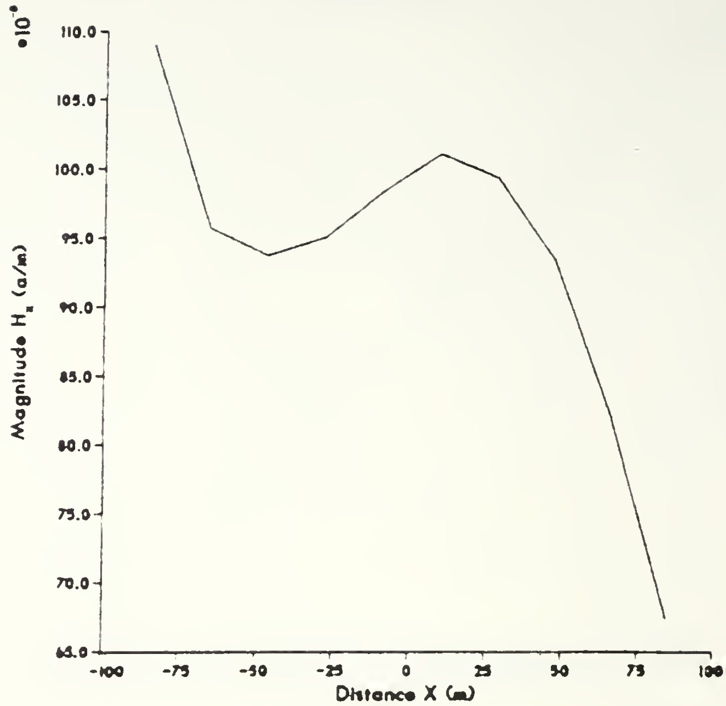


DIST VS PHASE

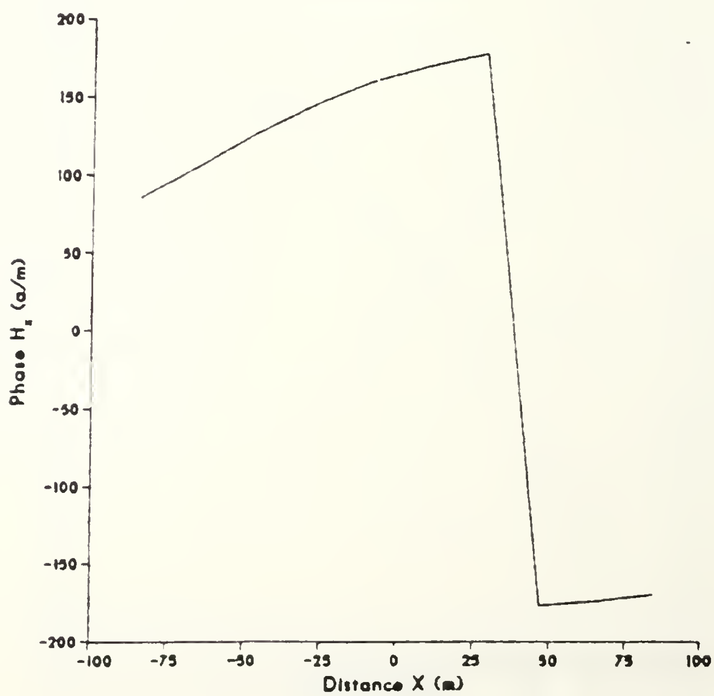

APPENDIX C-NEAR FIELD EXPERIMENTAL RESULTS FOR THE QUARTER SQUARE ARRAY WITH A STRAIGHT TRANSMISSION LINE

F=2MHZ

DIST VS MAG

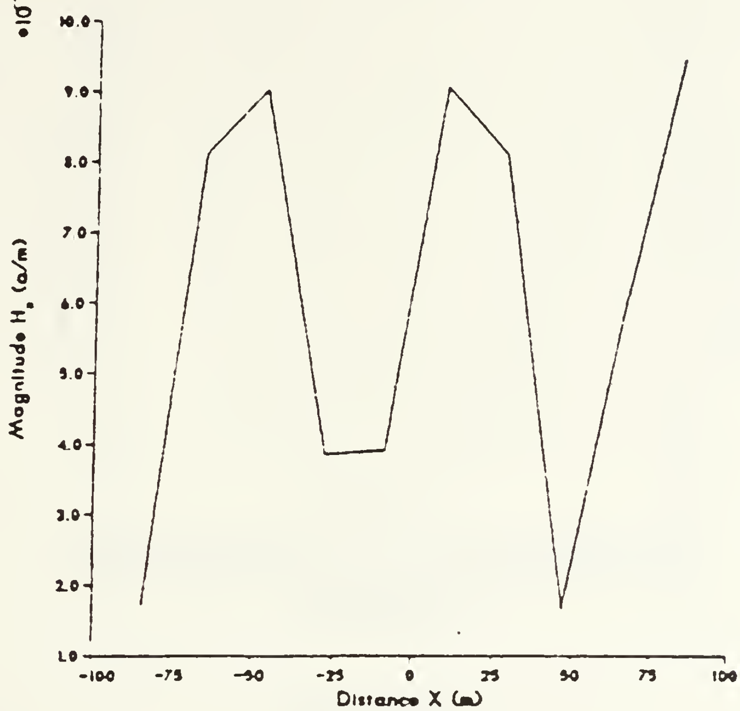


F=4MHZ

DIST VS MAG

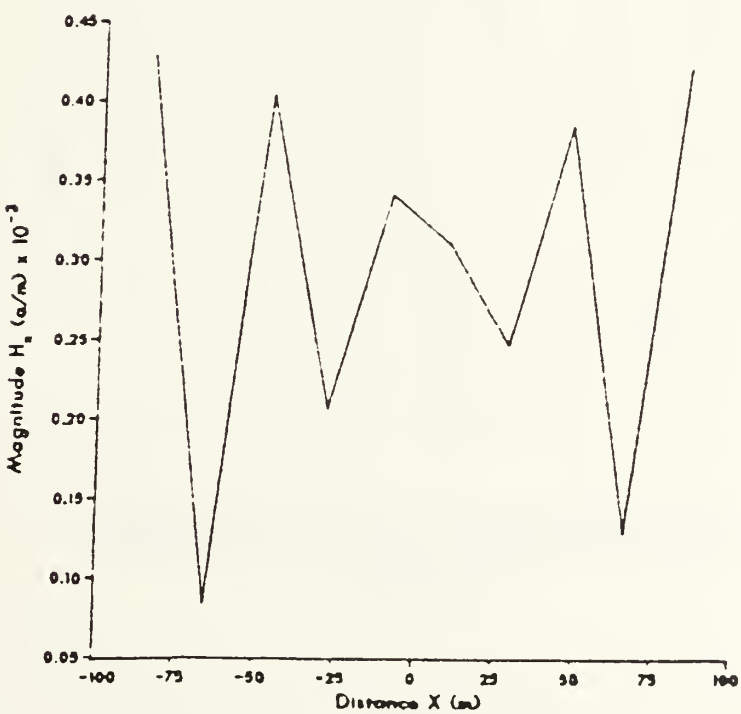

F=8.5MHZ

DIST VS MAG

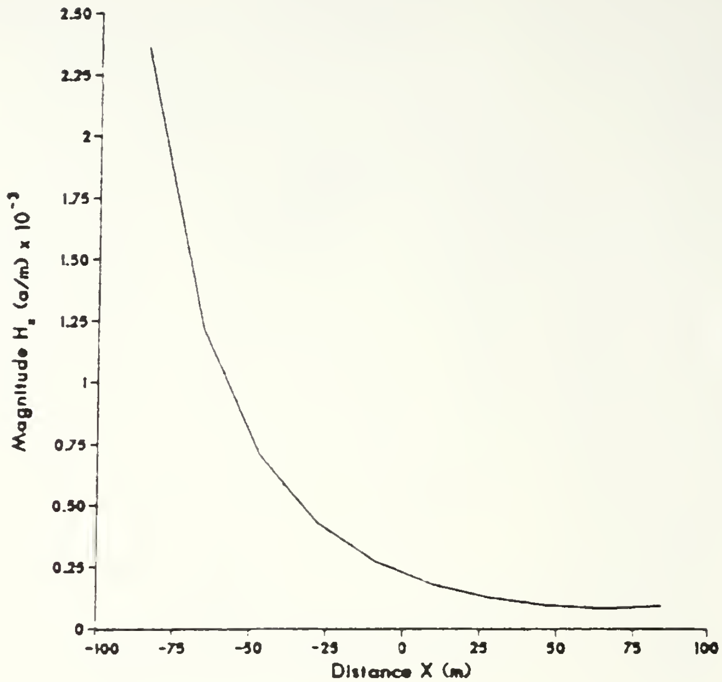


DIST VS PHASE

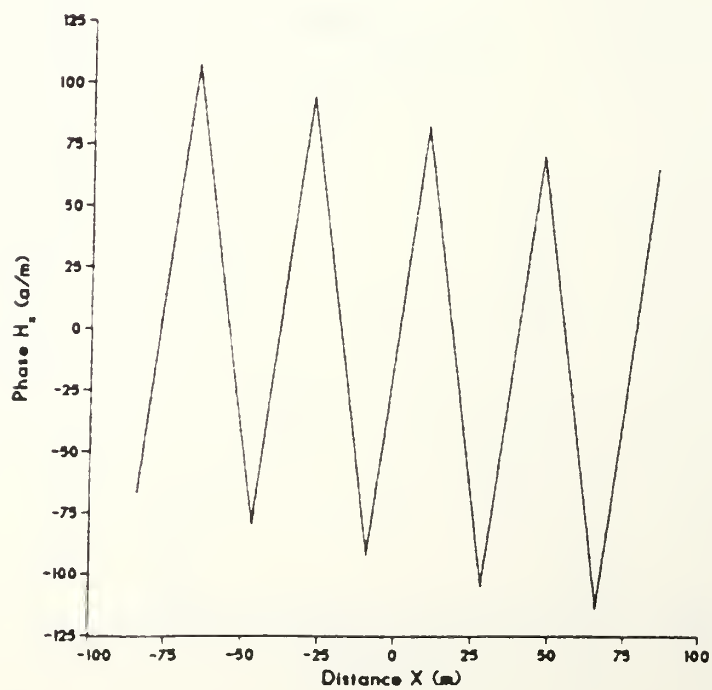

F=7.5MHZ

DIST VS MAG

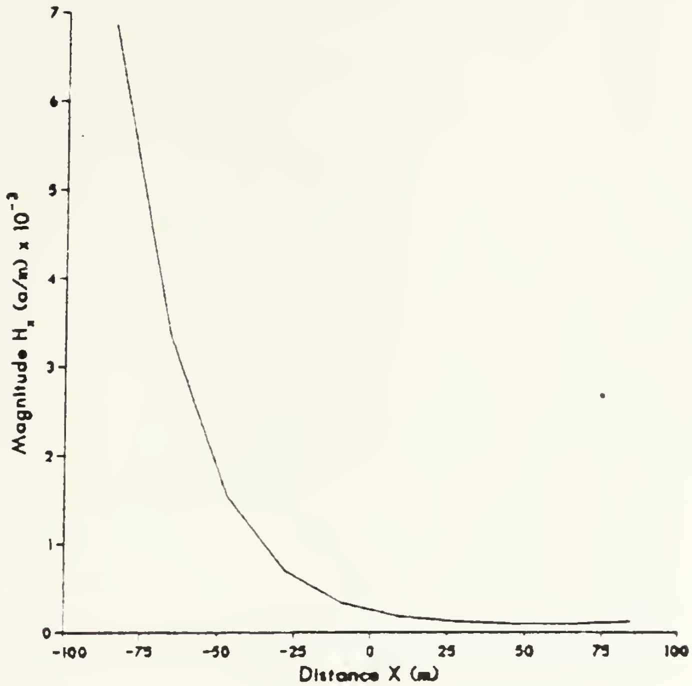


DIST VS PHASE

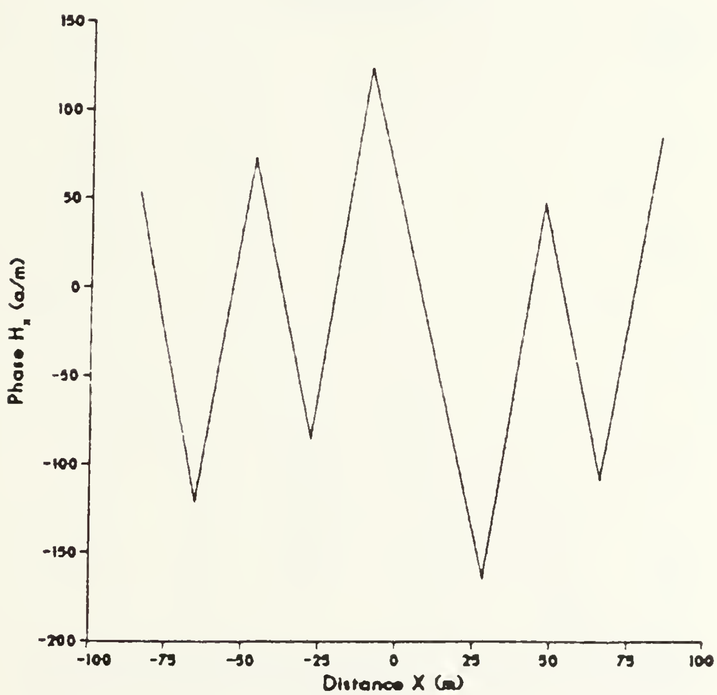

F=7MHZ

DIST VS MAG

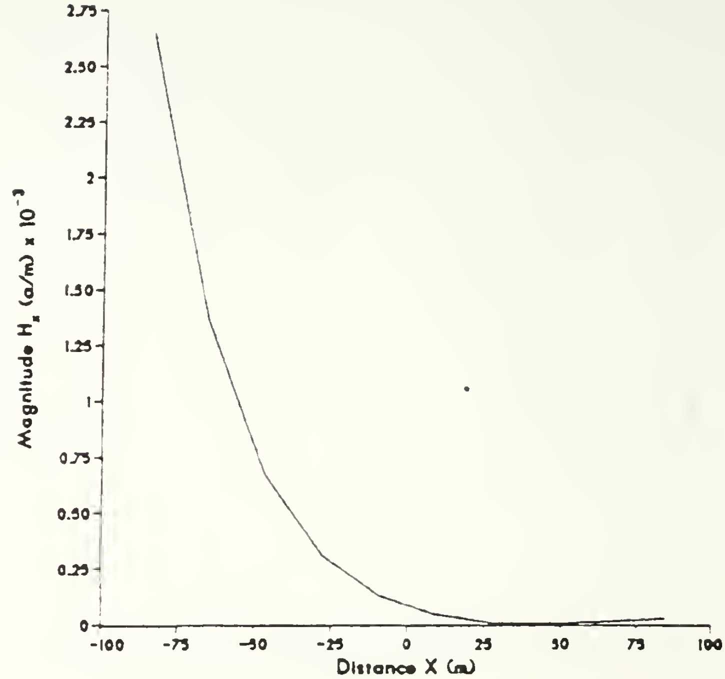


DIST VS PHASE

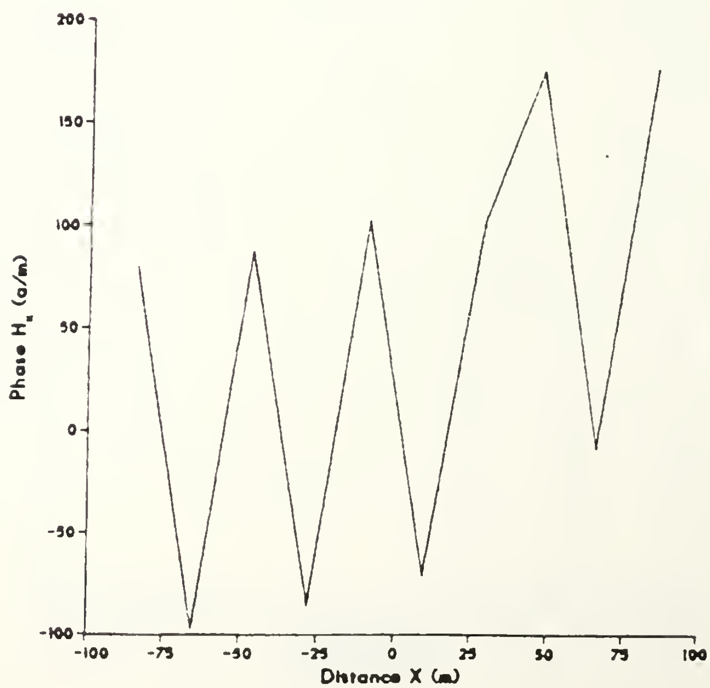

F=6.5MHZ

DIST VS MAG

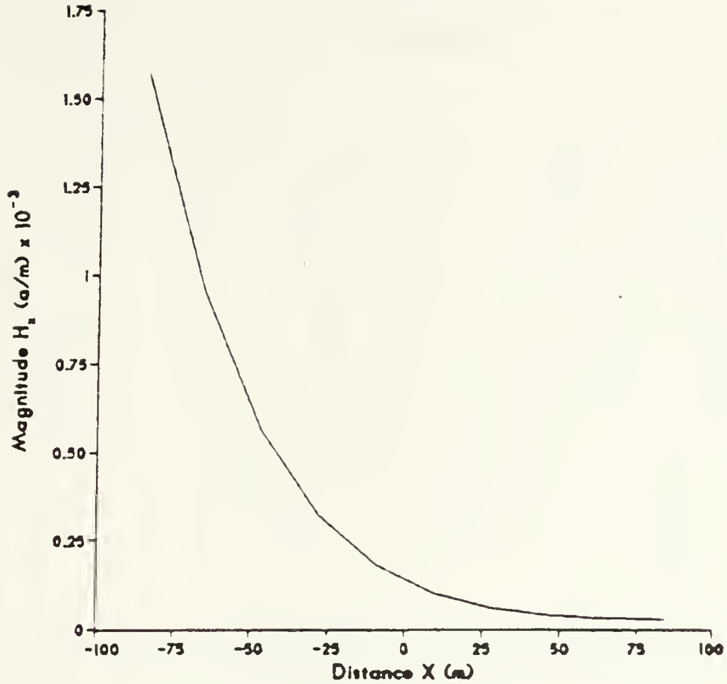


DIST VS PHASE

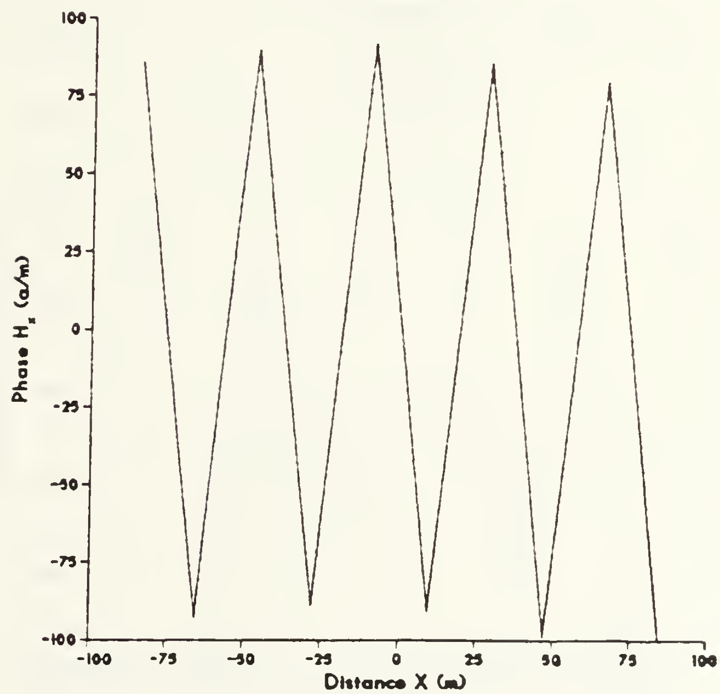

# APPENDIX D-NEAR FIELD EXPERIMENTAL RESULTS OF THE HALF SQUARE ARRAY WITH IN-PHASE FEED SOURCE

F=2MHZ

DIST VS MAG

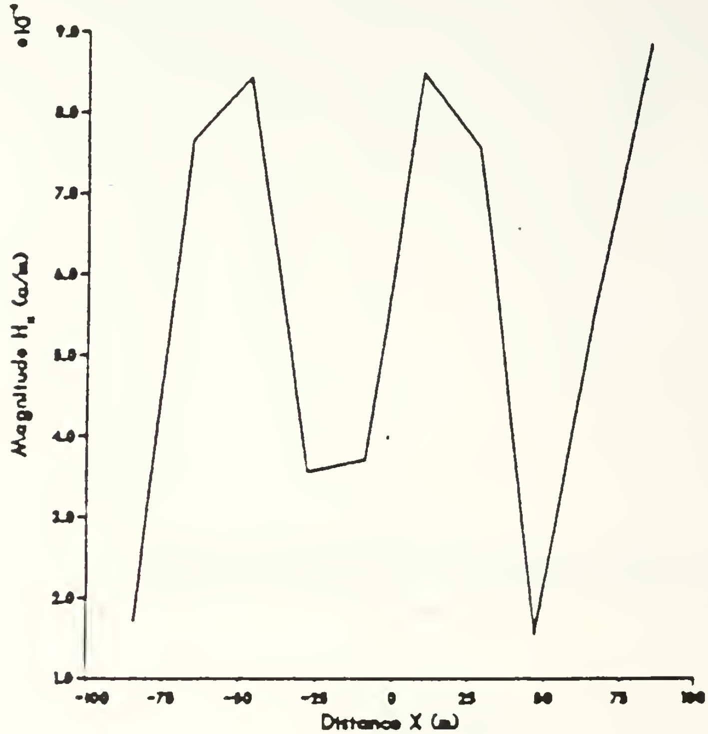


F=4MHZ

DIST VS MAG

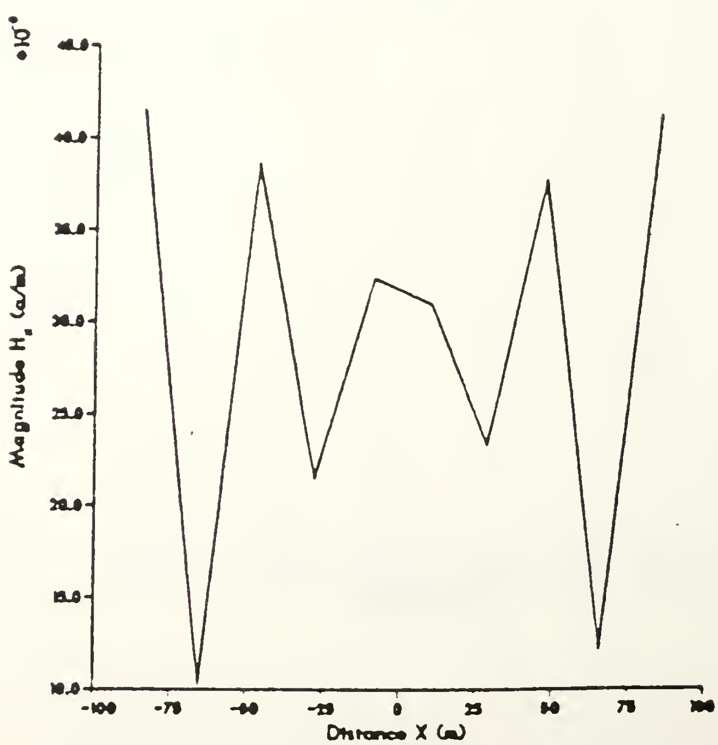

F=15MHZ

DIST VS MAG

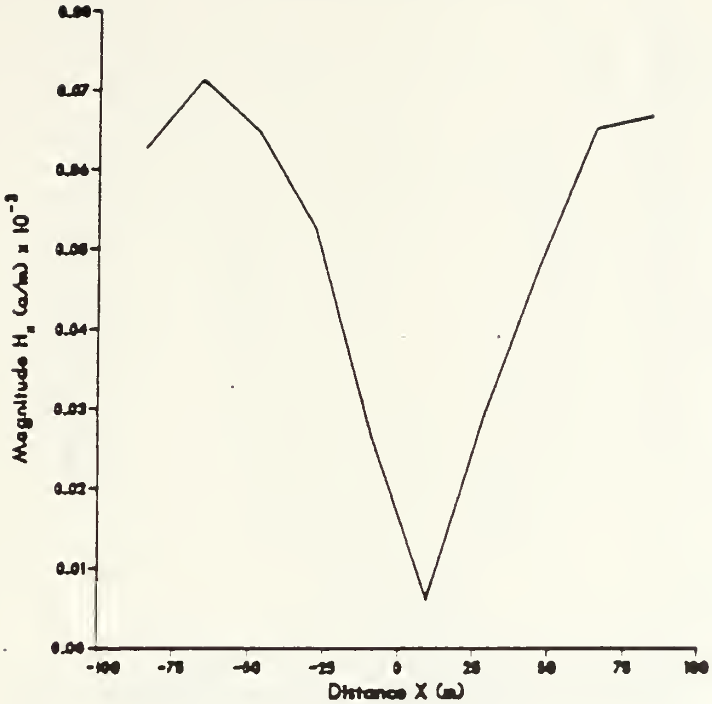


F=30MHZ

DIST VS MAG

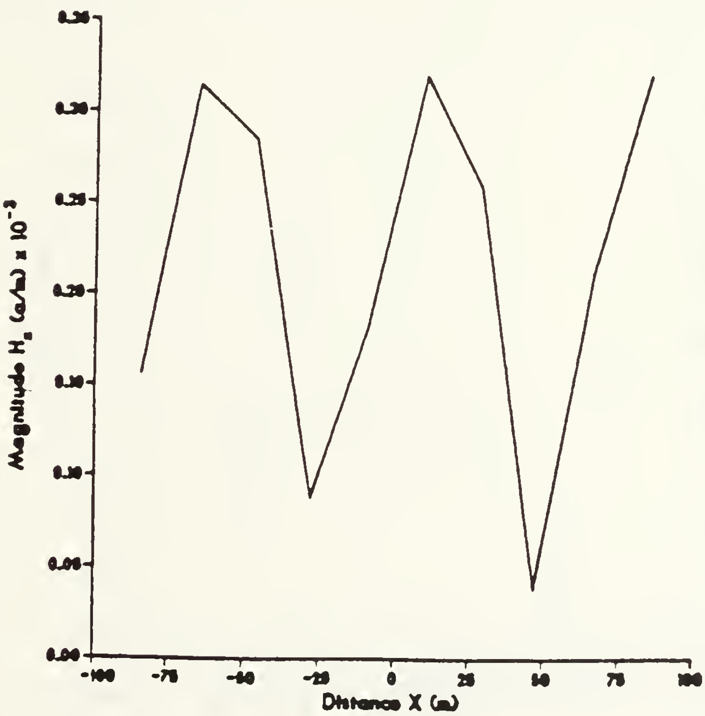

F=8.5MHZ

DIST VS MAG

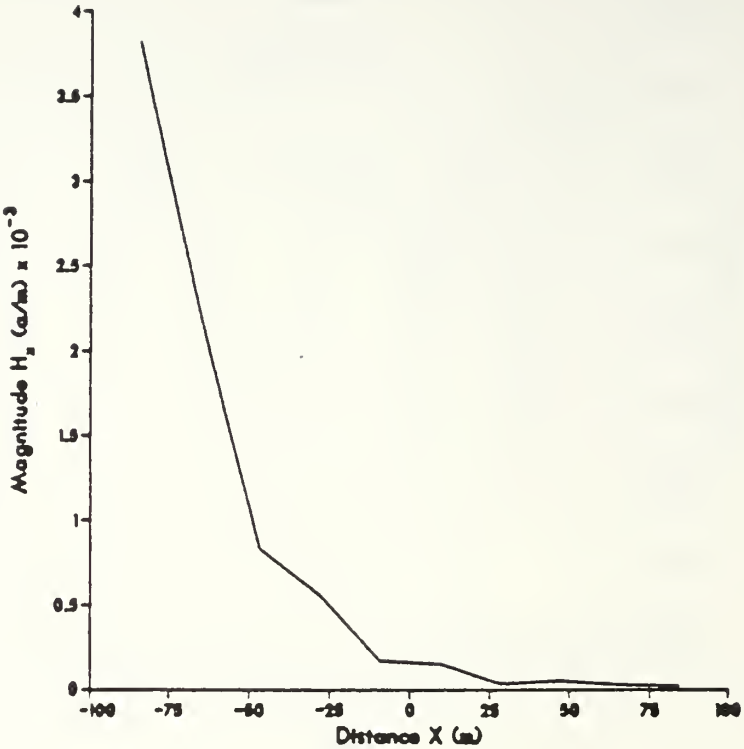


DIST VS PHASE

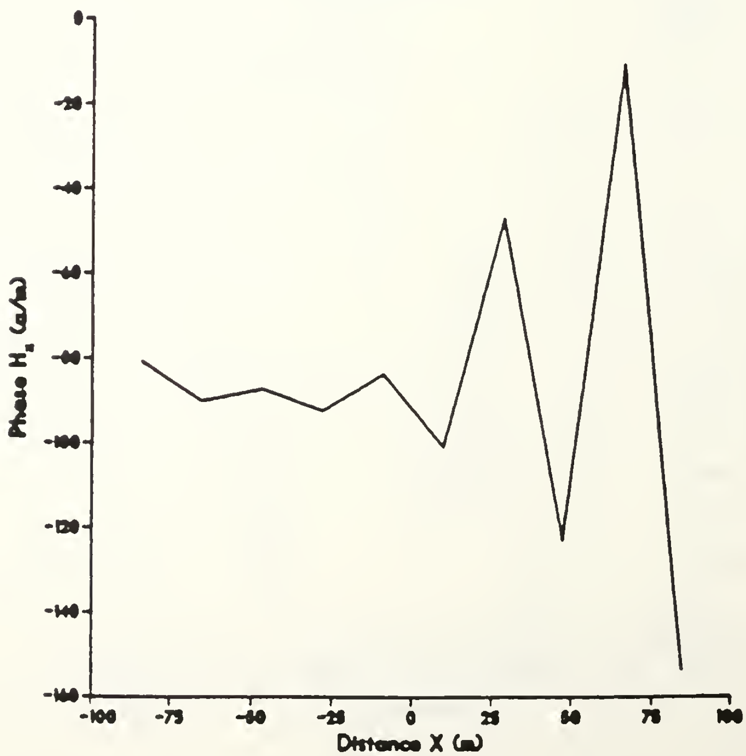

F=8.25 MHZ

DIST VS MAG

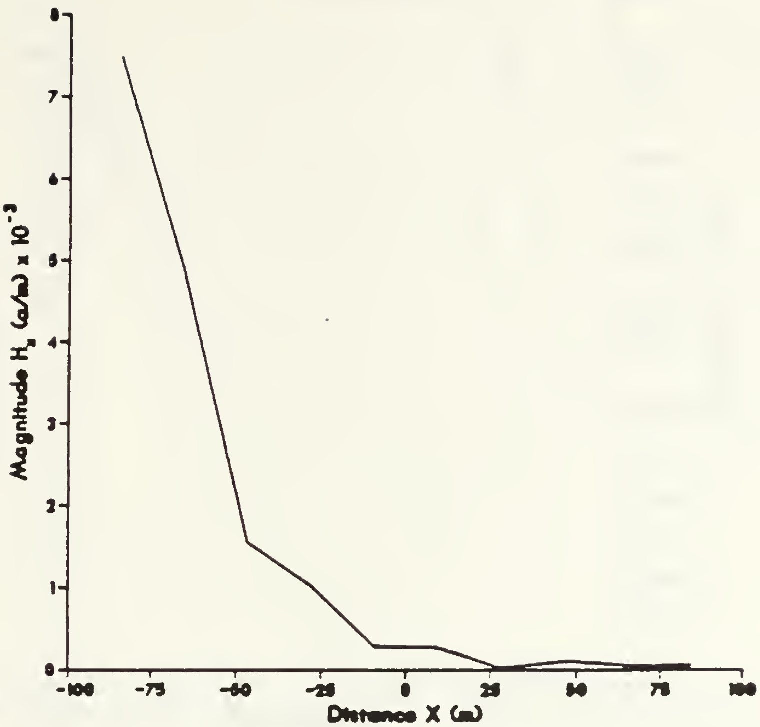


DIST VS PHASE

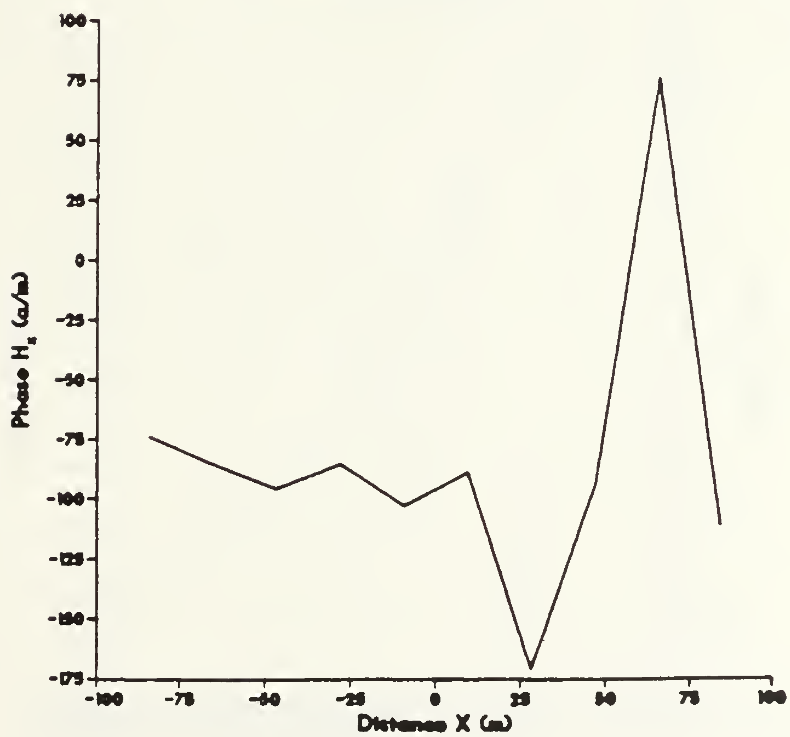

F=8MHZ

DIST VS MAG

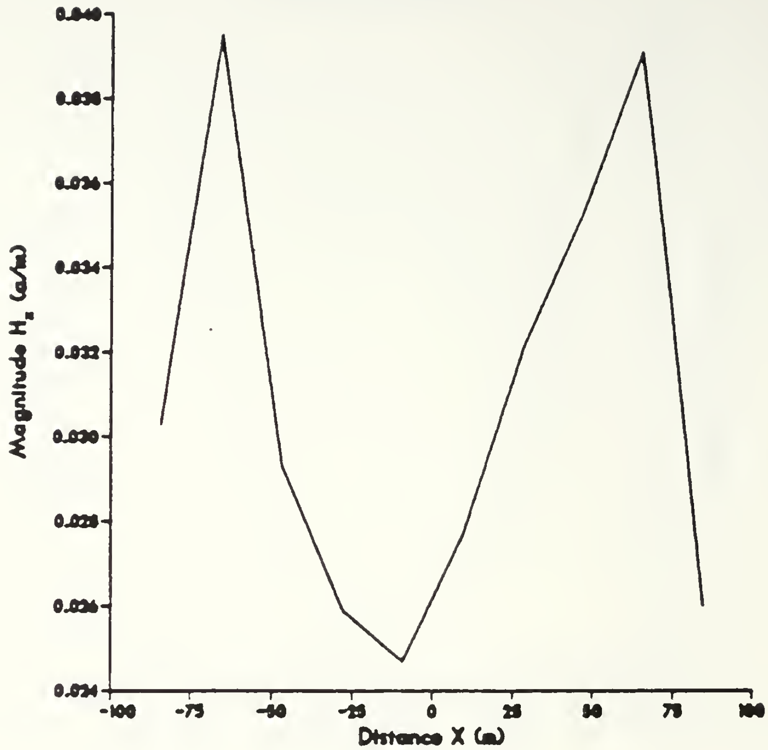


DIST VS PHASE

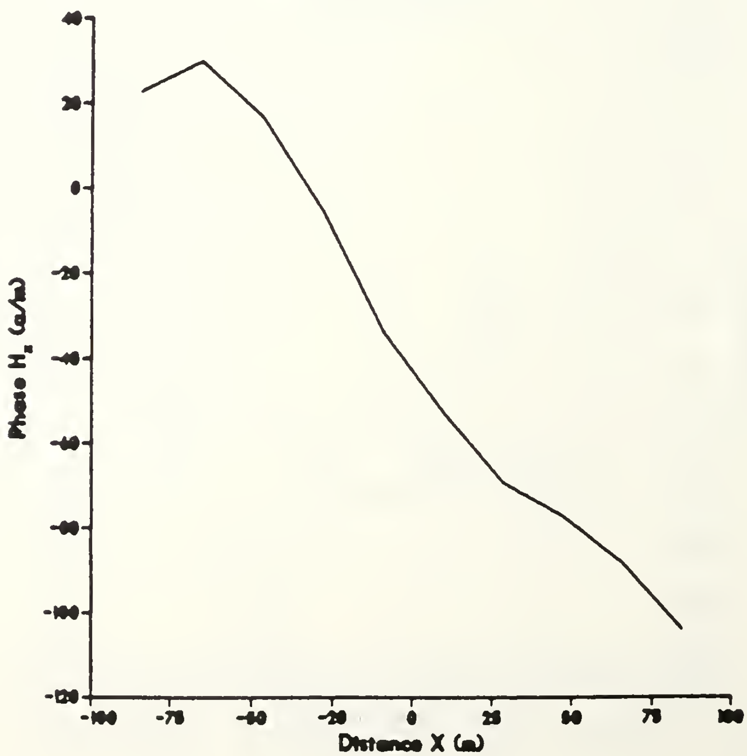

HSA F=7.75 MHZ

DIST VS MAG

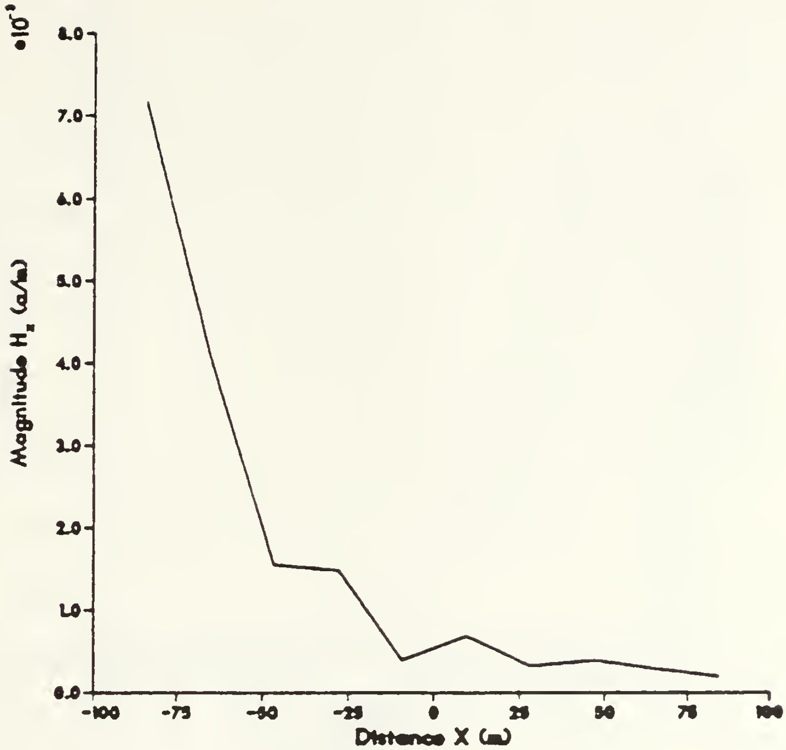


DIST VS PHASE

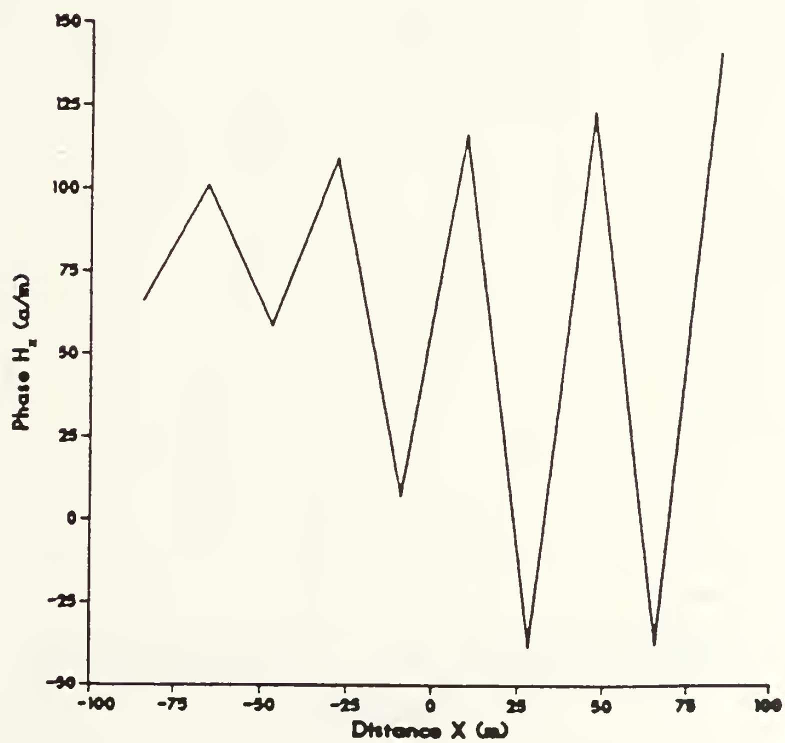

F=7.5MHZ

DIST VS MAG

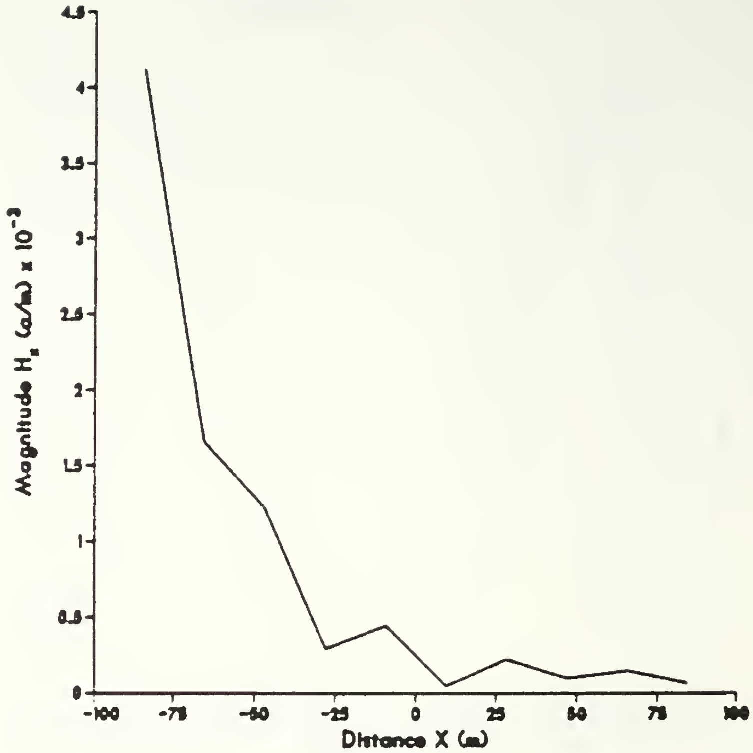


DIST VS PHASE

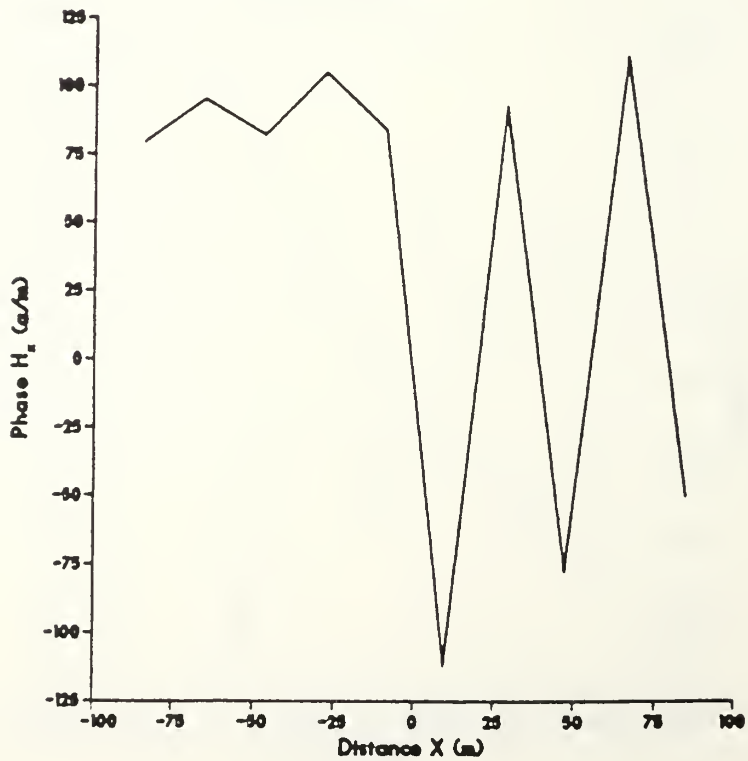

F=7MHZ

DIST VS MAG

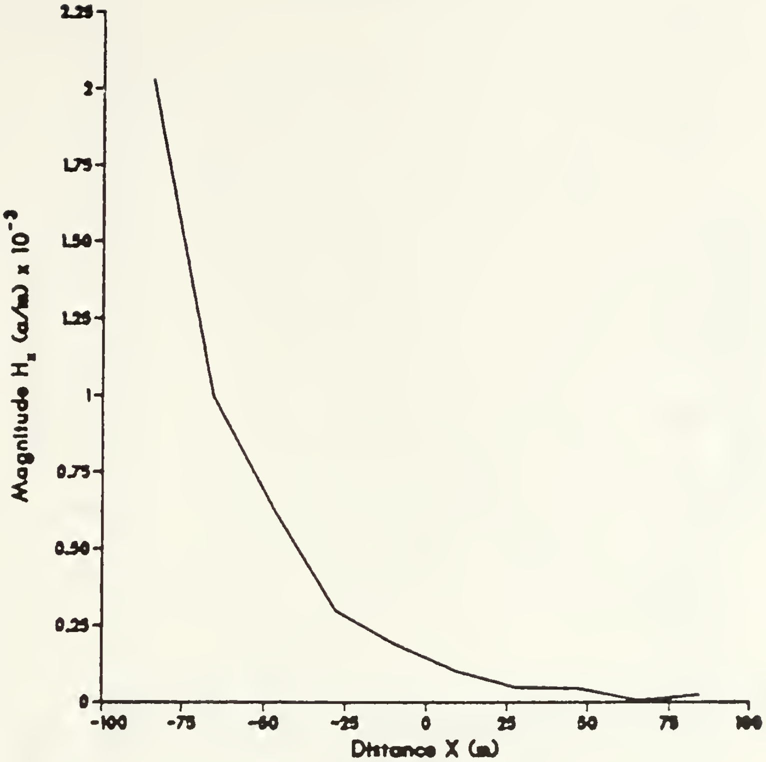


DIST VS PHASE

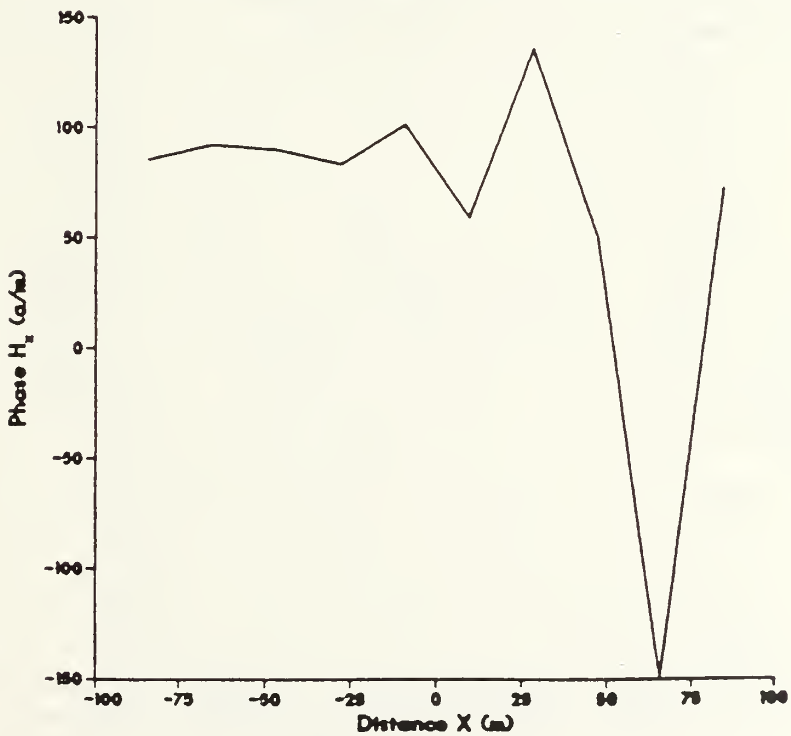

F=6.5MHZ

DIST VS MAG

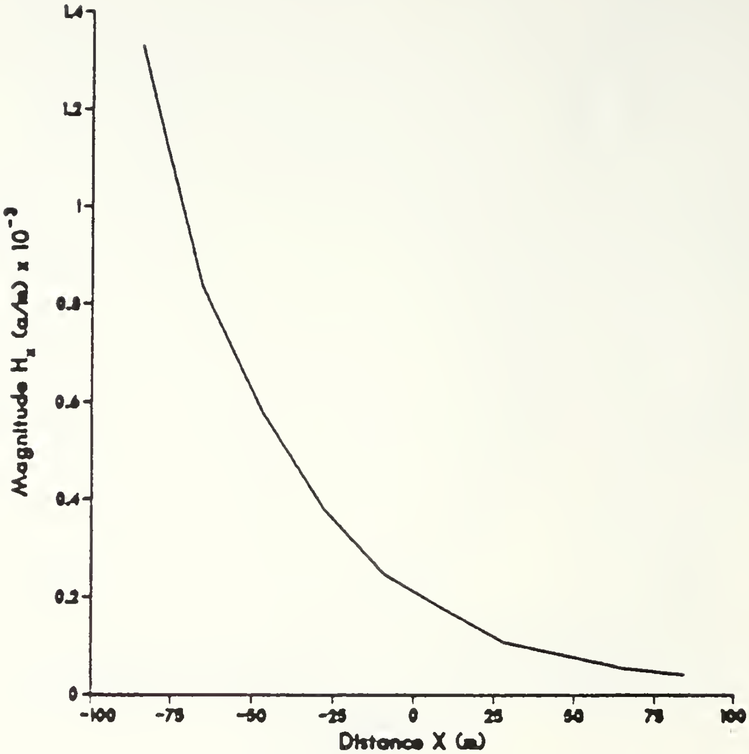


DIST VS PHASE

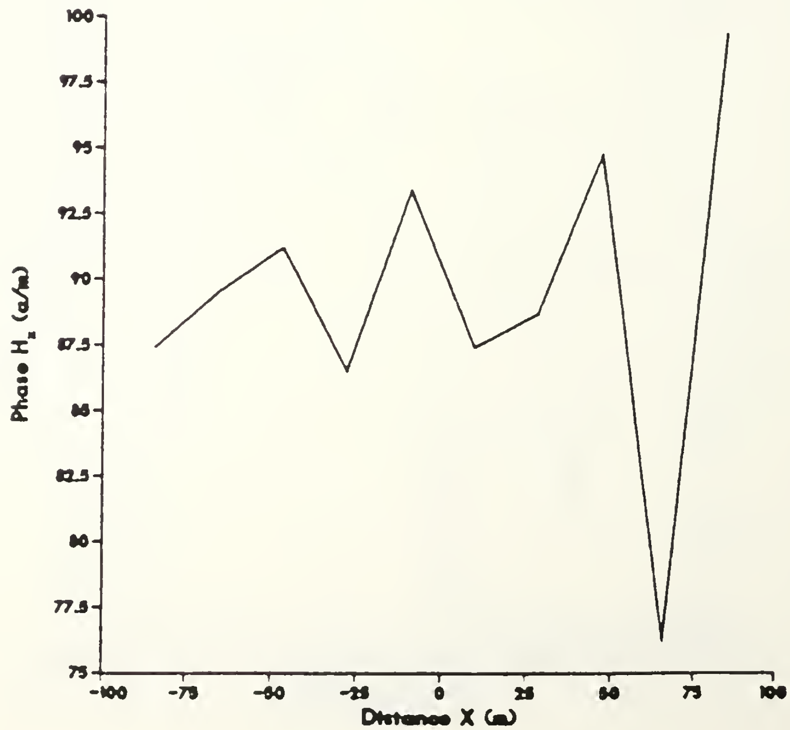

F=6.25MHZ

DIST VS MAG

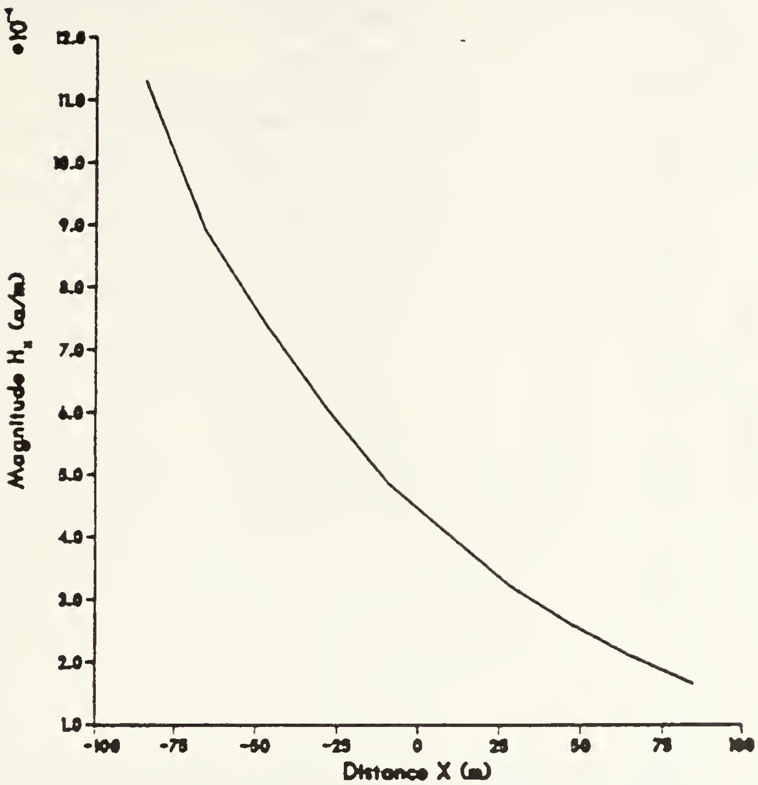


DIST VS PHASE

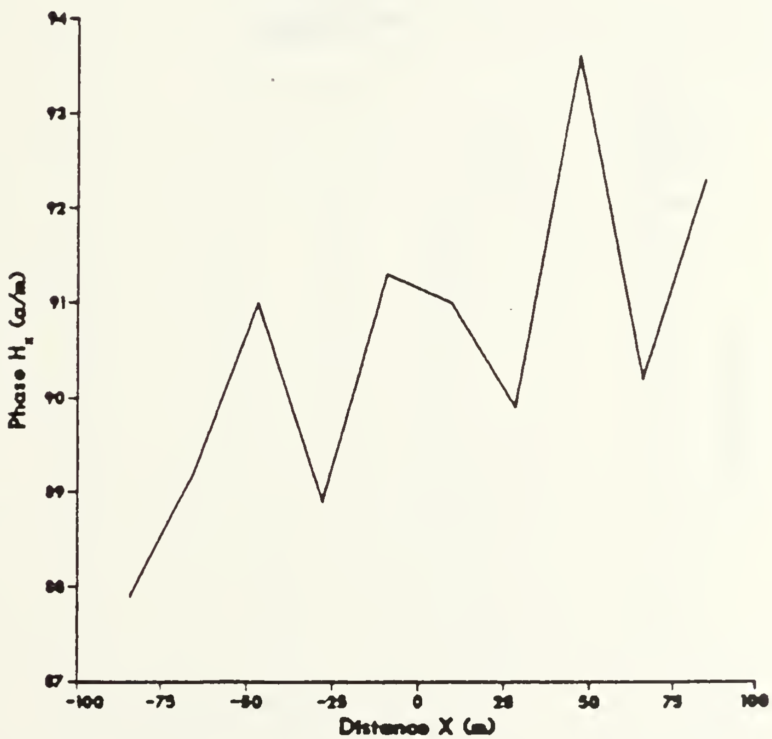

F=6MHZ

DIST VS MAG

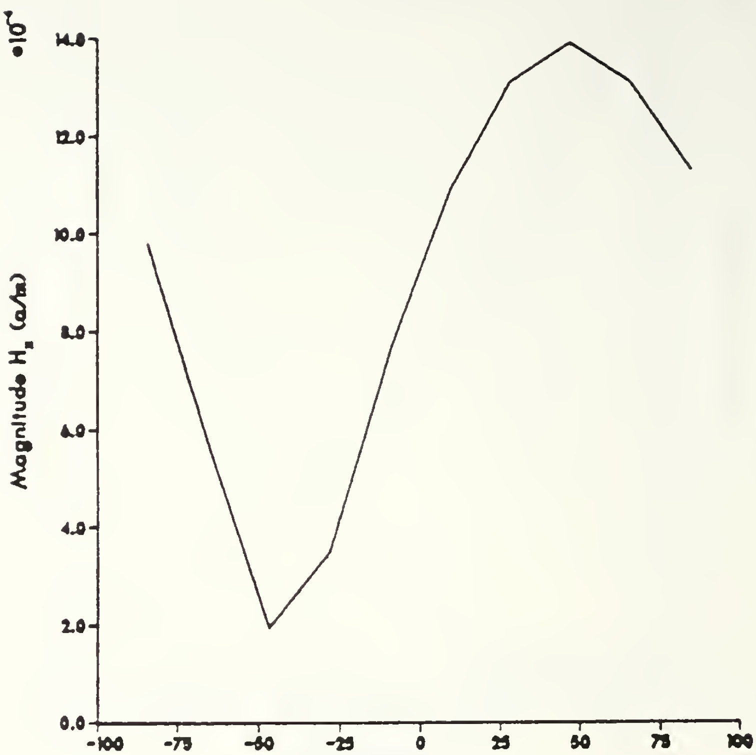


DIST VS PHASE

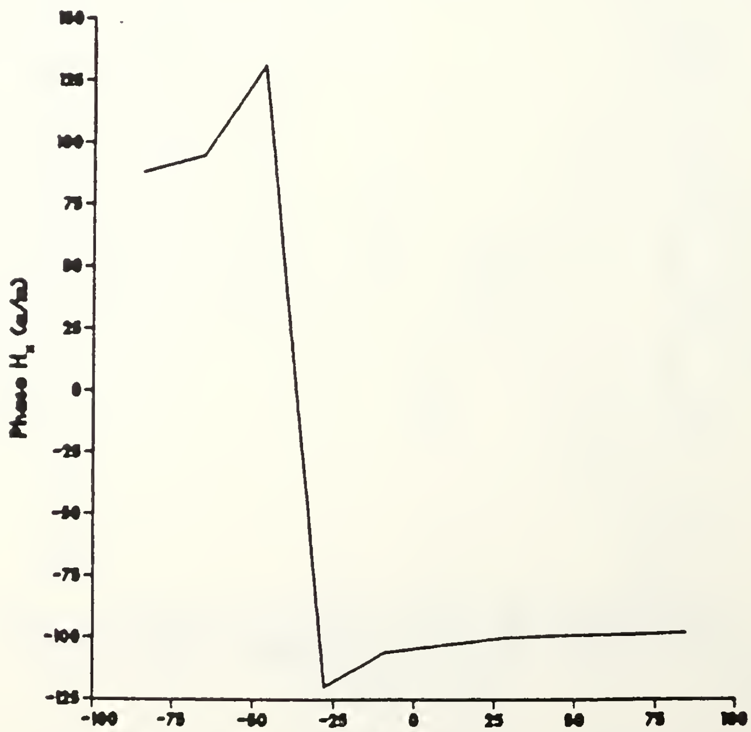

## APPENDIX E-NEAR FIELD EXPERIMENTAL RESULTS OF THE HALF SQUARE ARRAY WITH ANTI-PHASE FEED SOURCE

F=2 MHZ

DIST VS MAG

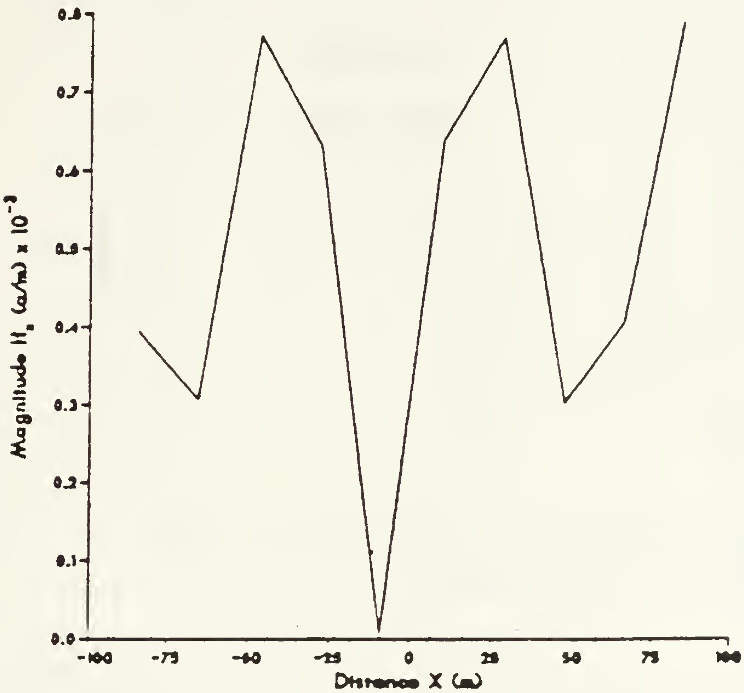


F=3 MHZ

DIST VS MAG

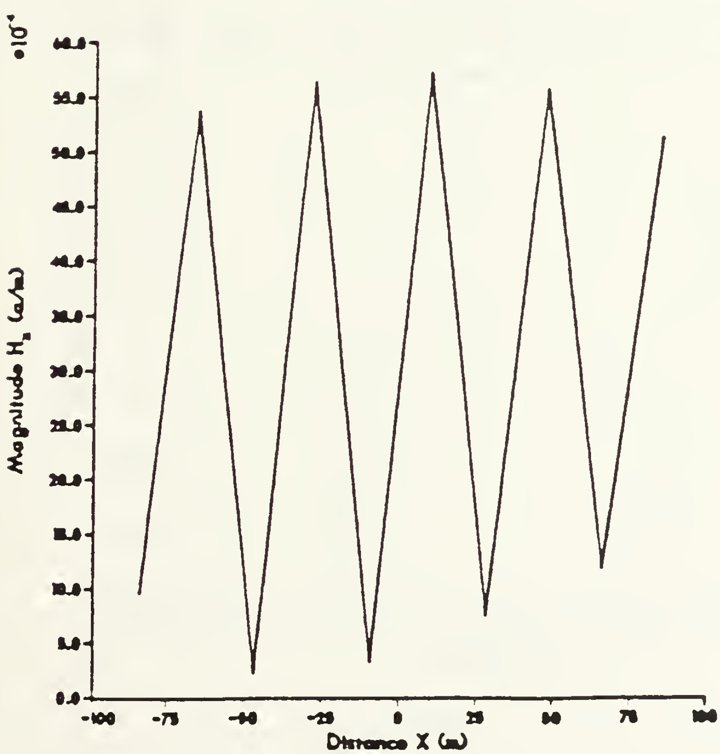

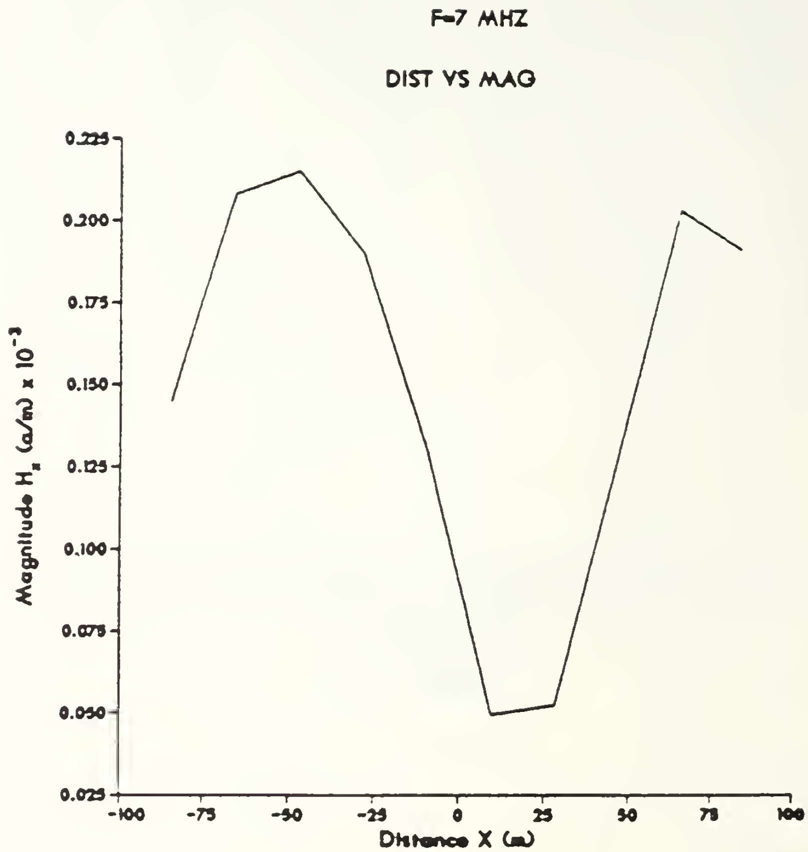
F=7 MHZ
DIST VS MAG
Magnitude $H_x$ (a/m) x $10^{-3}$
0.225
0.200
0.175
0.150
0.125
0.100
0.075
0.050
0.025
-100
-75
-50
-25
0
25
50
75
100
Distance X (m)

F=6 MHZ

DIST VS MAG

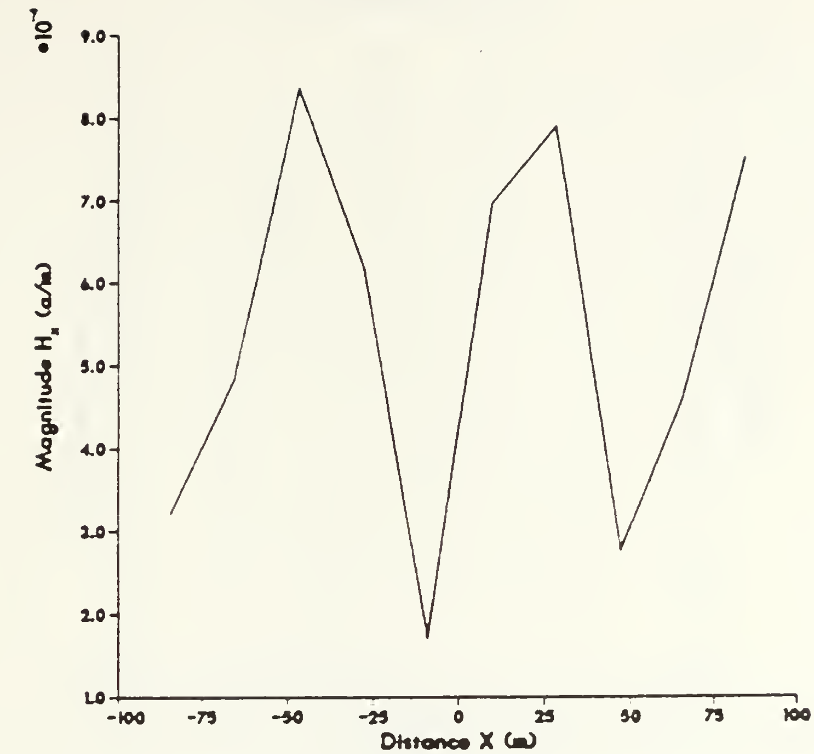


F=6.5 MHZ

DIST VS MAG

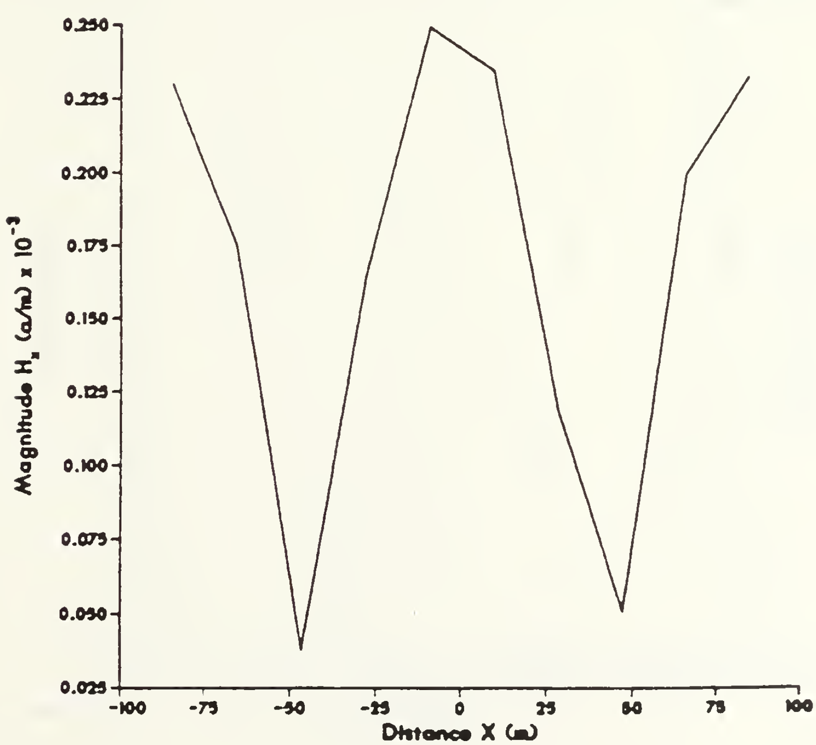

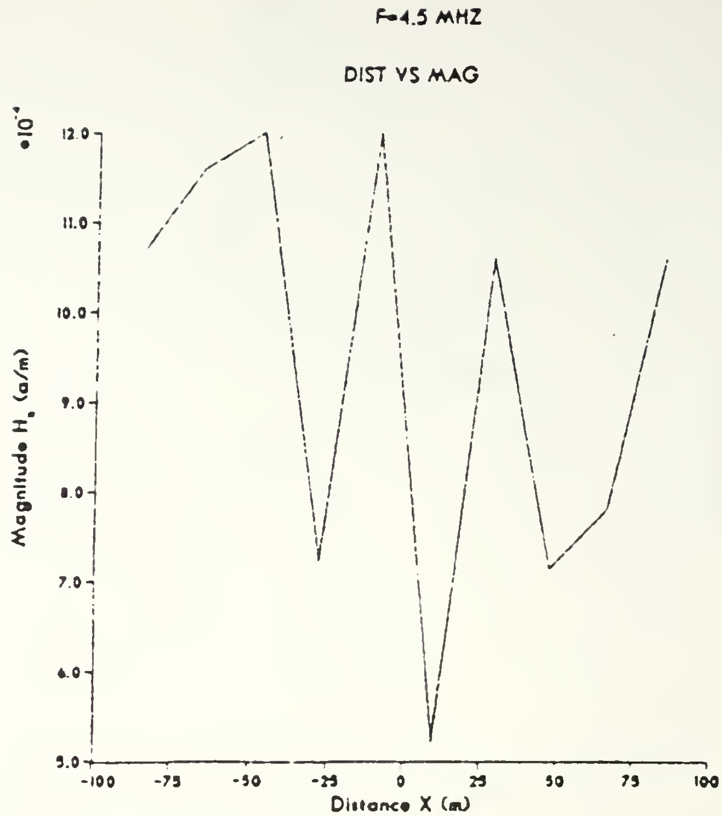
F=4.5 MHZ
DIST VS MAG
*10^-4
Magnitude H_z (a/m)
Distance X (m)

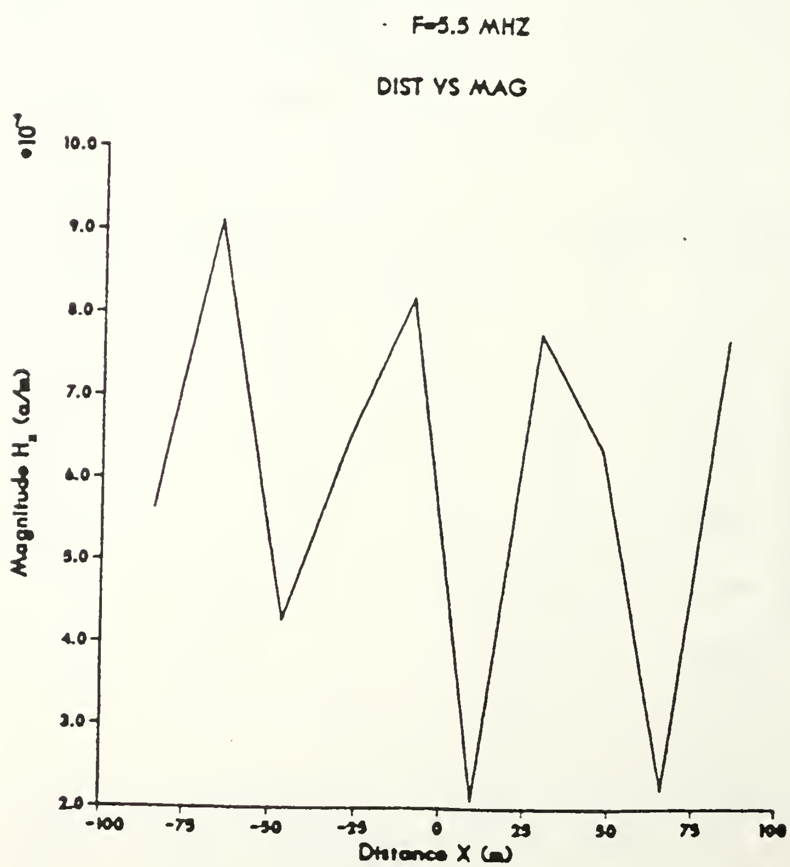
F=5.5 MHZ
DIST VS MAG
*10^-4
Magnitude H_z (a/m)
Distance X (m)

F=4 MHZ

DIST VS MAG

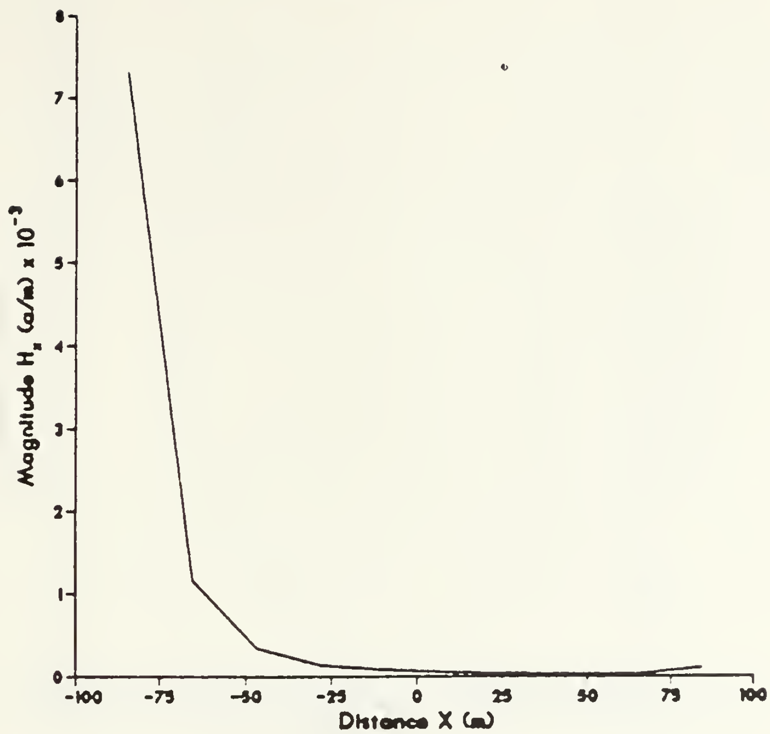


DIST VS PHASE

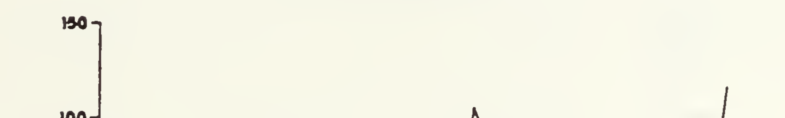

F=3.85 MHZ

DIST VS MAG

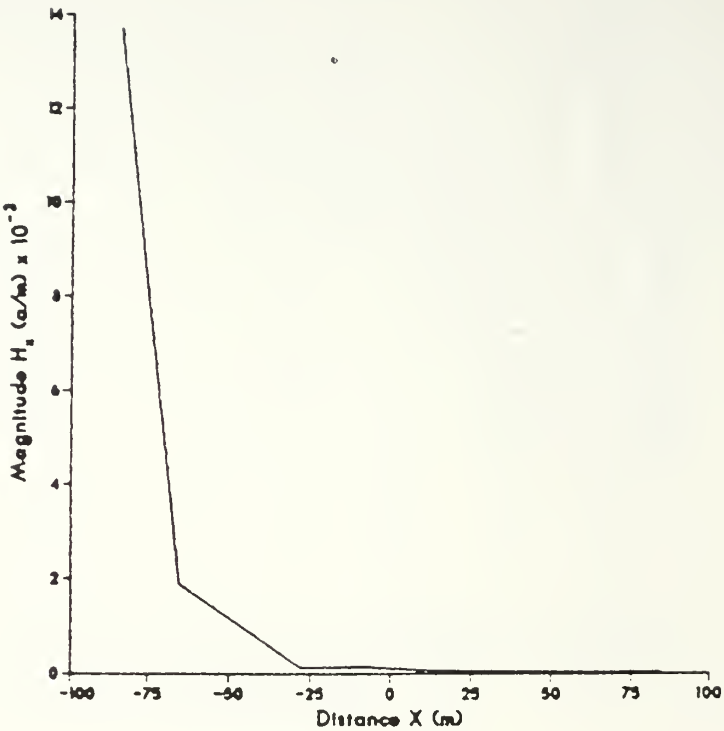


DIST VS PHASE

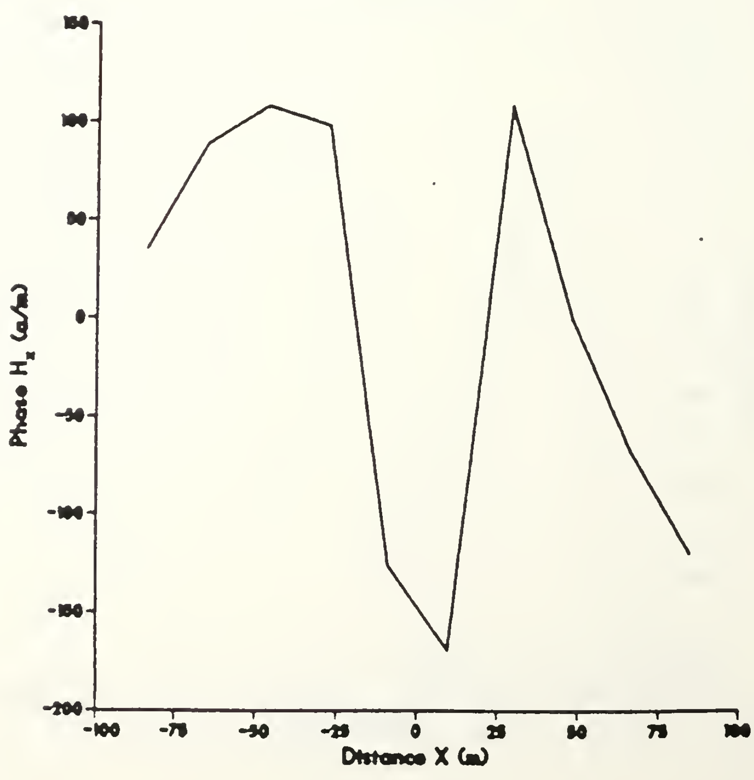

F=3.75 MHZ

DIST VS MAG

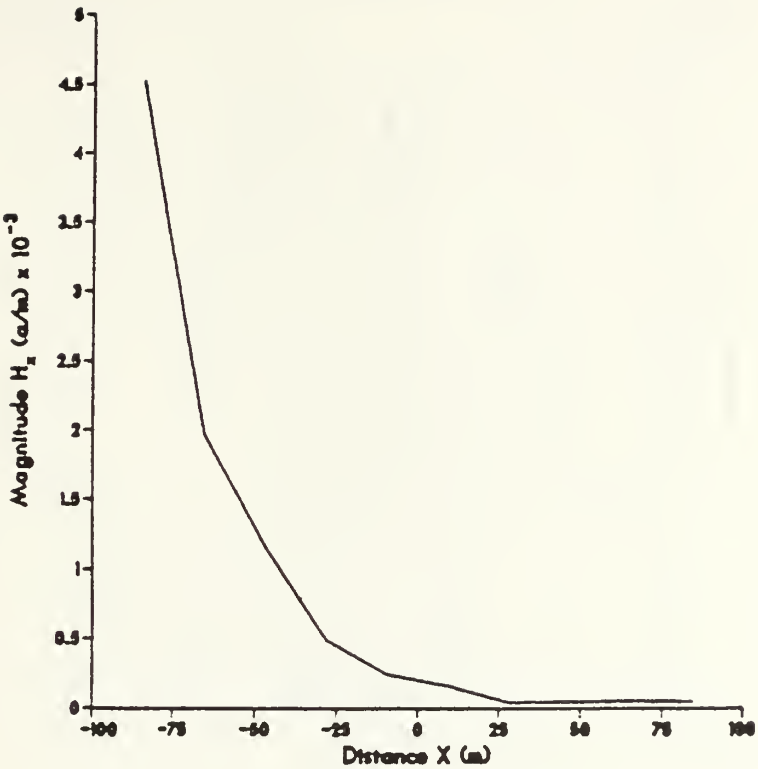


DIST VS PHASE

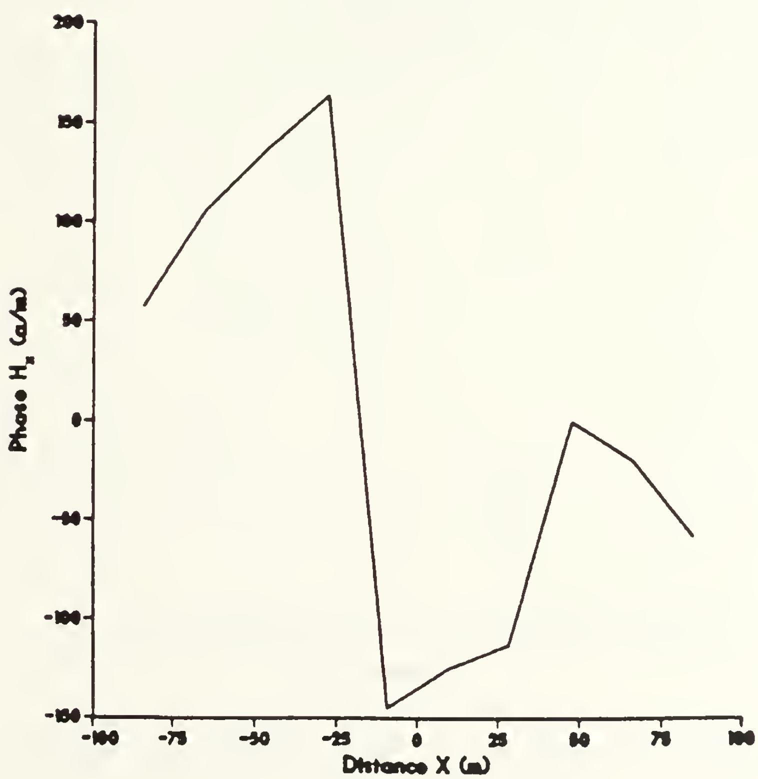

F=3.5 MHZ

DIST VS MAG

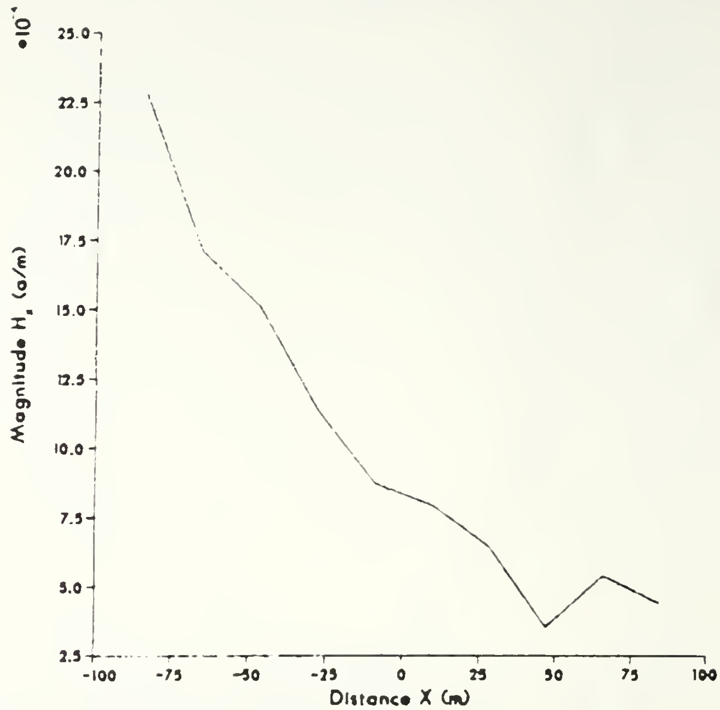


DIST VS PHASE

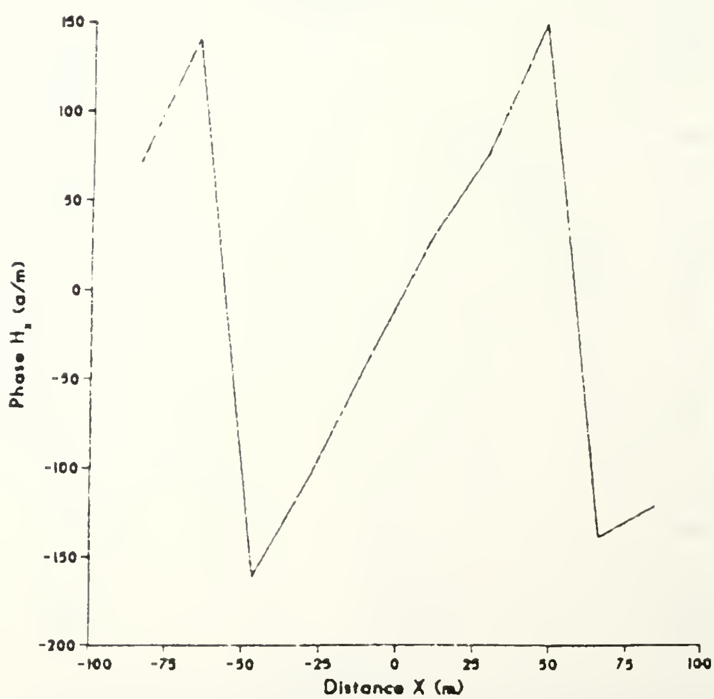

F=3.25 MHZ

DIST VS MAG

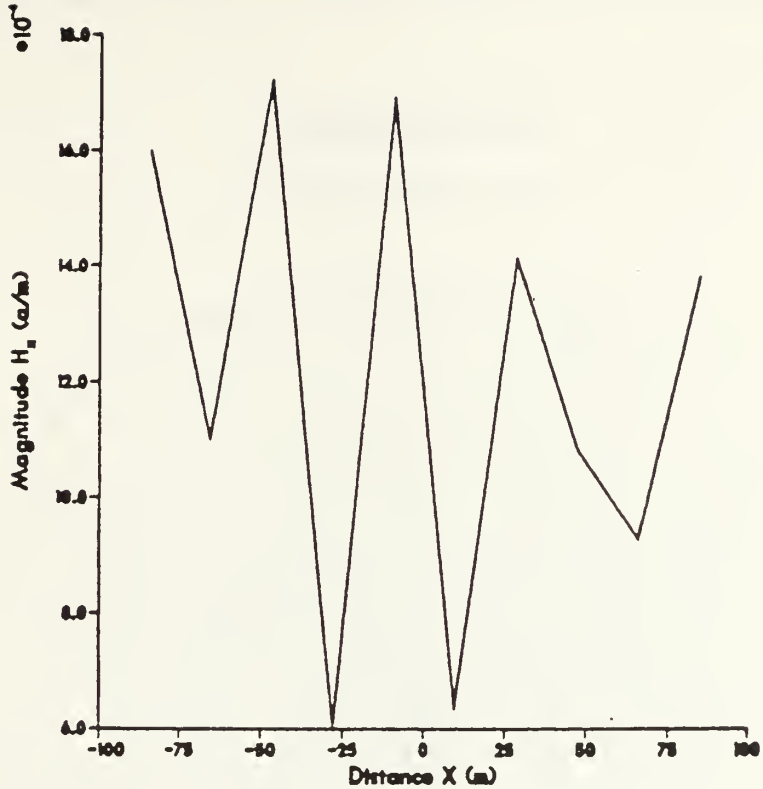


F=3.4 MHZ

DIST VS MAG

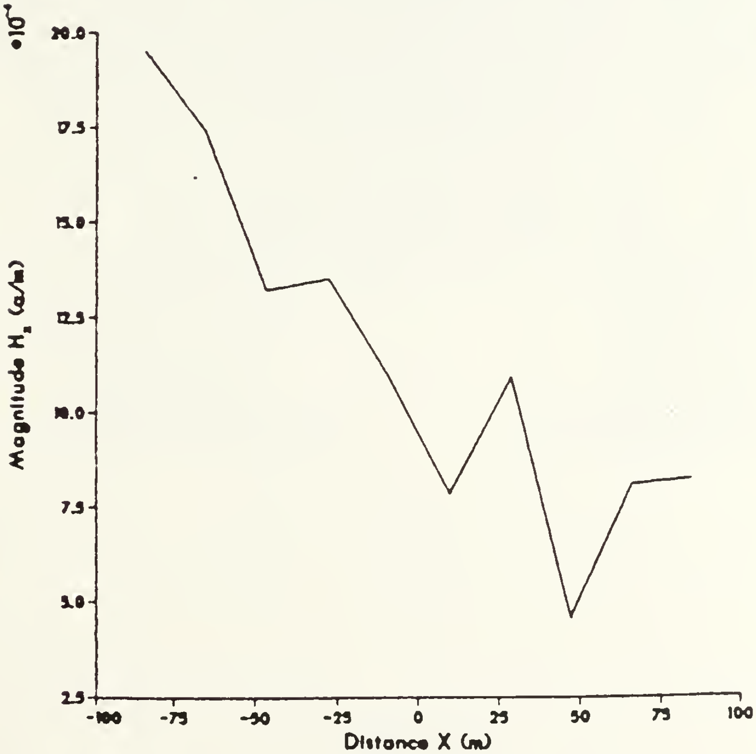

# APPENDIX F-HALF SQUARE ANTENNA RADIATION PATTERNS

F=2 MHZ

ANTI-PHASE

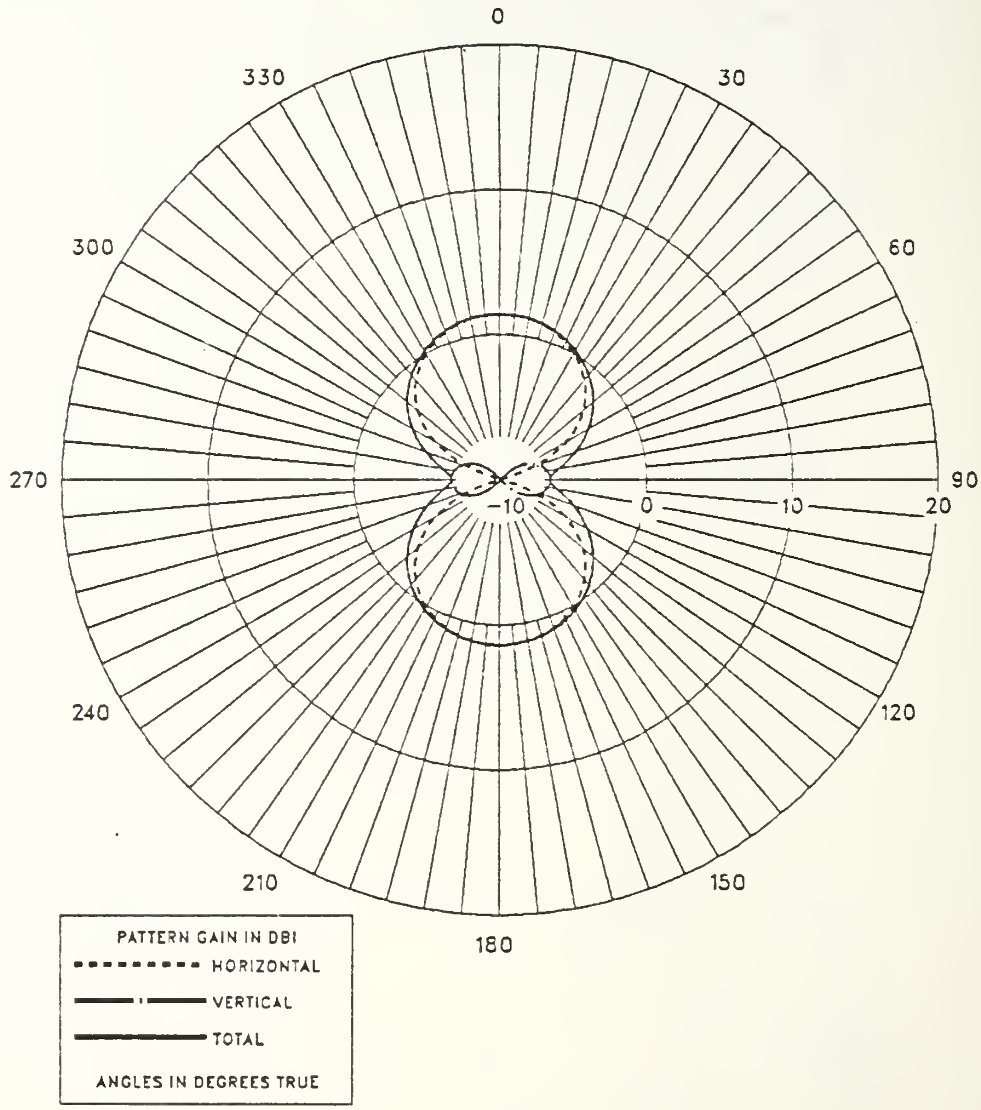

F=3 MHZ

ANTI–PHASE

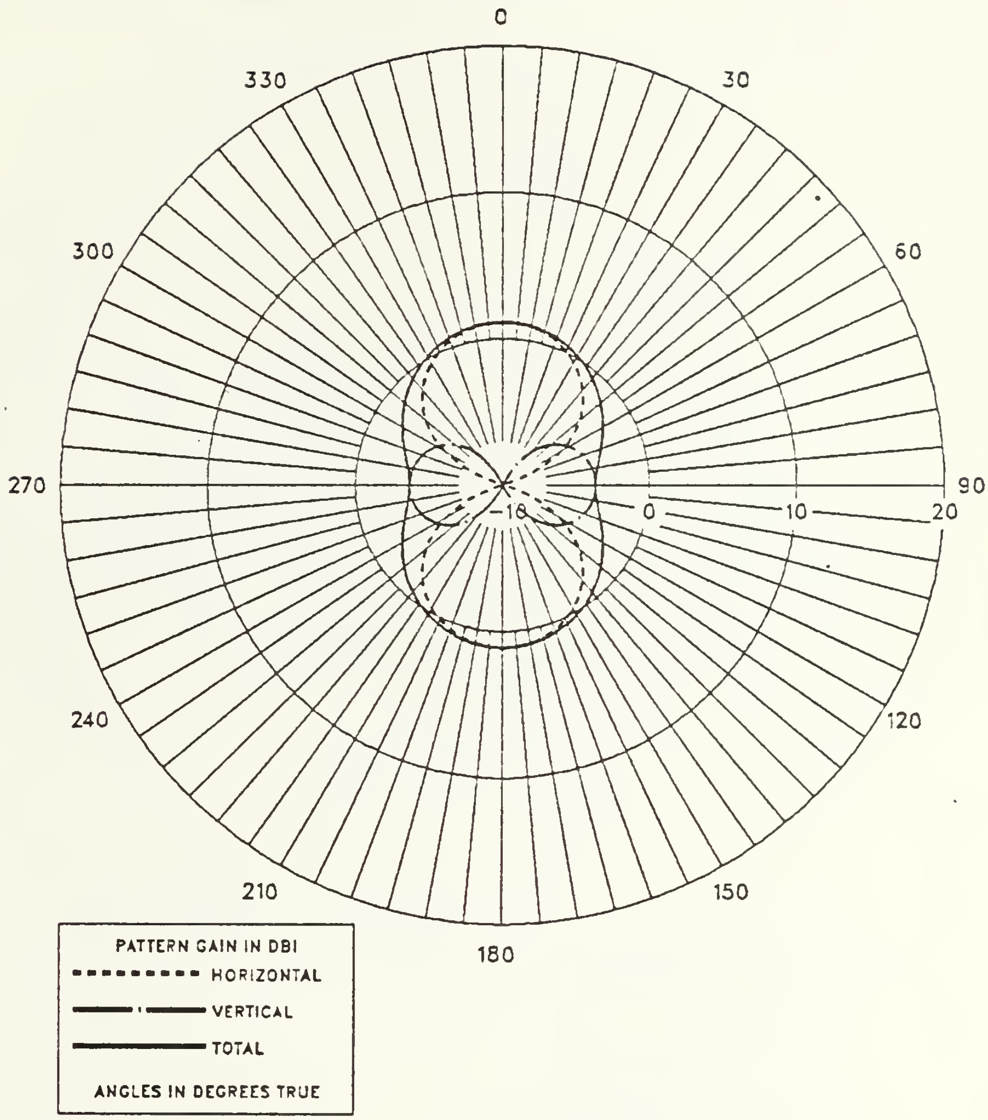

F=4 MHZ

ANTI-PHASE

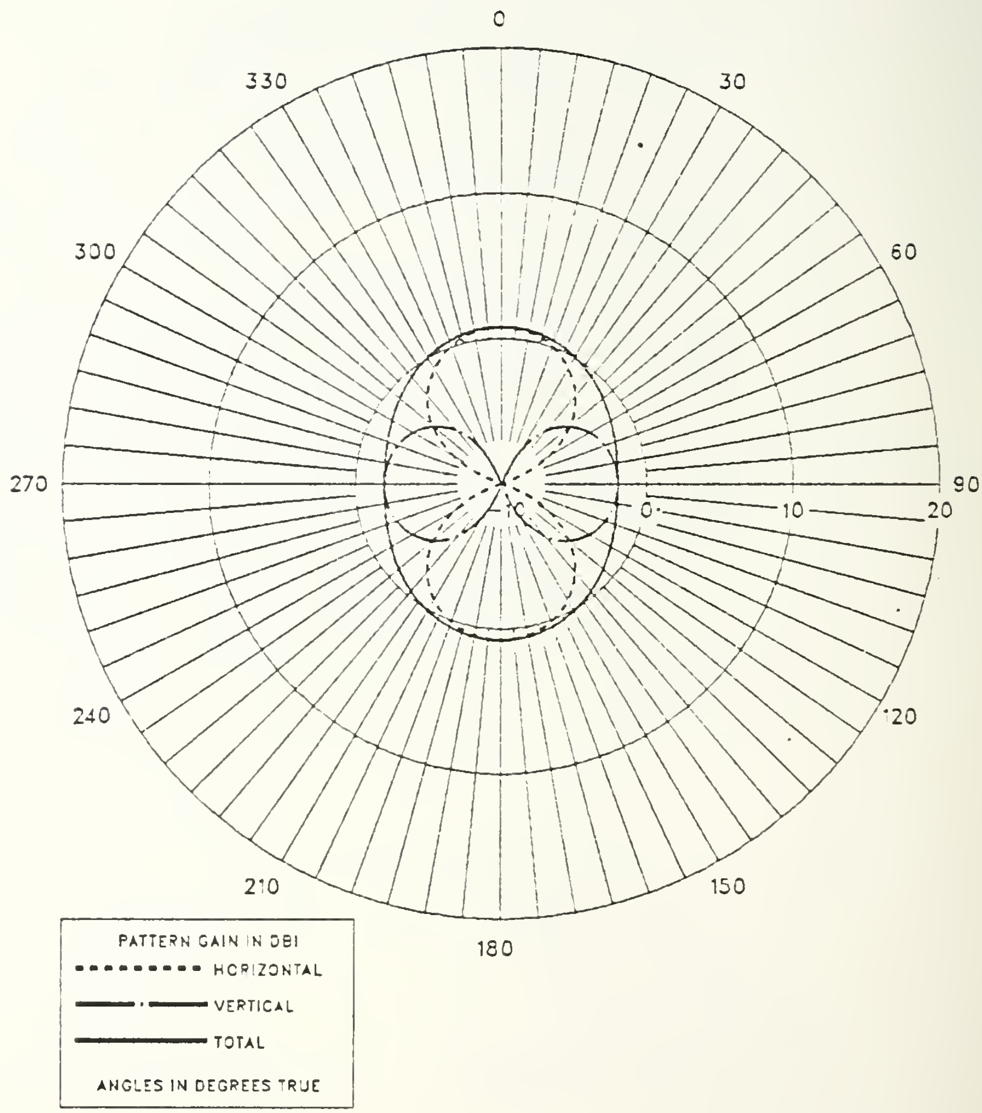

F=6 MHZ

ANTI–PHASE

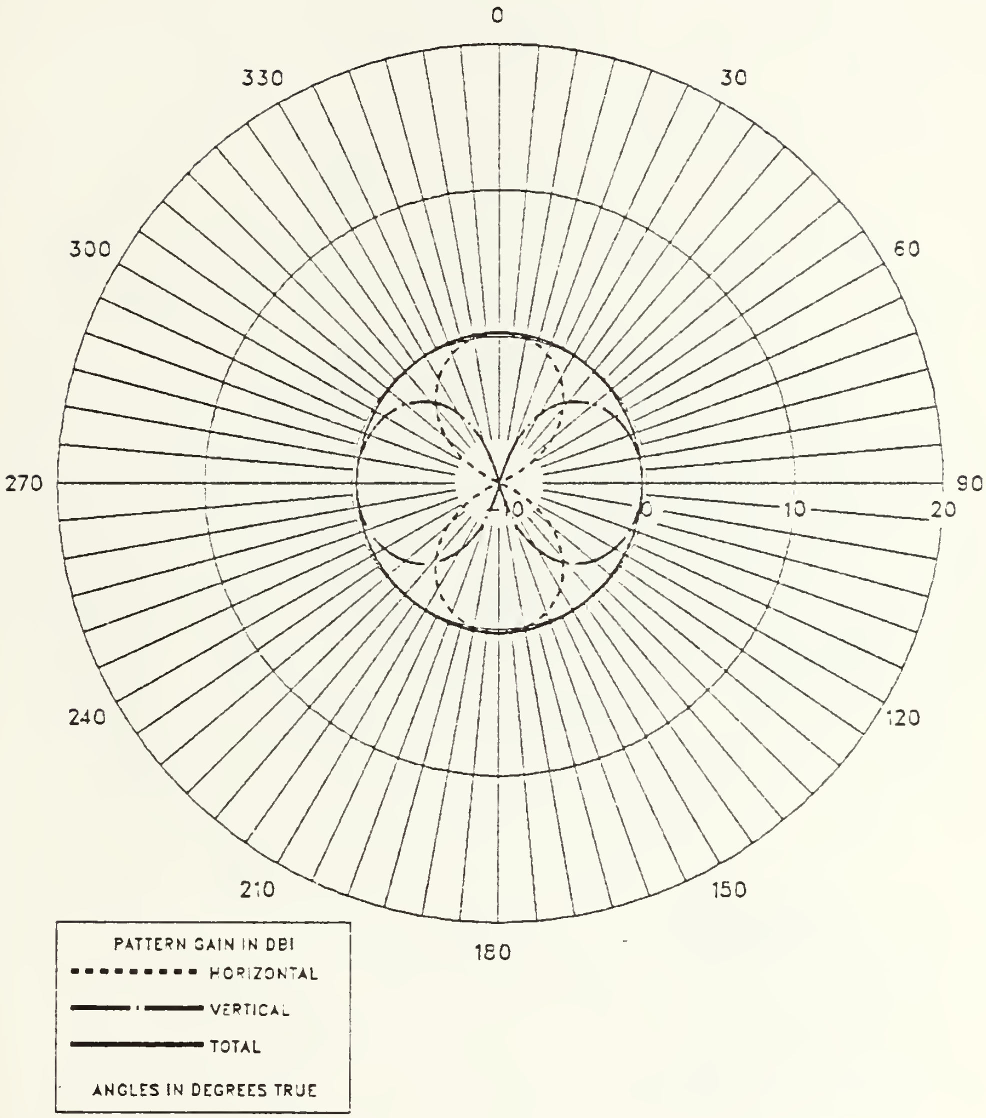

F=8 MHZ

ANTI-PHASE

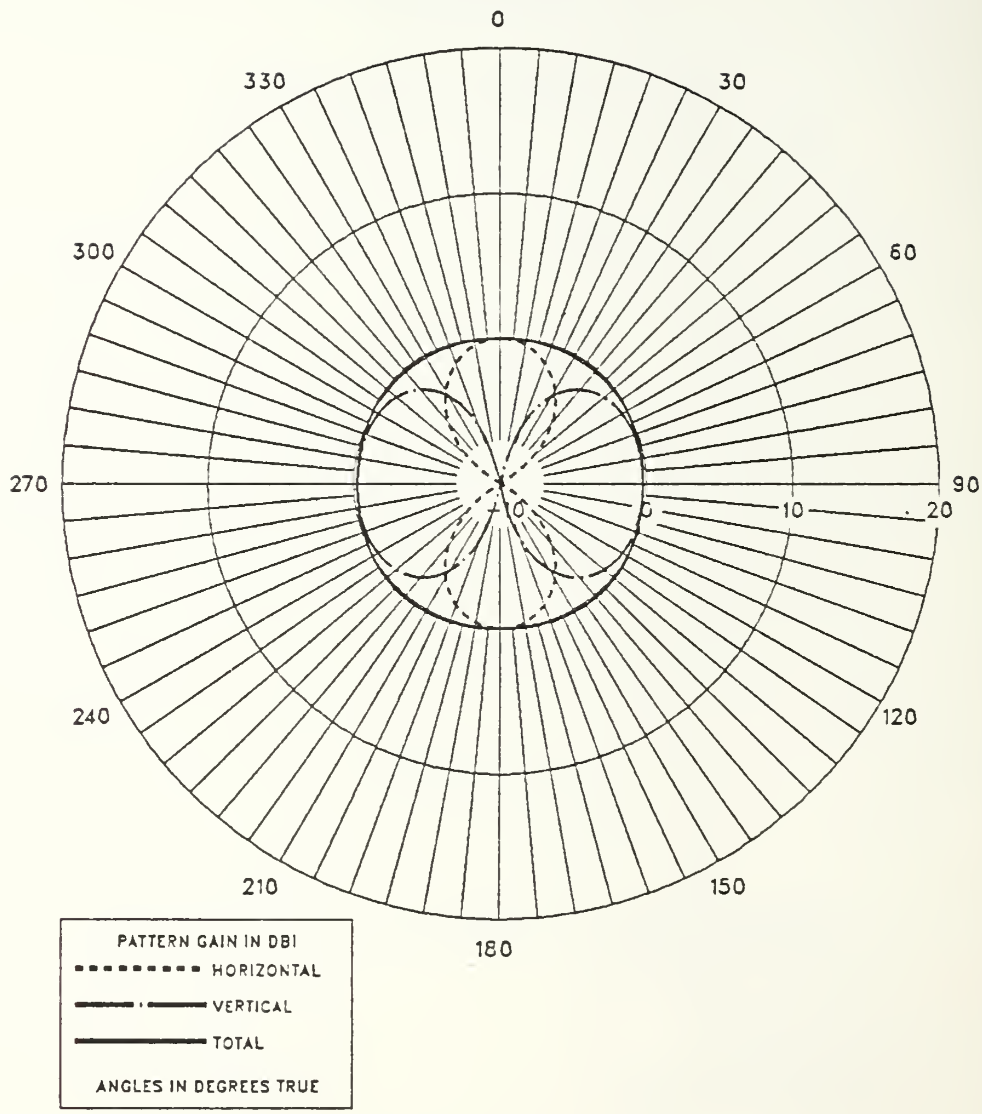

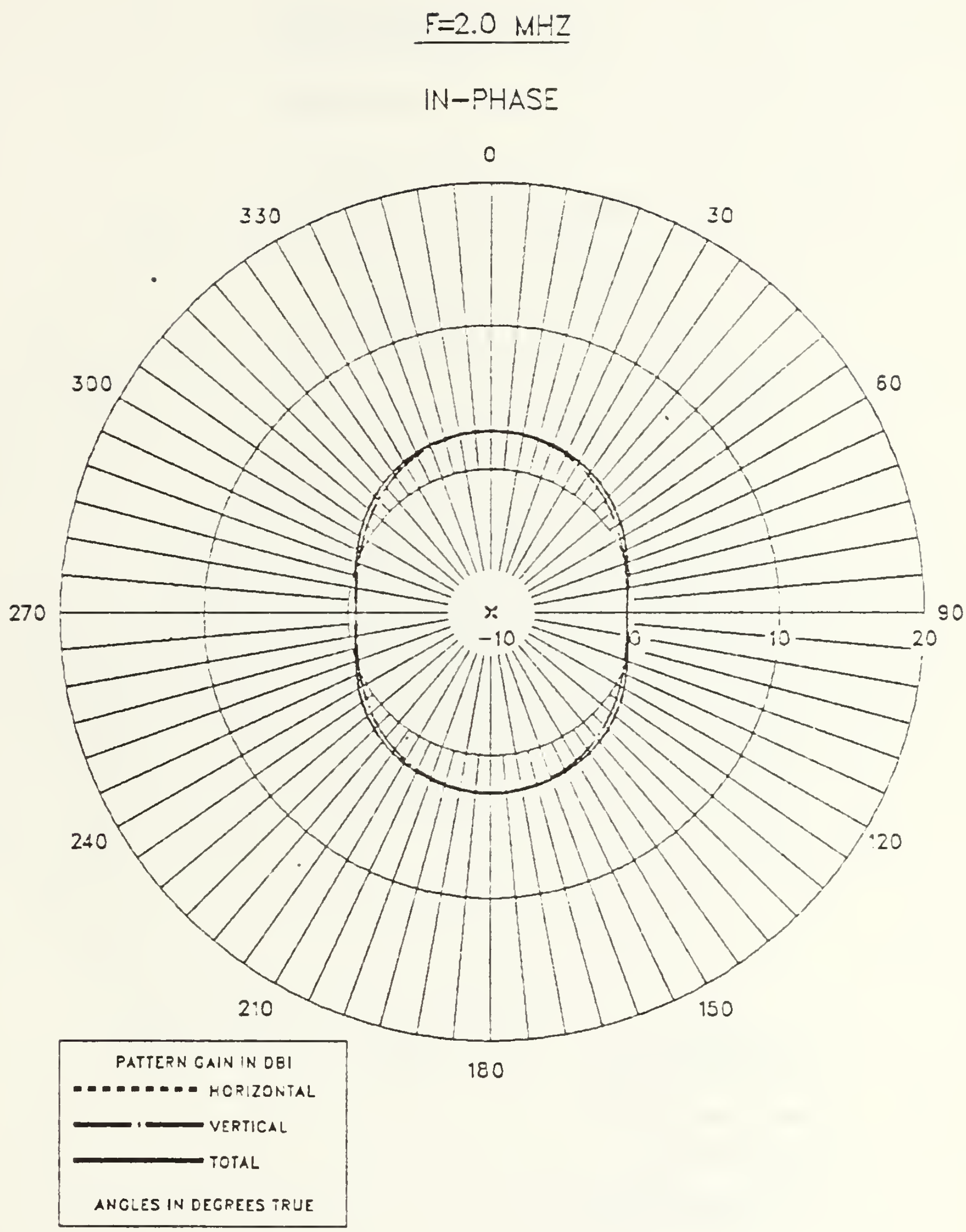
F=2.0 MHZ
IN-PHASE
0
30
60
90
120
150
180
210
240
270
300
330
-10
0
10
20
PATTERN GAIN IN DBI
HORIZONTAL
VERTICAL
TOTAL
ANGLES IN DEGREES TRUE

F=4.0 MHZ

IN-PHASE

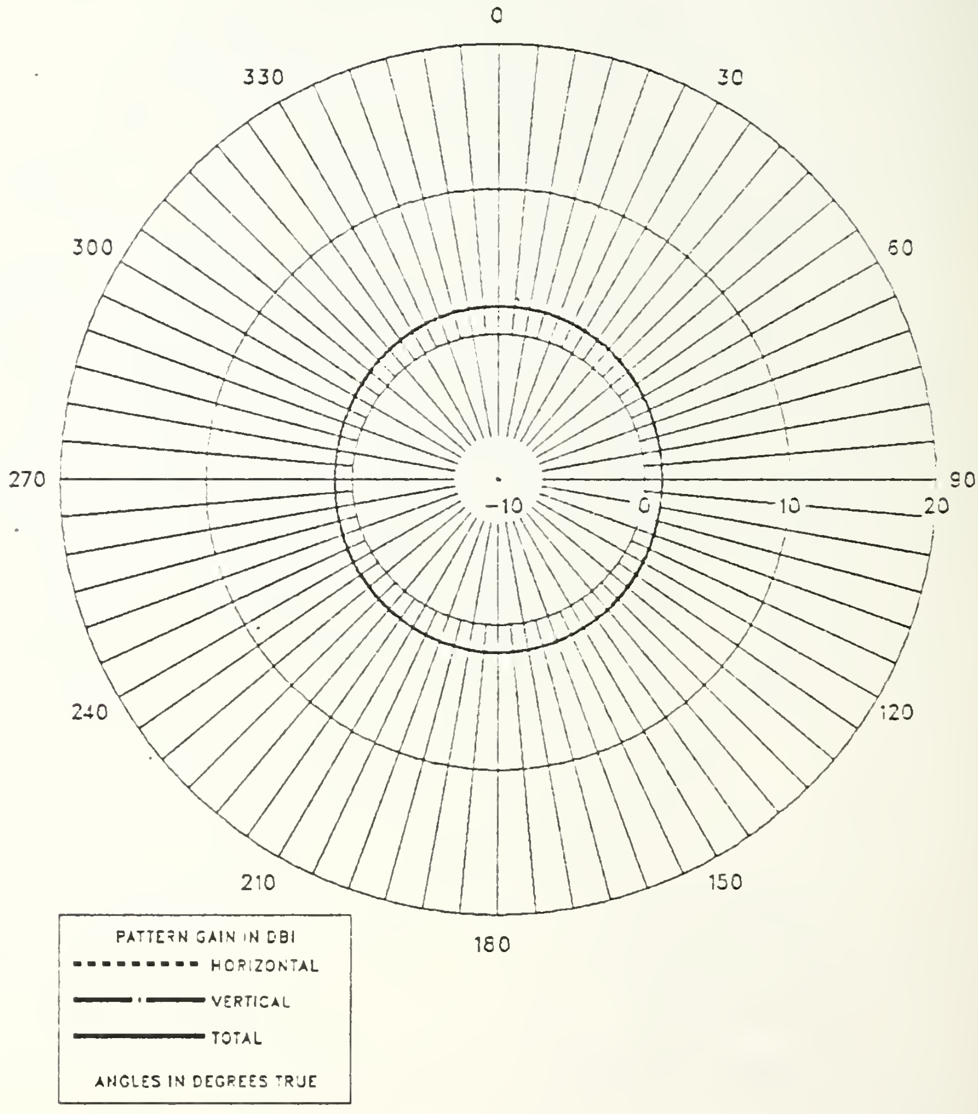

F=6.0 MHZ

IN-PHASE

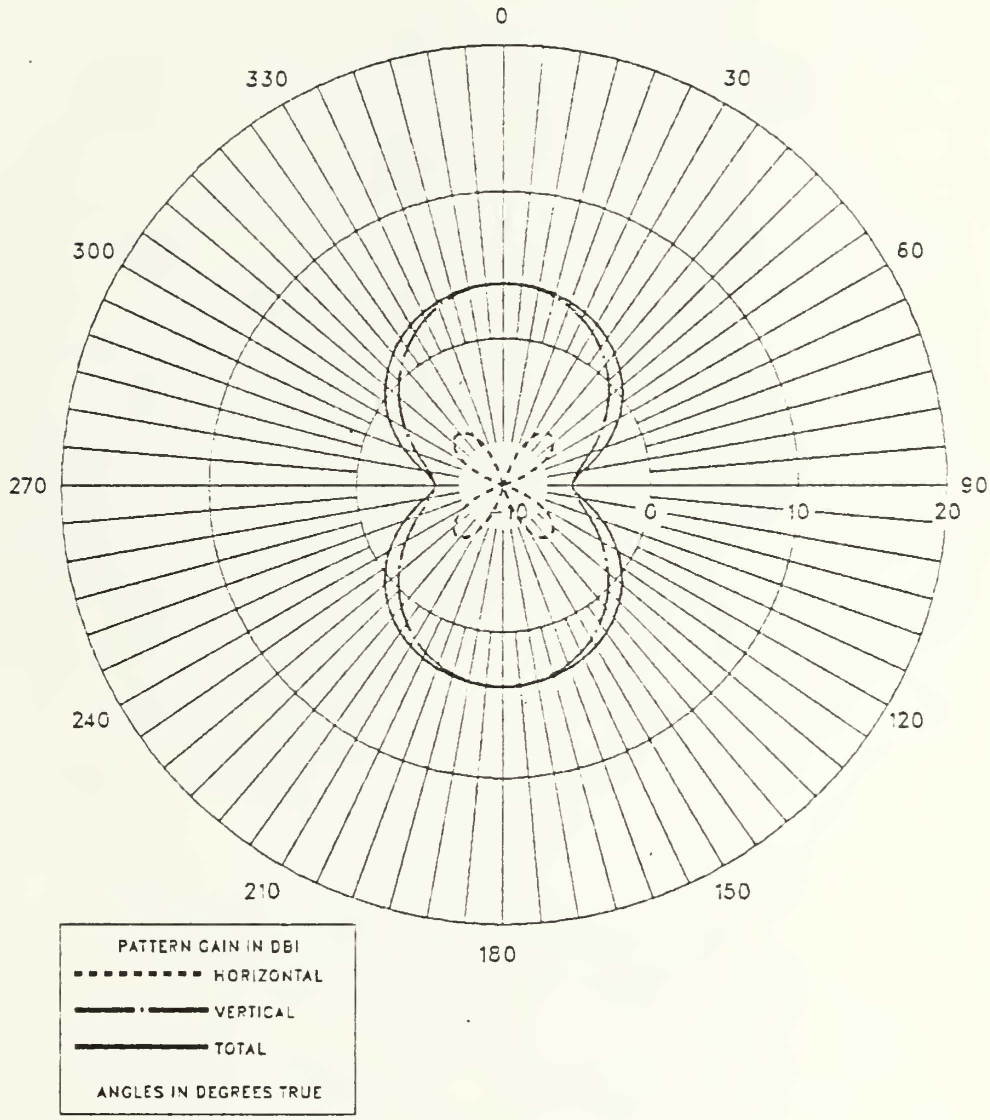

F=8.0 MHZ

IN-PHASE

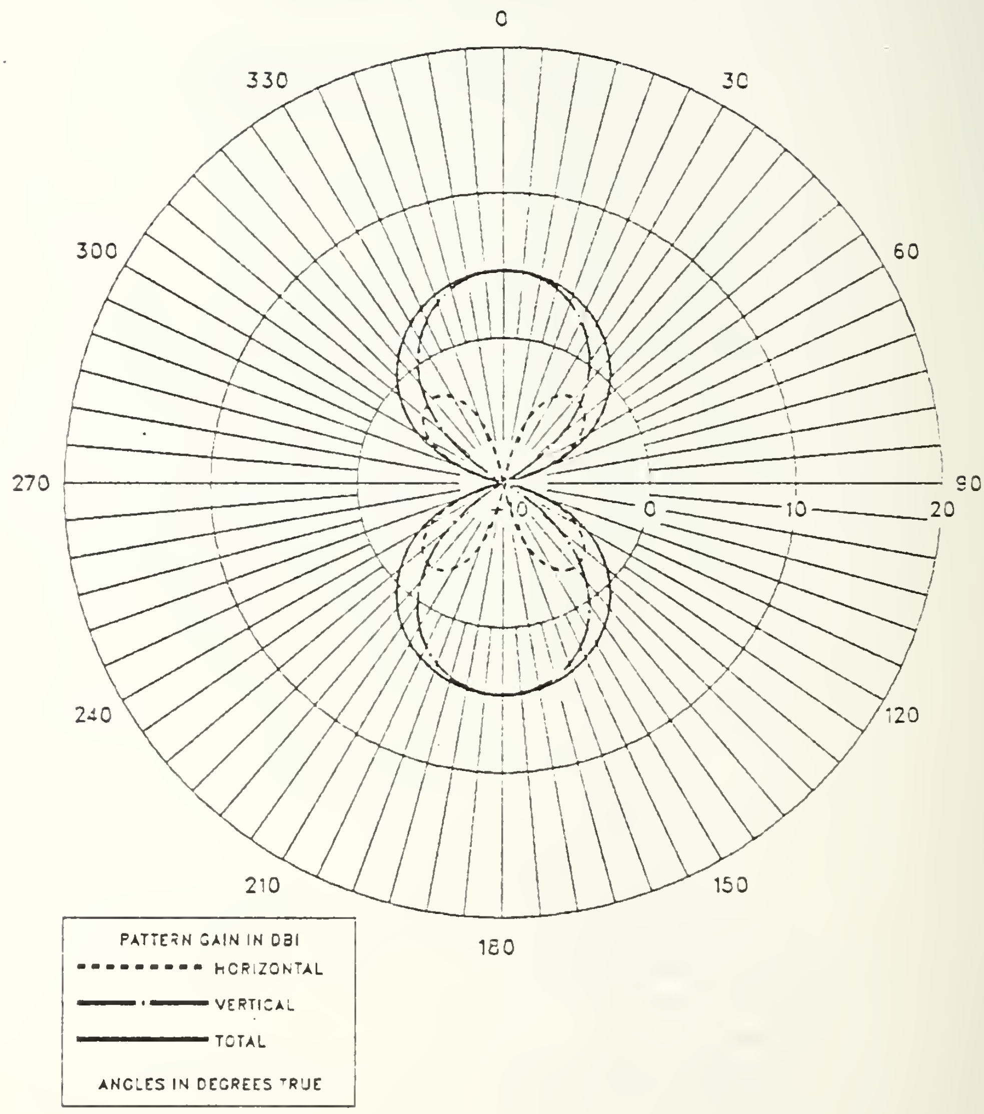

F=10.0 MHZ

IN-PHASE

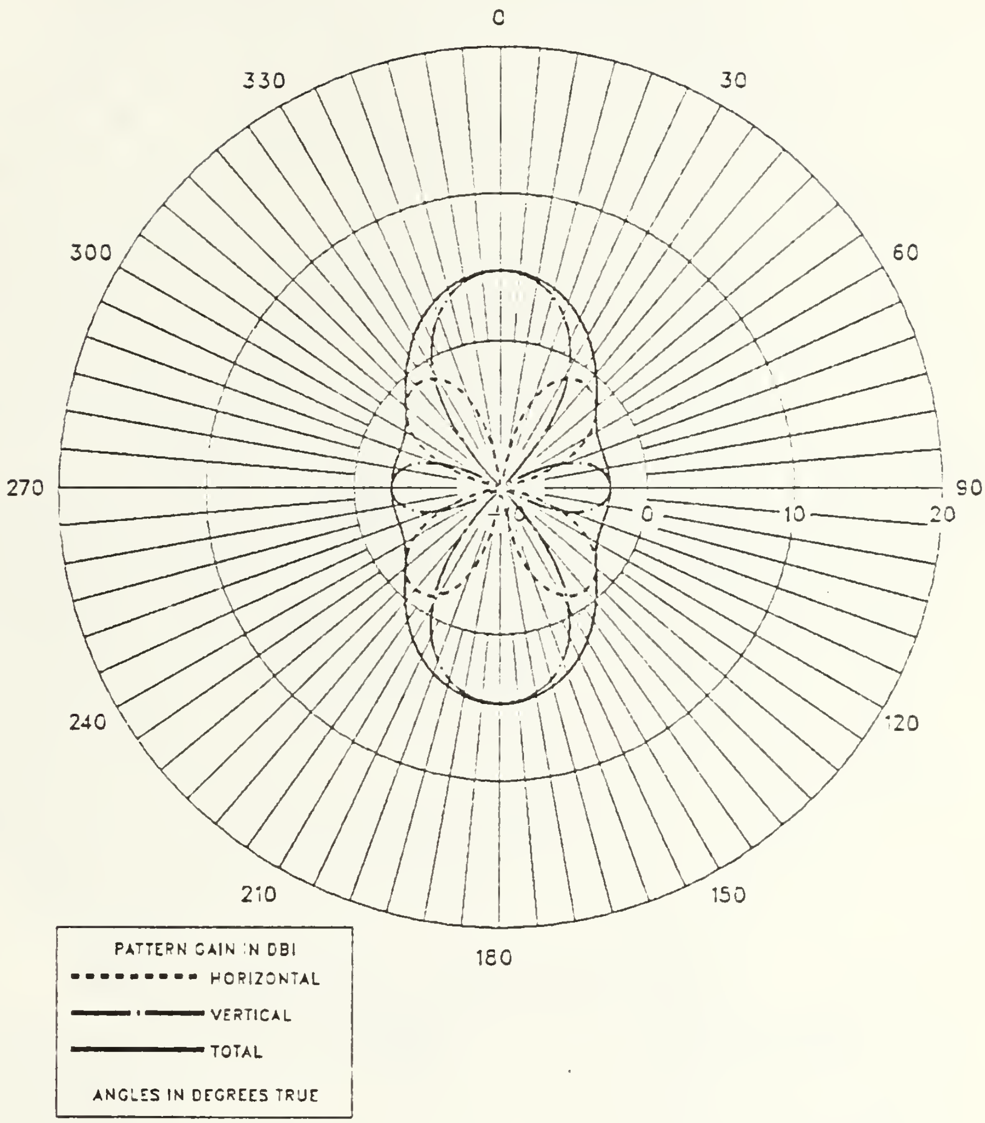

# APPENDIX G-HALF SQUARE ARRAY ANTENNA RADIATION PATTERNS

F=3.6 MHZ

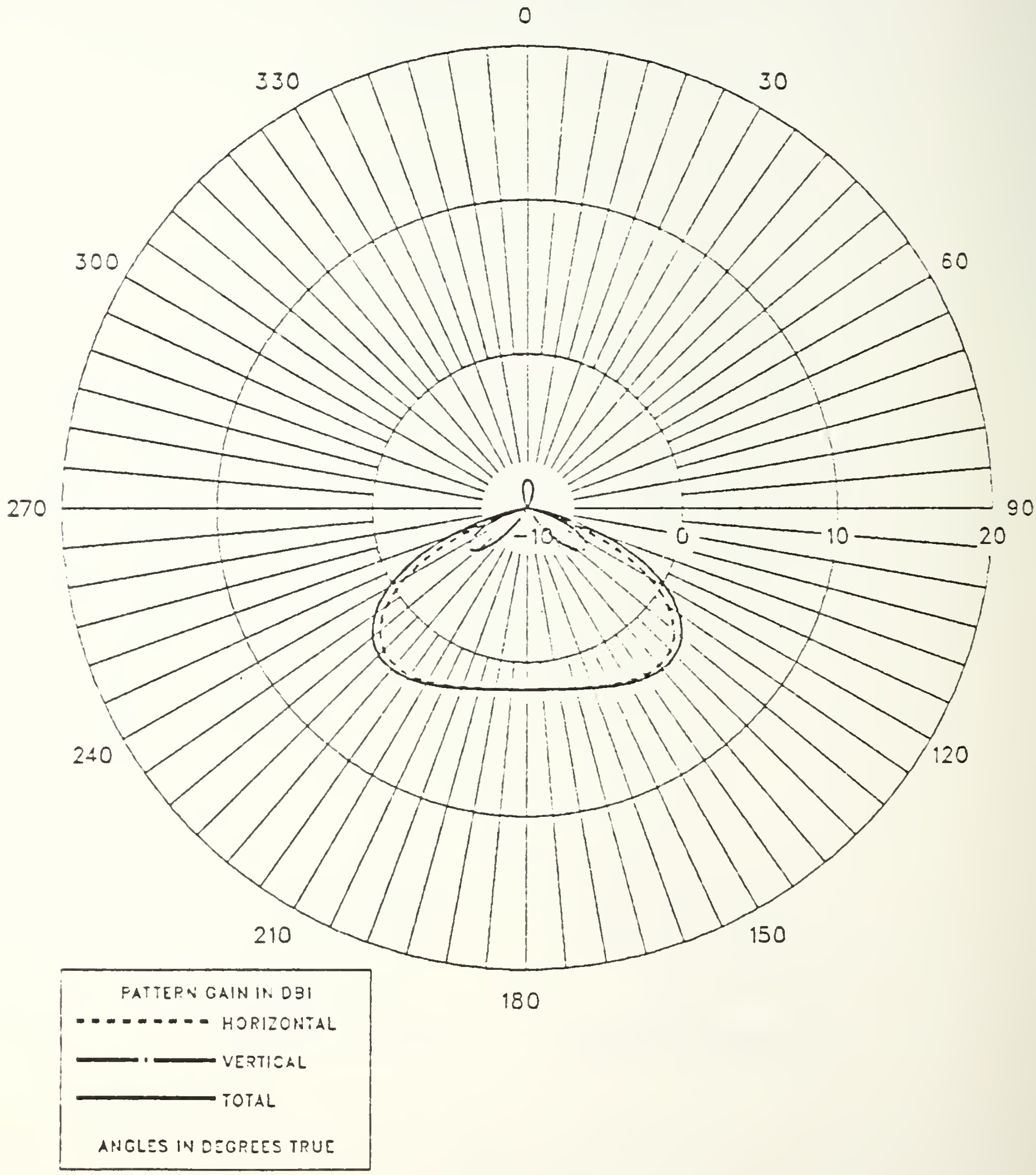

# F= 3.8 MHZ

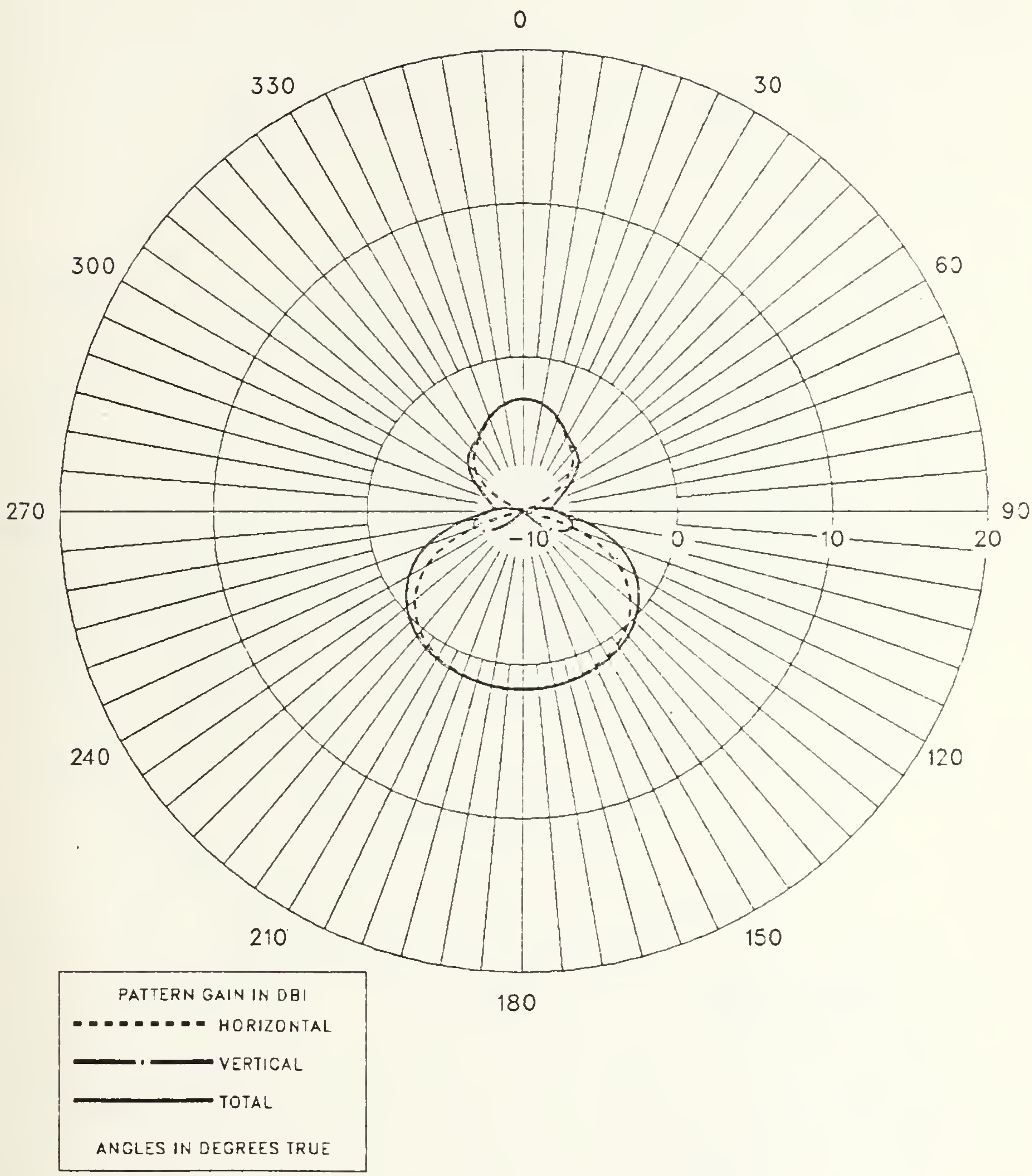
0
30
60
90
120
150
180
210
240
270
300
330
-10
0
10
20
PATTERN GAIN IN DBI
HORIZONTAL
VERTICAL
TOTAL
ANGLES IN DEGREES TRUE

F=7.2 MHZ

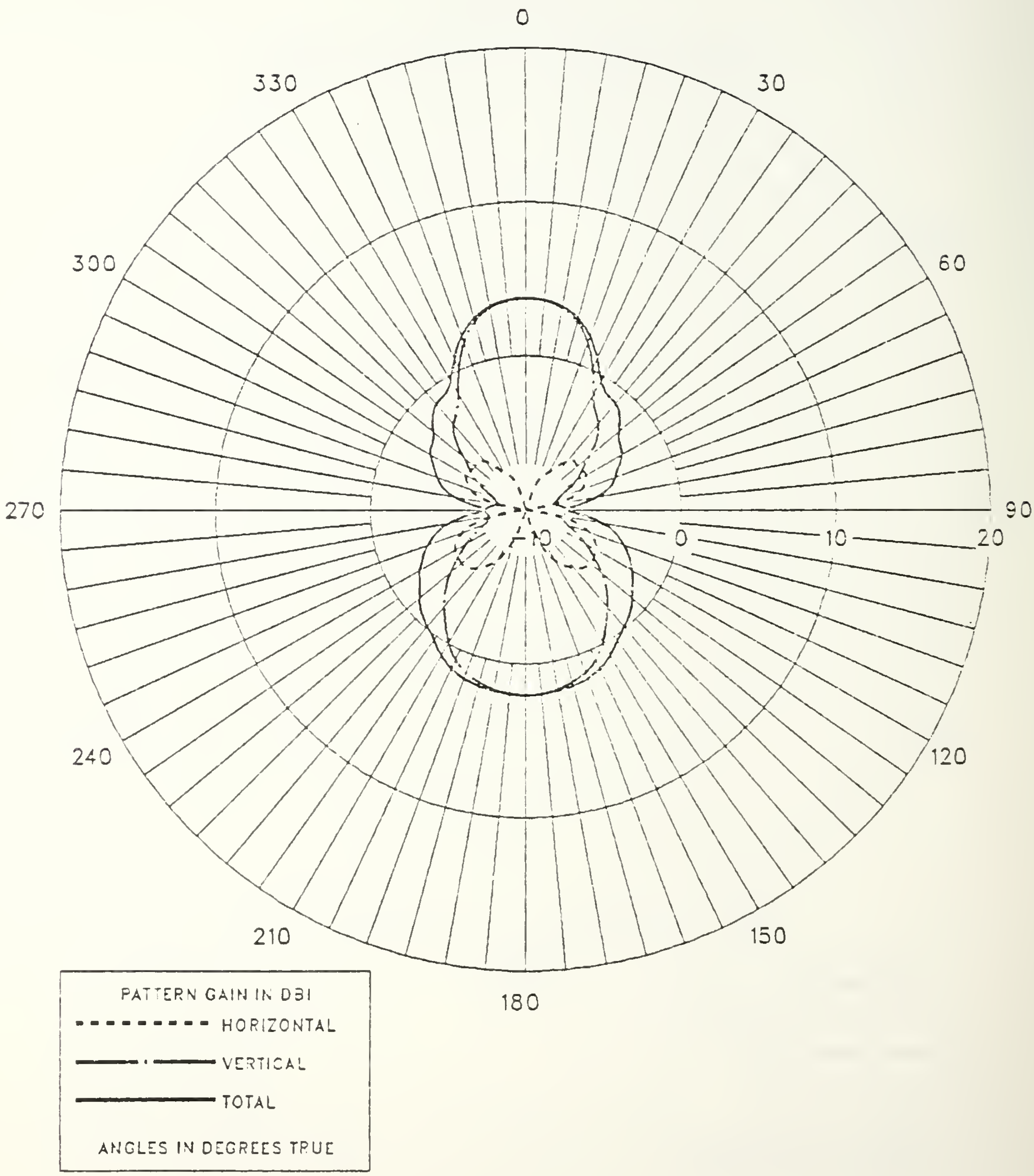
0
30
60
90
120
150
180
210
240
270
300
330
-10
0
10
20
PATTERN GAIN IN DBI
HORIZONTAL
VERTICAL
TOTAL
ANGLES IN DEGREES TRUE

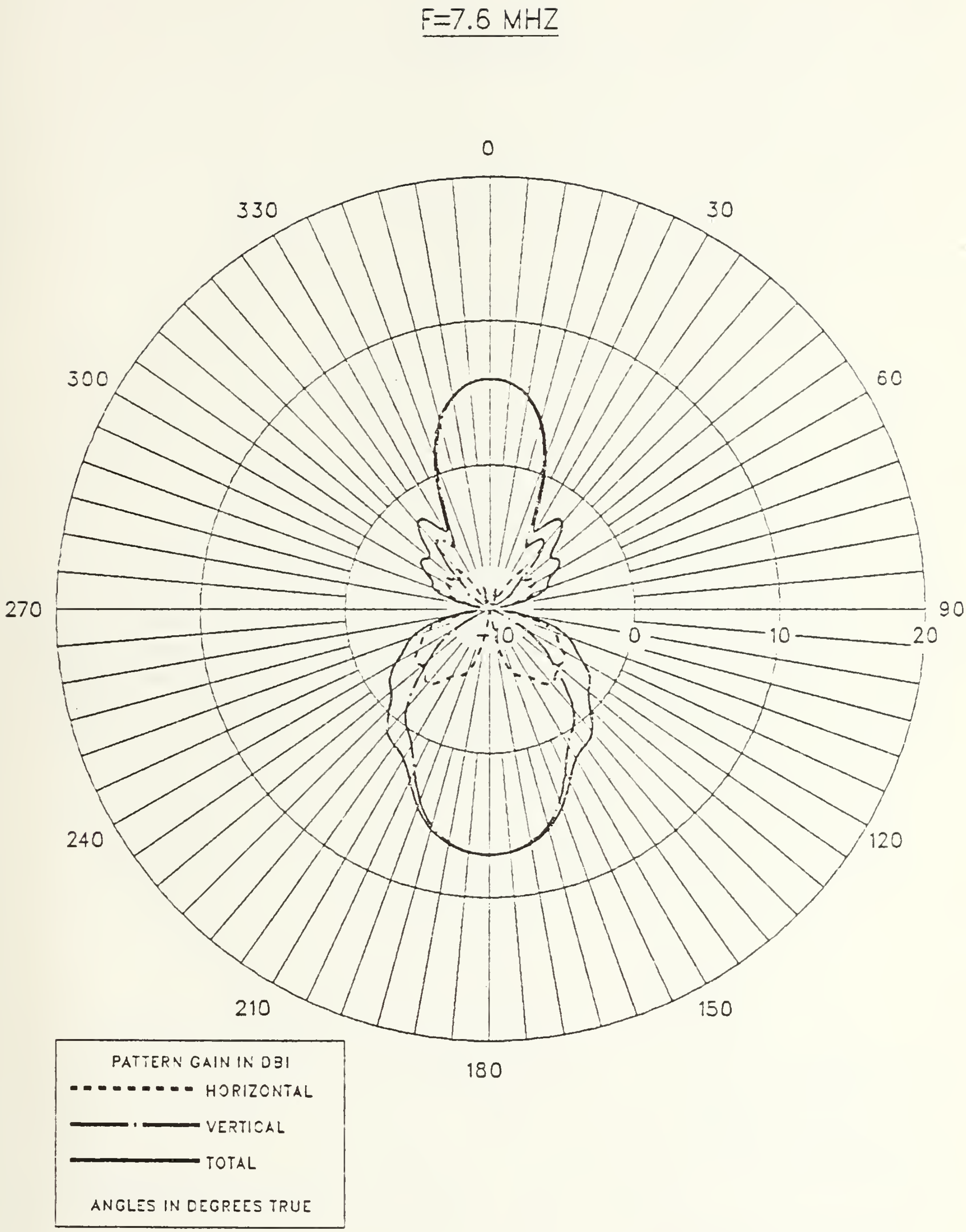
F=7.6 MHZ
0
30
60
90
120
150
180
210
240
270
300
330
-10
0
10
20
PATTERN GAIN IN DBI
HORIZONTAL
VERTICAL
TOTAL
ANGLES IN DEGREES TRUE

F=7.80 MHZ

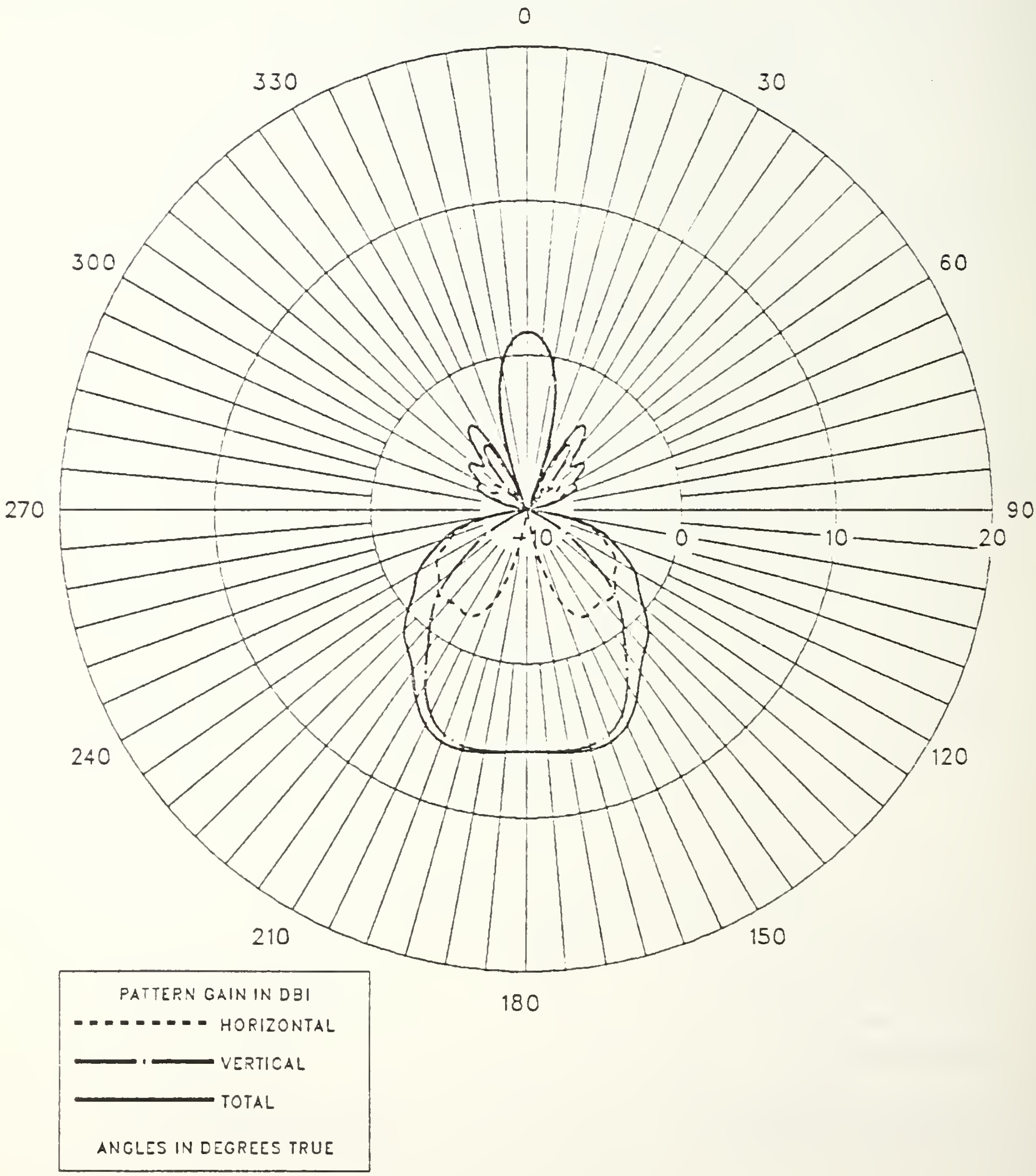
0
30
60
90
120
150
180
210
240
270
300
330
-10
0
10
20
PATTERN GAIN IN DBI
HORIZONTAL
VERTICAL
TOTAL
ANGLES IN DEGREES TRUE

F=7.9 MHZ

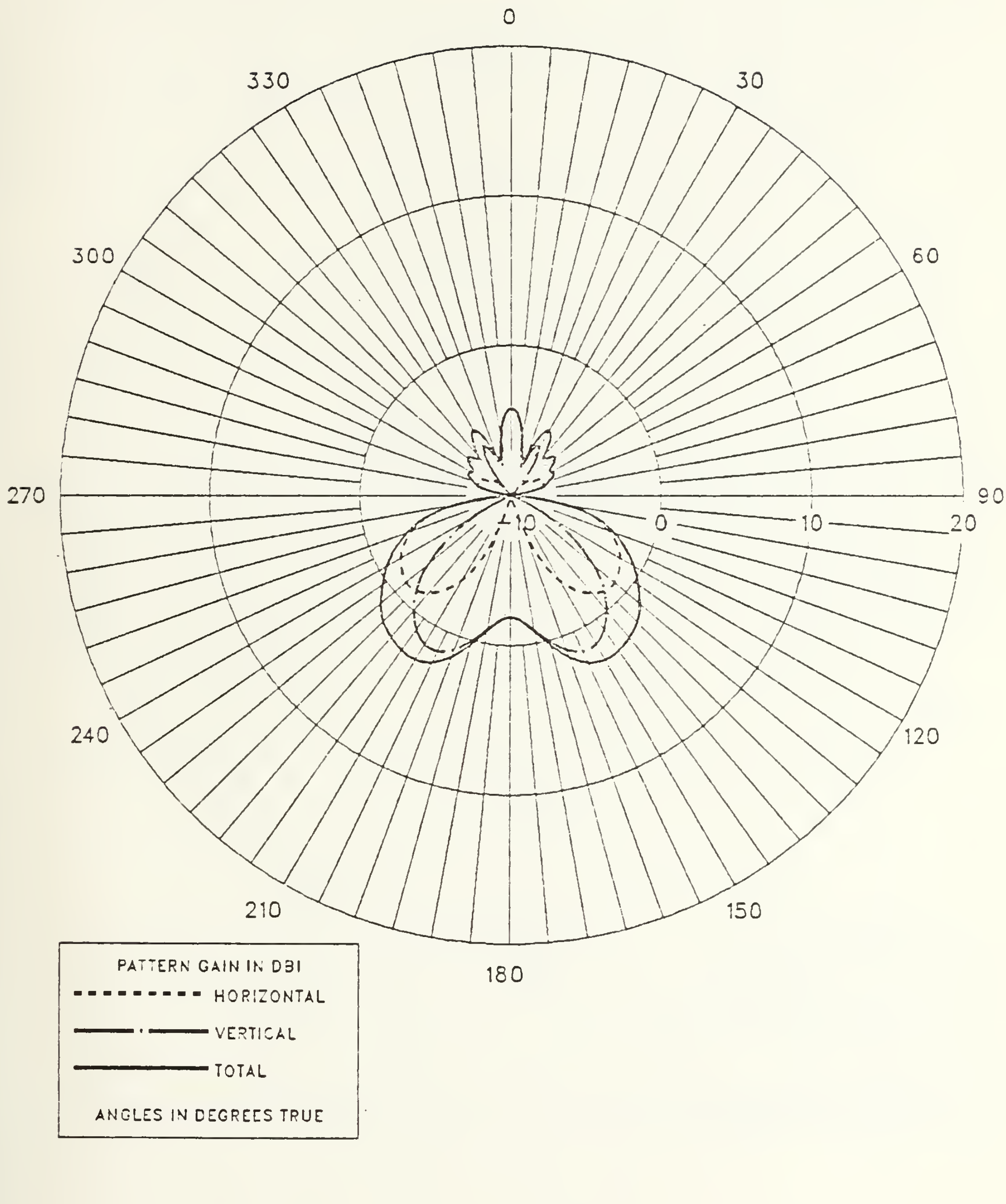

0
30
60
90
120
150
180
210
240
270
300
330
-10
0
10
20
PATTERN GAIN IN DBI
HORIZONTAL
VERTICAL
TOTAL
ANGLES IN DEGREES TRUE

F=8.0 MHZ

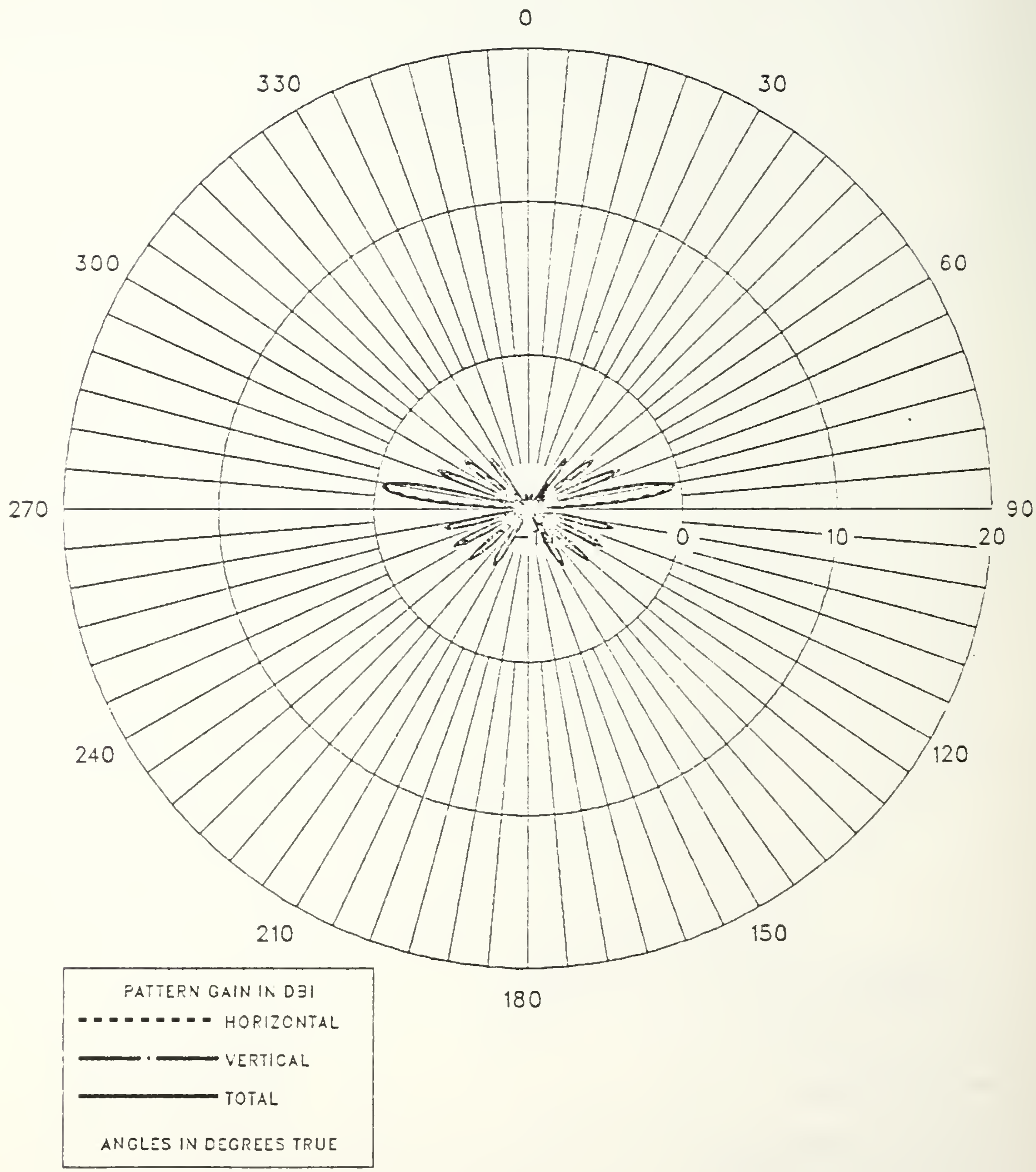
0
30
60
90
120
150
180
210
240
270
300
330
0
10
20
PATTERN GAIN IN DBI
HORIZONTAL
VERTICAL
TOTAL
ANGLES IN DEGREES TRUE

F=8.25 MHZ

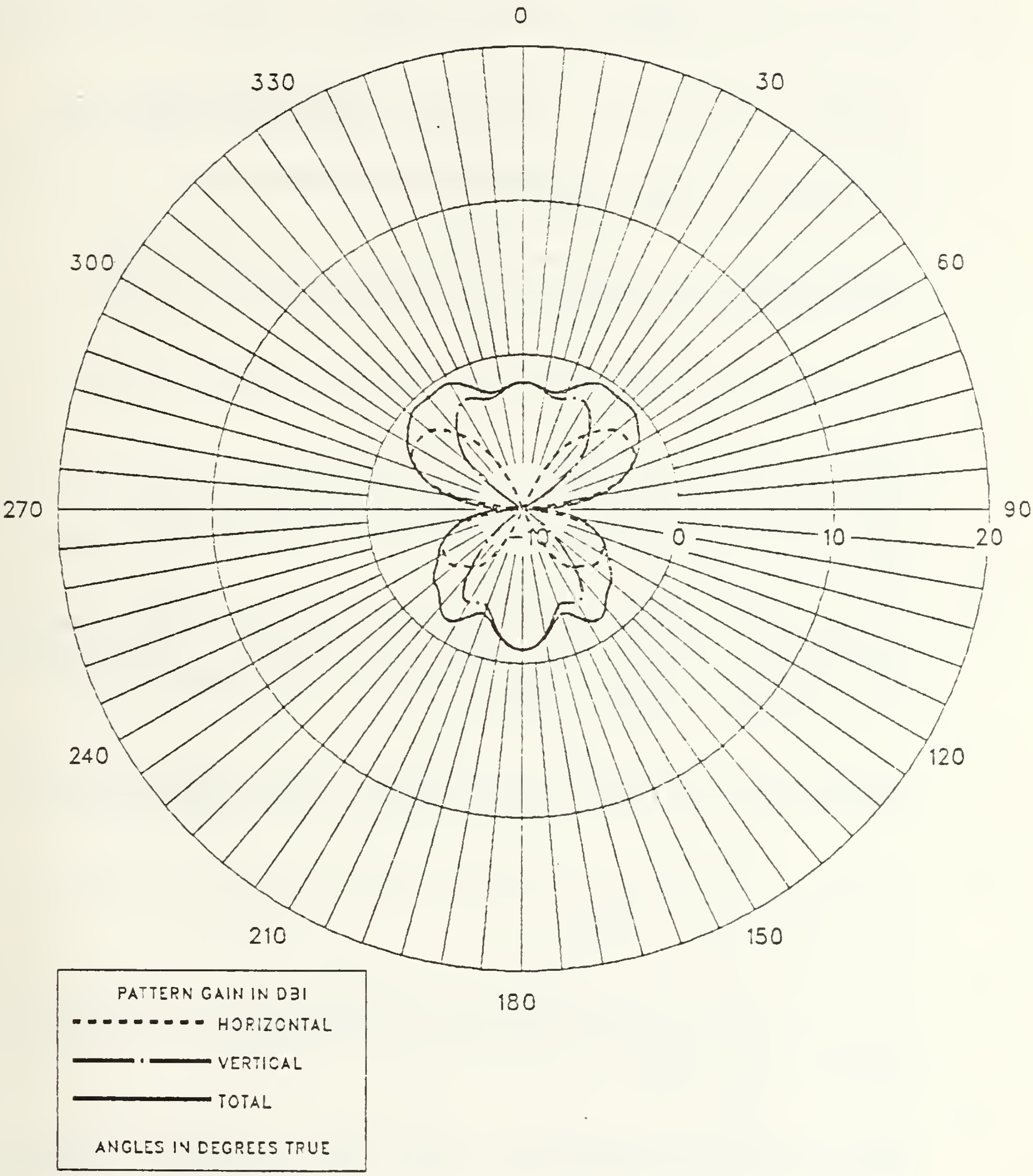
0
30
60
90
120
150
180
210
240
270
300
330
-10
0
10
20
PATTERN GAIN IN DBI
HORIZONTAL
VERTICAL
TOTAL
ANGLES IN DEGREES TRUE

# LIST OF REFERENCES


1. Campbell, D.V., and others, A Dual Feed-Dual Polarized Log-Periodic HF Antenna System, paper presented at the 1985 Antenna Applications Symposium, Urbana, Illinois, 18 September 1985.

2. Weeks, W.L., Antenna Engineering, pp. 267-291, McGraw-Hill, Inc., 1968.

3. Stutzman, W.L. and Thiele, G.A., Antenna Theory and Design, pp. 287-311, John Wiley and Sonc, Inc., 1981.

4. Jasik, H., Antenna Engineering Handbook, pp. 18.1-18.17, McGraw-Hill, Inc., 1961.

5. Isabell, D.E., "Log Periodic Dipole Arrays," IRE Transactions on Antennas and Propagation, V. AP-8, pp. 260-267, May 1960.

6. Vester, B., "The Half Square Antenna," QST, V. 48, pp. 11-14, March 1974.

7. Mayes, P.E., Deschamps, G.A. and Patton, W.T., Backward Wave Radiation from Periodic Structures and Application to Design of Frequency Independent Antennas", Proceedings IRE, V. 49, pp. 962-963, May 1961.

8. Antenna Laboratory Department of Electrical Engineering, University of Illinois, Technical Report 1, Near Field Investigation of Uniformly Periodic Monopole Arrays, by E. Hudock, 30 May 1963.

9. Tezmen, E., A Near Field Investigation of Two Uniformly Periodic Loop Arrays, MSEE Thesis, Naval Postgraduate School, Monterey, California, December 1970.

10. Mittra, R. and Jones, K.E., "How to Use k-$\beta$ Diagrams in Log-Periodic Antenna Design," Microwaves, V. 4, pp. 18-27, June 1965.

11. Electrical Engineering Research Laboratory, University of Illinois Technical Report 59, Theoretical Study of a Class of Lagarithmically Periodic Circuits, by R. Mittra, July 1962.

12. Naval Ocean Systems Center Technical Document 116, Numerical Electromagnetics Code (NEC)-Method of Moments, January 1981.

13. Brown, R.G., and others, Line, Waves, and Antennas, 2d ed., pp. 79-83, John Wiley and Sons, Inc., 1973.

INITIAL DISTRIBUTION LIST

| | | No. Copies |
|---|---|---|
| 1. | Defense Technical Information Center<br>Cameron Station<br>Alexandria, Virginia 22304-6145 | 2 |
| 2. | Library, Code 0142<br>Naval Postgraduate School<br>Monterey, California 93943-5002 | 2 |
| 3. | Commander<br>U.S. Army Signal Center and Ft. Gordon<br>ATTN: ATZH-PO-ACS (CPT Mayes)<br>Ft. Gordon, GA 30905-5300 | 1 |
| 4. | U.S. Army CECOM<br>ATTN: AMSEL-RD-COM-TA-1 (Ken Loffer)<br>Ft. Monmouth, NJ 07703-5202 | 1 |
| 5. | Professor R.W. Adler, Code 62Ab<br>Department of Electrical and Computer Engineering<br>Naval Postgraduate School<br>Monterey, California 93943-5000 | 2 |
| 6. | Donn V. Campbell<br>Military Electronics and Avionics Division<br>TRW Electronics Systems Group<br>One Rancho Carmel<br>San Diego, CA 92128 | 1 |
| 7. | CPT John R. Johnsen, USA<br>HQ, USCOB/USAB<br>ACSIM/DOIM<br>APO, New York 09742 | 2 |
| 8. | Mr. Pete Cunningham<br>CENCOM-CECOMS<br>DRSEL-COM-RN-4<br>Ft. Monmouth, N.J. 07703 | 1 |
| 9. | Air Force Communications and Communication Engineering Institute Center<br>EIE/EIEUS<br>Air Force Base<br>Oklahoma City, OK 73145 | 1 |

10. Sylvania Systems Group/West Division 1
100 Ferguson Drive
Mountain View, CA 94042

11. Hi-Gain Telex Coms Inc 1
8691 NE Hwy 6
Lincoln, NE 68505

12. Barker and Williamson 1
Attn: SR Antenna Desing Engineer
10 Canal Street
Briston, PA 19007

13. DHV/Antenna Production Division 1
Attn: SR Antenna Design Engineer
Box 520
Mineral Wells, TX 76067

14. Mr. Harold Askins 1
NESEC/Charleston
4600 Goer Road
N. Charleston, SC 29406

15. CAPT W. P. Averill 1
U.S. Naval Academy
Dept. of Electrical Engineering
Annapolis, MD 21402

16. Mr. Lawrence Behr 1
Lawrence Behr Assoc. Inc.
P. O. Box 8026
210 W. 4th
Greenville, NC 27834

17. Mr. John Belrose 1
Communications Research Centre
P. O. Box 11490
STN H
Ottawa, Ontario Canada K2H8S2

18. Mr. Lawrence J. Blum 1
Tech For. Comm. Int'l
1625 Stierlin Road
Mt. View, CA 94043

19. Mr. Edwin Bramel 1
P. O. Box 722
Ft. Huachuca, AZ 85613

20. Mr. J. K. Breakall 1
Lawrence Livermore Nat'l Lab
P. O. Box 5504
L-156
Livermore, CA 94550

21. Mr. R. Corry 1
USACEEIA
CCC-CE-TP
Ft. Huachuca, AZ 85613

22. Dr. Roger A. Cox 1
Telex Communications Inc.
8601 NE Hwy 6
Lincoln, NE 68505

23. Mr. W. Decormier 1
Dielectric Products
Tower Hill Rd
Raymond, ME 04071

24. Mr. E. Domning 1
Lawrence Livermore Nat'l Lab
P. O. Box 5504
L-153
Livermore, CA 94550

25. Mr. Dave Faust 1
Eyring Research Int
1455 W 820 N
Provo, UT 84601

26. Dr. A. J. Ferraro 1
Penn State Univ
Ionosphere Res. Lab
University Park, PA 16802

27. Mr. G. H. Hagn 1
SRI International
1611 N. Kent Street
Arlington, VA 22209

28. Mr. Lawrence Harnish 1
SRI International
1611 N. Kent Street
Arlington, VA 22209

29. Mr. J. B. Hatfield 1
Hatfield and Dawson
4226 Sixth Avenue, NW
Seattle, WA 98107

30. Mr. Jackie Ervin Hipp 1
SW Res Inst/EMA
P. O. Drawer 28510
San Antonio, TX 78284

31. Mr. Howard Hochman 1
GTE Sylvania
Box 7188
Mountain View, CA 94039

32. Mr. R. T. Hoverter 1
U.S. Army CECOM
AMSEL-COM-RN-R
Ft. Monmouth, NJ 07703

33. Mr. S. W. Kershner 1
Kershner and Wright
5730 Gen. Washington Dr
Alexandria, VA 22312

34. Mr. Moray King 1
Eyring Research Institute
1455 W 820 N
Provo, UT 84601

35. Mr. H. Kobayaski 1
1607 Cliff Dr
Edgewater, MD 21037

36. Mr. George Lane 1
Voice of America/ESBA
601 D Street, NW
Washington, D.C. 20362

37. Mr. Jim Logan 1
NOSC Code 822(T)
271 Catalina Blvd
San Diego, CA 92152

38. Ms. Janet McDonald 1
USAISESA
ASBH-SET-P
Ft. Huachuca, AZ 85613-5300

39. Mr. David P. Pinion 1
74 Harper Street
San Francisco, CA 94131

40. Mr. J. J. Reaves, Jr. 1
Naval Elec Sys Eng Center
4600 Marriott Dr
N. Charleston, SC 29413

41. Mr. Alfred Resnick 1
WLS Radio
360 N. Michigan Ave
Chicago, IL 60601

42. Mr. R. B. Riegel 1
NSA
8806 Crandal Rd
Lanham, MD 20801

43. Dr. John W. Rockway 1
NOSC Code 8112(T)
271 Catalina Blvd
San Diego, CA 92152

44. Mr. Joseph R. Romanosky 1
NSA
Electronic Engineer
Ft. Meade, MD 20755

45. Mr. R. Royce 1
Naval Research Lab
Washington, D.C. 20375

46. Dr. Jacob Z. Schanker 1
Scientific Radio Systems
367 Orchard St
Rochester, NY 14606

47. Mr. N. Skousen 1
Eyring Res. Inst, Inc.
1455 W 820 N
Provo, UT 84601

48. Mr. W. D. Stuart 1
IIT Research Institute
185 Admiral Cochrane Dr.
Annapolis, MD 21402

49. Mr. R. Tanner 1
Tech Com Int'l
1625 Stierlin Rd
Mountain View, CA 94045

50. Mr. E. Thowless 1
NOSC Code 822(T)
271 Catalina Blvd
San Diego, CA 92152

51. Mr. Hung-Mou Lee, Code 62Lh 1
Naval Postgraduate School
Monterey, California 93943-5000

52. Mr. Ray Vinson, Code 62 1
Naval Postgraduate School
Monterey, California 93943-5000

Thesis
J54975 Johnsen
c.1 An investigation into the potential for developing a successful log-periodic half square antenna with dual feed.